DTIC

AD-A135806


This document has been approved for public release and sale; its distribution is unlimited.

DTIC ELECTE DEC 1 4 1983 A

DEPARTMENT OF THE AIR FORCE

AIR UNIVERSITY (ATC)

# AIR FORCE INSTITUTE OF TECHNOLOGY

Wright-Patterson Air Force Base, Ohio

DTIC FILE COPY

83 12 13 198

AFIT/GE/EE/82D-66

# LOWER BOUNDS APPLIED TO THE MEAN-SQUARE TRACKING ERROR OF AN AMPLITUDE-COMPARISON MONOPULSE RADAR

THESIS

AFIT/GE/EE/82D-66 William P. Tross
lLt USAF

Approved for public release; distribution unlimited

AFIT/GE/EE/82D-66

A-1

# LOWER BOUNDS APPLIED TO THE MEAN-SQUARE TRACKING ERROR OF AN AMPLITUDE-COMPARISON MONOPULSE RADAR

DTIC
COPY
INSPECTED
3

THESIS

Presented to the Faculty of the School of Engineering
of the Air Force Institute of Technology
Air University
in Partial Fulfillment of the
Requirements for the Degree of
Master of Science

by

William P. Tross, B.S.
1Lt USAF

Graduate Electrical Engineering

December 1982

Approved for public release; distribution unlimited

## Acknowledgements

I would like to thank Lt. Col Carpinella for suggesting this thesis and for his valuable advice and guidance in solving this problem. His strong knowledge of the subject and his experience enabled me to overcome many obstacles. I would also like to thank Major Castor for his help in Estimation Theory. I am also grateful to Capt. Rick Floyd for saving me weeks of time by helping me obtain plotted results from the ASD computer system. I am, most of all, grateful for my wife, Chris, and our five children for their support and encouragement and for helping me prove that family life does not have to be altogether sacrificed while at AFIT.

## Contents

## List of Figures

## Notation

### Letter Symbols

| | |
|---|---|
| $A$ | Amplitude of Incoming Signal |
| $\hat{A}$ | Estimate of Amplitude of Incoming Signal |
| dB | Decibels |
| $E$ | Energy of Incoming Signal |
| $E\{\ \}$ | Expected Value Function |
| $g(\ )$ | Antenna Function |
| $\dot{g}(\ )$ | Derivative of Antenna Function |
| $H$ | Decision Hypothesis |
| $k_o$ | Propagation Constant |
| $\ell(r)$ | Likelihood Ratio |
| $N_o$ | Noise Spectral Density |
| $n(t)$ | Noise Signal |
| $P(\ )$ | Probability of |
| $p(\ )$ | Probability Density of |
| PRF | Pulse Repetition Frequency |
| Var( ) | Variance of |

### Greek Letter Symbols

| | |
|---|---|
| $\Sigma$ | Sum Channel for Two-Dimensional Case |
| $\epsilon$ | Error Voltage |
| $\Delta_{az}$ | Difference Channel for Azimuth in Two-Dimensional Case |

| | |
|---|---|
| $\Delta_{el}$ | Difference Channel Elevation in Two-Dimensional Case |
| $\rho$ | Correlation Coefficient |
| $\sigma^2$ | Variance |
| $\theta$ | Azimuth Angle for One-Dimensional Case, Elevation Angle for Two-Dimensional Case |
| $\hat{\theta}$ | Estimate of Azimuth or Elevation Angle |
| $\phi$ | Azimuth Angle for Two-Dimensional Case |
| $\hat{\phi}$ | Estimate of Azimuth Angle for Two-Dimensional Case |

## Abstract

This thesis addresses the problem of estimating the target angle with respect to the boresite of an Amplitude-Comparison Monopulse Radar. The maximum likelihood estimate is used to track the target and produce a mean-square error. This error is approximated from a computer simulated tracking loop and then compared to the Cramer-Rao and Ziv-Zakai bounds.

At high signal-to-noise ratios (SNR), the Cramer-Rao bound is useful in lower bounding the mean-square error. At low SNR levels a phenomena known as the threshold effect occurs and the Cramer-Rao bound becomes unreliable as a lower bound. The Ziv-Zakai bound is a tighter bound and can be used to lower bound the mean-square error at very low SNR levels. It also proves useful in determining the SNR level at which the threshold effect occurs.

# LOWER BOUNDS APPLIED TO THE MEAN-SQUARE TRACKING ERROR OF AN AMPLITUDE-COMPARISON MONOPULSE RADAR

## I. Introduction

### Background

A monopulse radar tracks by maintaining the radar boresite on the target. As the target moves off of boresite an error voltage is developed proportional to the angle off boresite. This information is fed to the radar angle servo which in turn steers the boresite toward the target. Theoretically, this process is done using information gained from a single pulse. Breaklock occurs at a certain signal-to-noise ratio (SNR) per pulse when the information gained from the pulse is not sufficient to steer the boresite to the target accurately. Consequently, the target moves out of the antenna beam width.

At a certain minimum SNR level, a phenomena known as the threshold effect occurs. Consider the example of a probability density function (pdf) of an observation z. Assume that the density function has several maximums, the largest of which is at the center. The maximum likelihood (ML) estimate of z is that value of z which maximizes the pdf [Ref 6].

For the case of no noise in the observation z, the maximum is at the origin (Figure 1). For the low noise situation, the maximum is shifted a small distance from the origin which is proportional to the standard deviation of the additive noise. When the noise becomes comparable to the mean of the pdf, not only is the local maximum near the origin shifted but it is highly probable that some other local maximum of the pdf becomes the largest. Now the error is much larger than the error caused by the shifting of the central local maximum. These large errors are referred to as anomalous errors. When anomalous errors occur, the system behaves nonlinearly and its performance degrades rapidly. This is what is known as the threshold effect [Ref 11].

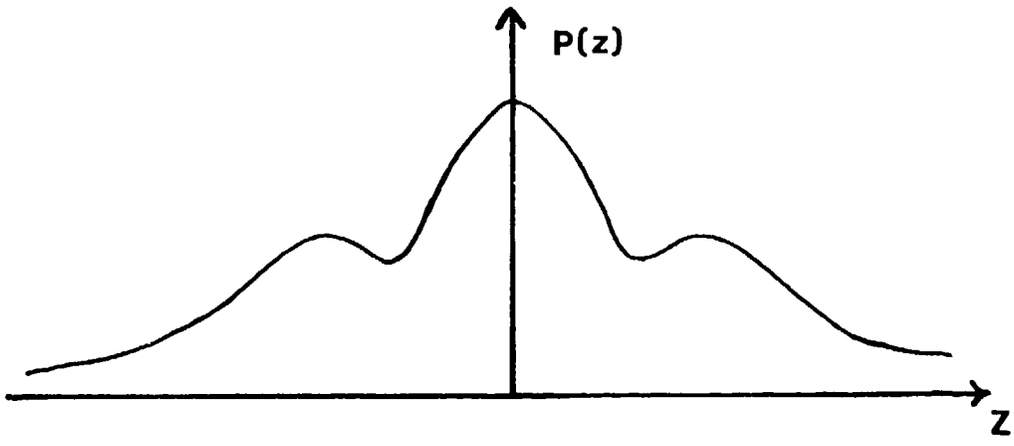


Fig. 1. Probability Density Function of Observation z

The incoming target return is processed in the monopulse radar by weighting the amplitude of the return by the antenna gain factor of its sum and difference beams.

This amplitude weighting is proportional to the target angle off of boresite and is used to steer the radar boresite to the target. Because of random channel noise however, the boresite will be steered to the vicinity of the actual target position. The vicinity is described in terms of the mean-square error (MSE). It will be shown hereafter that as the SNR level decreases, the MSE increases.

The threshold can be quantified by describing a mean-square tracking error, driving its lower bound and then comparing the two. It can be shown [Ref 2] that the Cramer-Rao (CR) bound for the variance of the probability density of the angle off boresite estimate is proportional to the beam-width and SNR.

$$\mathrm{Var}(\hat{\theta}) \propto \frac{BW}{SNR} \tag{1}$$

This bound tells us that no matter what SNR, the variance is kept small by maintaining a narrow beam-width. However, the CR bound is only useful when the SNR level is well above the system threshold. Below threshold the CR bound becomes inaccurate and proves unable to predict breaklock. A much tighter bound (one good at low SNR) is needed to quantify and predict the system threshold or breaklock point.

Problem and Scope

The purpose of this thesis is to develop a maximum likelihood estimate of the target angle off boresite and use it to track the target. From this procedure the MSE can be derived through simulation and used to determine at what SNR the MSE becomes large enough to be considered a breaklock point. The simulation results will then be compared to the CR and Ziv-Zakai bounds to see which bound will provide an accurate prediction of the breaklock point.

The Ziv-Zakai (ZZ) bound is designed to be tighter at low SNR levels [Ref 11]. The bound was derived by considering the suboptimal detection procedure which involves an estimate of one of two possible values of a parameter. A criteria was developed for determining which value of the parameter was estimated. This approach is called the Estimation Theorist's Approach. The probability of error associated with this approach is lower bounded by the probability of error achieved by the optimal detection scheme (which is referred to as the Hypothesis Tester's Approach). This entire process resulted in new bounds based on known results in detection theory. The advantage of the ZZ bound is that it is independent of biases associated with estimators and is therefore tighter than other bounds [Ref 11].

The ZZ bound was modified to fit a problem involving the bearing estimate of a linear array [Ref 8]. This

modified version is adapted and used to derive a lower bound for the MSE for this problem.

Assumptions

This problem is approached assuming a one-dimensional Amplitude-Comparison Monopulse Radar (i.e., azimuth case only). The channel noise is assumed to be white gaussian noise (WGN) independent from channel to channel and pulse to pulse with zero mean and variance $N_o/2$. The antenna functions used to describe the sum and difference beams are derived assuming the two radar antennas are point sources in a linear array. The amplitude of the return signal, A, is assumed to be random and unknown since the target radar cross-section is unknown. However, A can be estimated as will be shown and used in the estimation of the target angle relative to boresite.

The radar's 3 dB beam-width is 3° and the PRF is 200 pps.

A stationary target will be tracked first after which a moving target will be considered.

General Approach

The first step is to develop adequate antenna functions which can weight the return signal amplitude proportional to the target angle relative to boresite. The antenna functions are used to form the observation r(t). The product of the return signal s(t), its amplitude A,

and the antenna function, added to the channel noise makes up an observation.

$$r(t) = As(t)g(\theta) + n(t)$$

It is shown that the one-dimensional monopulse radar has two channels and will therefore have two observations $r_1(t)$ and $r_2(t)$. With these observations and their joint pdf, the maximum likelihood estimate can be derived by finding

$$\frac{\partial \ \ell n}{\partial \theta} \ p(r_1 r_2/A,\theta) = 0 \qquad (2)$$

where $p(r_1 r_2/A,\theta)$ is the joint pdf of $r_1$ and $r_2$, A is the amplitude of the return signal and $\theta$ is the target angle relative to boresite.

This results in an equation that is a function of $\theta$, the actual target position relative to boresite, and $\hat{\theta}$, the estimated target position. It is then shown that this equation is zero when $\hat{\theta} = \theta$, or when the radar boresite is pointing at the actual target position. This equation is called the error equation and is used to steer the antenna toward the target.

Once the error equation is obtained, the ZZ bound is derived following the steps outlined in reference [8].

At this point, a computer simulated tracking loop is designed and implemented. The tracking loop will yield an error between the actual target position and the

boresite position. This error is developed into an MSE and then plotted for different SNR levels. The MSE will be a function of time since an error will develop for each pulse or observation received. The breaklock point will occur when the MSE grows unbounded as the number of pulses (or observations) increases. The level of SNR where this occurs is compared to the Cramer-Rao and Ziv-Zakai bounds to quantify the system threshold or breaklock point.

Both the stationary and nonstationary targets are used to determine breaklock.

## II. The Radar Model

### The Antenna Functions

A simple block diagram of a one-dimensional monopulse radar is shown in Figure 2.

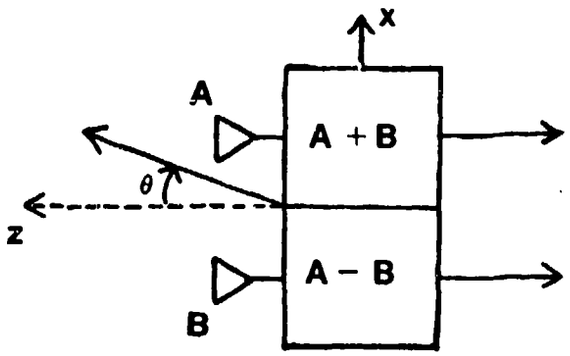


Fig. 2. Simple Block Diagram of Radar

The patterns of antennas A and B are combined so as to produce two beams. The sum beam, A+B, is represented as an antenna function $g_{\Sigma}(\theta)$. Likewise, the difference beam, A-B, is represented as $g_{\Delta}(\theta)$. The antenna functions are used to describe the amplitude weighting of the target return. The maximum gain occurs at the antenna boresite ($\theta=0$) and decreases as $\theta$ increases.

To derive the antenna functions, the two antennas are considered as point sources in a two-element linear array (see Figure 3).

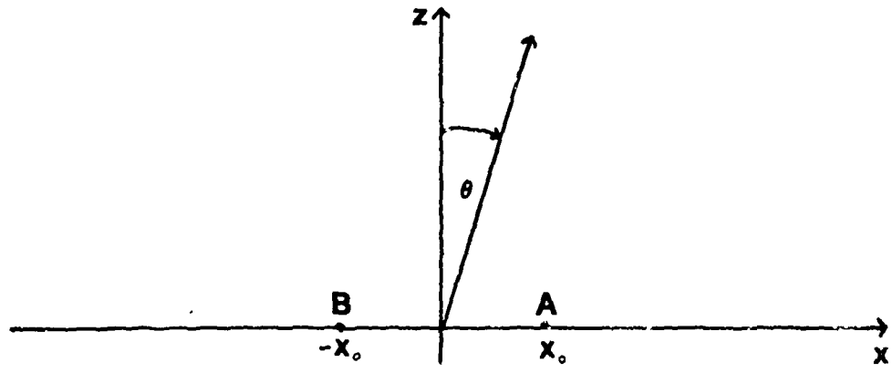


Fig. 3. Two Point Sources in the x-z Plane

A plane wave approaching from an arbitrary direction in the x-z plane can be described as

$$E_A = E_o e^{j\bar{k}_A \cdot \hat{r}} \tag{2}$$

$$E_B = E_o e^{j\bar{k}_B \cdot \hat{r}} \tag{3}$$

where $E_o$ is the amplitude of the plane wave and

$$\bar{K}_A = k_o x_o \hat{x}$$

$$\bar{K}_B = -k_o x_o \hat{x}$$

and

$$\hat{r} = \hat{x} \sin\theta \cos\phi + \hat{y} \sin\theta \sin\phi + \hat{z} \cos\theta$$

Performing the dot product and substituting back into equations (2) and (3) gives

$$E_A = E_o e^{jk_o x_o \sin\theta} \tag{4}$$

$$E_B = E_o e^{-jk_o x_o \sin\theta} \quad (5)$$

Equations (4) and (5) can now be used to form the sum and difference beams of the monopulse radar.

$$E_A + E_B = E_o(e^{jk_o x_o \sin\theta} + e^{-jk_o x_o \sin\theta}) \quad (6)$$

$$E_A - E_B = E_o(e^{jk_o x_o \sin\theta} - e^{-jk_o x_o \sin\theta}) \quad (7)$$

Using Euler's equation and taking the magnitude yields [Ref 8]

$$|E_A + E_B| = 2E_o \cos u \quad (8)$$

$$|E_A - E_B| = 2E_o \sin u \quad (9)$$

where $u = k_o x_o \sin\theta$.

The antenna functions for the radar model can be obtained by normalizing equations (8) and (9) to produce

$$g_\Sigma(u) = \cos u \quad (10)$$

$$g_\Delta(u) = \sin u \quad (11)$$

These functions represent the monopulse sum and difference beams. The patterns from the two antennas are approximated in Figure 4. To obtain the sum beam these two patterns are summed and yield the pattern shown in Figure 5a. The difference beam is obtained by subtracting the two patterns which yields the pattern in Figure 5b.

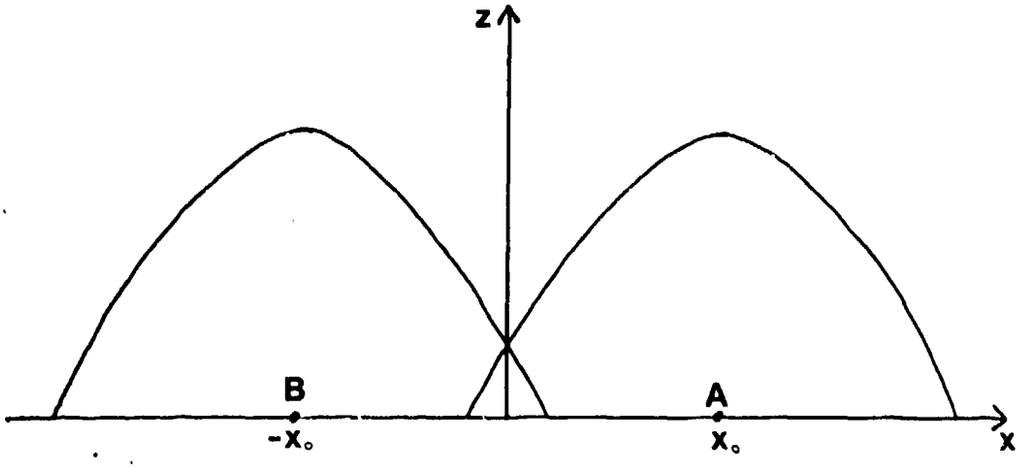


Fig. 4. The Antenna Patterns of the Two Ideal Antennas of the Monopulse Radar

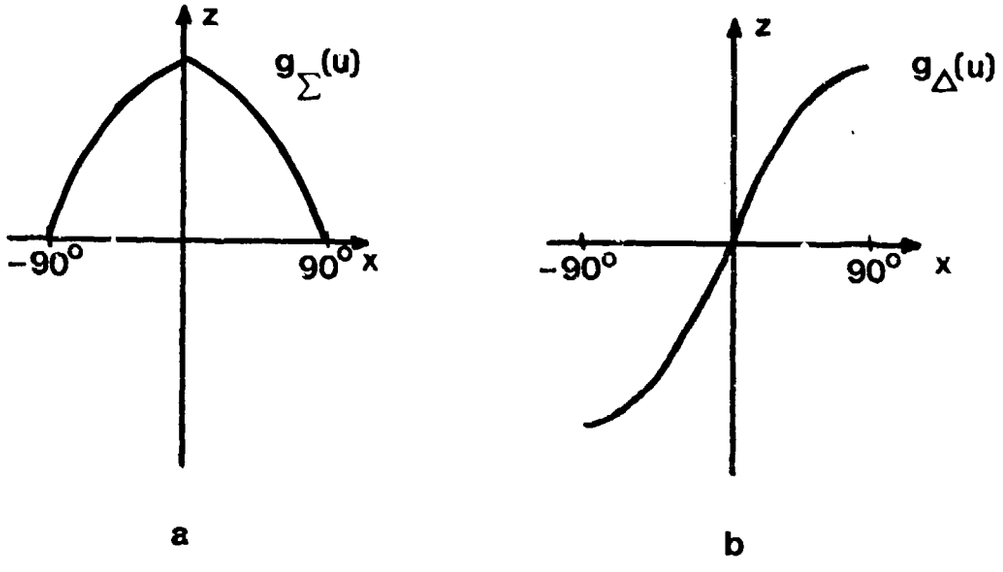


Fig. 5. The Two Monopulse Beams
(a) The Sum Beam; (b) the Difference Beam

If the boresite is pointing directly at the target

$$g_{\Sigma}(u) = \cos(\sin(0)) = 1$$

and

$$g_{\Delta}(u) = \sin(\sin(0)) = 0$$

Now that the antenna functions have been established, a model for estimating the angle off boresite can be developed.

The block diagram in Figure 6 shows the basic system. The signal s(t) with unknown amplitude A is weighted by the antenna functions $g_{\Sigma}(u)$ and $g_{\Delta}(u)$. The channel noise n(t) is added to each channel output to produce the observations $r_1(t)$ and $r_2(t)$. These observations enter the estimator which produces an output (an estimate of the target position relative to boresite) that is used as input to the angle servo. The angle servo then moves the radar boresite.

The Estimator

A maximum likelihood estimate will be taken with respect to the observations $r_1(t)$ and $r_2(t)$. To do this a joint probability density function of $r_1(t)$ and $r_2(t)$ is needed.

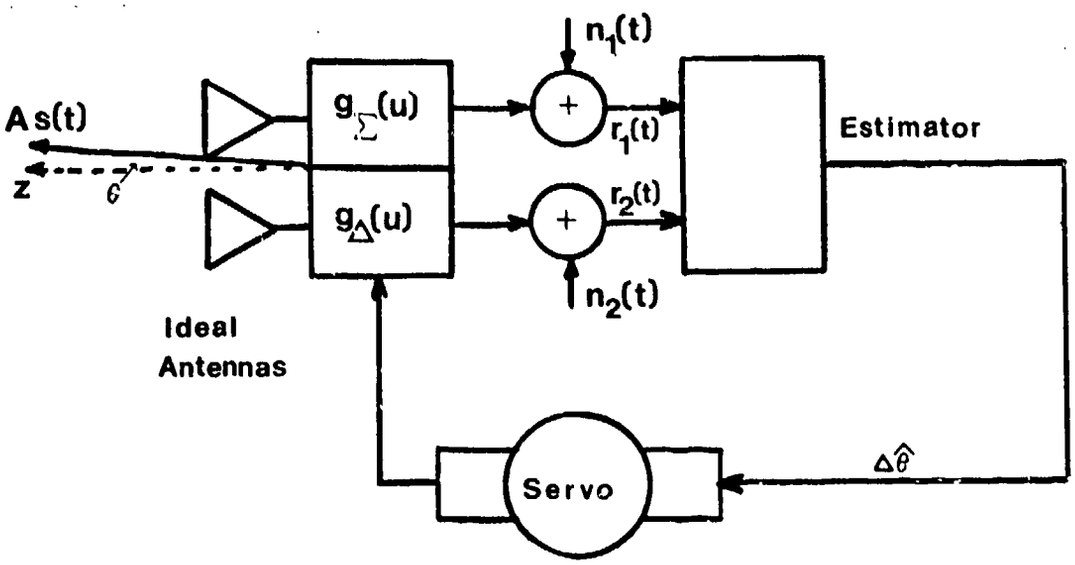


Fig. 6. Block Diagram of the Radar Model Showing the Addition of the Estimator and Servo

The observations $r_1(t)$ and $r_2(t)$ are

$$r_1(t) = Ag_\Sigma(u)s(t) + n(t) \tag{12}$$

$$r_2(t) = Ag_\Delta(u)s(t) + n(t) \tag{13}$$

where n(t) is additive white gaussian channel noise and A is the unknown amplitude of the target return.

For convenience, let $g_\Sigma(u) = g_1(u)$ and $g_\Delta(u) = g_2(u)$.

The maximum likelihood estimator is formed by operating on the density function of the observations. Since the observation, $r(t) = As(t)g(u)+n(t)$, falls under the category of an uncountable infinite number of points, it needs to be transformed into a set of countable

infinite vectors to form the probability density function. The set of vectors is formed by decomposing the observations $r_1(t)$ and $r_2(t)$ into a basis set formed by applying the Gram-Schmidt orthogonalization method [Ref 10]. For the single pulse problem the orthonormal basis set is one-dimensional with

$$\phi_i(t) = \begin{cases} s(t)/\sqrt{E} & 0 \leq t \leq T \\ 0 & \text{else} \end{cases}$$

then

$$r_{11} = \int_0^T r_1(t)\phi_1(t)dt$$

$$= \int_0^T r_1(t)s(t)/\sqrt{E}\ dt$$

$$= \int_0^T [As(t)g_1(u) + n_1(t)]s(t)/\sqrt{E}\ dt$$

$$= A\sqrt{E}g_1(u) + n_1 \qquad (14)$$

where

$$n_1 = 1/\sqrt{E}\int_0^T s(t)n_1(t)\ dt$$

Similarly,

$$r_{21} = \int_0^T r_2(t)\phi_1(t)\ dt$$

and then

$$r_{21} = A\sqrt{E}g_2(u) + n_2 \qquad (15)$$

Since the noise components, $n_i$, are independent gaussian random variables, $r_{11}$ and $r_{21}$ are gaussian and independent. Their statistics are

$$E\{r_{11}/A,u\} = A\sqrt{E}g_1(u); \quad Var(r_{11}/A,u) = N_o/2 \quad (16)$$

$$E\{r_{21}/A,u\} = A\sqrt{E}g_2(u); \quad Var(r_{21}/A,u) = N_o/2 \quad (17)$$

At this point only a single pulse is being considered so the second subscript on the vector observations will be dropped.

The pdf of the observations is the joint pdf of $r_1$ and $r_2$. Since they are independent, the joint pdf is

$$p(r_1r_2/A,u) = p(r_1/A,u)p(r_2/A,u)$$

$$p(r_1r_2/A,u) = \left(\frac{1}{\pi N_o}\right)^{\frac{1}{2}}$$

$$\exp\left\{\frac{-1}{N_o}\left[(r_1-A\sqrt{E}g_1(u))^2 + (r_2-A\sqrt{E}g_2(u))^2\right]\right\} \quad (18)$$

To obtain the maximum likelihood estimate [Ref 6] we find

$$\partial/\partial A[\ell n\ p(r_1r_2/A,u)] = 0$$

and

$$\partial/\partial u[\ell n\ p(r_1r_2/A,u)] = 0$$

Let $\partial/\partial u\, g(u) = \dot{g}(u)$

$$\ell n\, p(r_1 r_2/A,u) = \ell n\, k - 1/N_o[(r_1 - A\sqrt{E}g_1(u))^2 + (r_2 - A\sqrt{E}g_2(u))^2]$$

where k is a constant.

Then

$$\partial/\partial A[\ell n\, p(r_1 r_2/A,u)] = \frac{-1}{N_o}[2(r_1 - \hat{A}\sqrt{E}g_1(u))(-g_1(u)\sqrt{E}) + 2(r_2 - \hat{A}\sqrt{E}g_2(u))(-g_2(u)\sqrt{E})] = 0$$

Solving for $\hat{A}$ we get

$$\hat{A} = \frac{r_1 g_1(u) + r_2 g_2(u)}{\sqrt{E}(g_1^2(u) + g_2^2(u))} \tag{19}$$

Now to find $\hat{u}$

$$\partial/\partial u[\ell n\, p(r_1 r_2/A,u)] = \frac{-1}{N_o}[2(r_1 - A\sqrt{E}g_1(u))(-A\sqrt{E}\dot{g}_1(u)) + 2(r_2 - A\sqrt{E}g_2(u))(-A\sqrt{E}\dot{g}_2(u))] = 0$$

Solving for $A\sqrt{E}$ yields

$$A\sqrt{E} = \frac{r_1\dot{g}_1(u) + r_2\dot{g}_2(u)}{g_1(u)\dot{g}_1(u) + g_2(u)\dot{g}_2(u)}$$

Substituting equation (19) for $A\sqrt{E}$ yields

$$\frac{r_1 g_1(u) + r_2 g_2(u)}{g_1^2(u) + g_2^2(u)} = \frac{r_1\dot{g}_1(u) + r_2\dot{g}_2(u)}{g_1(u)\dot{g}_1(u) + g_2(u)\dot{g}_2(u)}$$

continuing we get

$$[r_1 g_1(u)+r_2 g_2(u)][g_1(u)\dot{g}_1(u)+g_2(u)\dot{g}_2(u)]$$

$$= [r_1\dot{g}_1(u)+r_2\dot{g}_2(u)][g_1^2(u)+g_2^2(u)]$$

$$r_1 g_1^2(u)\dot{g}_1(u) + r_1 g_1(u) g_2(u)\dot{g}_2(u) + r_2 g_1(u) g_2(u)\dot{g}_1(u)$$

$$+ r_2 g_2^2(u)\dot{g}_2(u)$$

$$= r_1 g_1^2(u)\dot{g}_1(u) + r_1 g_2^2(u)\dot{g}_1(u) + r_2 g_1^2(u)\dot{g}_2(u)$$

$$+ r_2 g_2^2(u)\dot{g}_2(u)$$

$$r_1 g_2(u)[g_1(u)\dot{g}_2(u)-\dot{g}_1(u)g_2(u)]$$

$$+ r_2 g_1(u)[\dot{g}_1(u)\, g_2(u)-g_1(u)\dot{g}_2(u)] = 0$$

which for $\hat{u} = u$ results in

$$r_1 g_2(u) - r_2 g_1(u) = 0 \qquad (20)$$

Equation (20) is the general error equation for a one-dimensional Amplitude-Comparison Monopulse Radar. This equation will be used to steer the radar boresite to the target. To see this, recall that $g_1(u) = \cos u$ and $g_2(u) = \sin u$. Substituting these into equation (20) gives

$$r_1 \sin \hat{u} - r_2 \cos \hat{u} = \varepsilon \qquad (21)$$

The expected value of equation (21) is

$$E\{r_1 \sin \hat{u} - r_2 \cos \hat{u}\}$$

$$= A\sqrt{E}[\cos u \sin \hat{u} - \sin u \cos \hat{u}]$$

$$\bar{\varepsilon} = A\sqrt{E} \sin(\hat{u} - u) \tag{22}$$

This represents the error equation for a no noise case. Clearly, if $\hat{u} = u$ the error is zero. This means that the radar boresite is pointing directly at the target. When the WGN is considered, however, the error is never zero and the error equation is random.

$$\varepsilon = r_1 \sin \hat{u} - r_2 \cos \hat{u} \tag{23}$$

The Discriminator Curve

If equation (22) is normalized with respect to the return signal amplitude and energy it becomes

$$\bar{\varepsilon} = \sin(\Delta u) \tag{24}$$

where $\Delta u = \hat{u} - u$. This equation, which is the mean of equation (23), describes a discriminator curve. The discriminator curve can be used to obtain a value for $\Delta u$ which is a function of the target angle $\theta$ (see Figure 7).

For each value of $\varepsilon$ on the discriminator curve there is a unique corresponding value for $\Delta u$ as long as the linear portion of the curve is used.

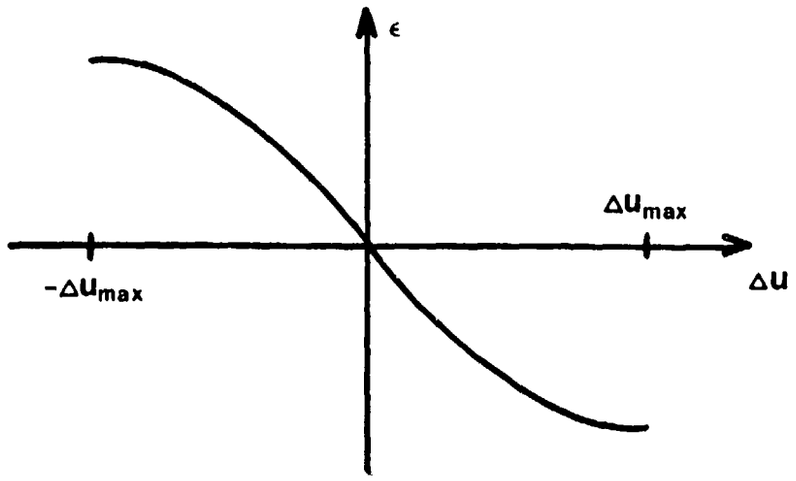


Fig. 7. Discriminator Curve

Equation (23) is also a discriminator curve. However, since $r_1$ and $r_2$ are random variables, a different curve is produced for each value of $r_1$ and $r_2$. This prevents the use of equation (23) to design a discriminator. Equation (24), being the average or mean of (23), is more practical for a discriminator design since it is unchanging with each observation. Both equations (23) and (24) are used to produce a $\Delta u$ to steer the radar boresite. Equation (23) produces the error value $\varepsilon$ which contains the target position information plus a noise component. Equation (24), or the discriminator curve in Figure 7, uses the value of $\varepsilon$ from equation (23) to produce a $\Delta u$ that does not include the noise component. When $\Delta u$ is sent to the angle servo to move the boresite, a tracking error develops.

This can best be seen by an example. Let the target position relative to boresite be 1.0°. Ideally, the error, $\varepsilon$, would produce a $\Delta u$ on the first return pulse that corresponds to 1.0°. However, due to the additive WGN, let $\Delta u$ from Figure 7 correspond to 0.9°. This value is sent to the angle servo to move the radar boresite and the resulting new target position relative to boresite is 0.1°. This is also the tracking error. On the next pulse an error is produced that corresponds to a target angle of 0.1° plus a noise component. Each time (i.e., observation), the boresite is moved closer to the target until a steady-state error is developed. As will be shown later, the steady-state error can be formed into an MSE.

To quantify the threshold of the radar system the MSE needs to be lower bounded. The lower bounds will reveal the minimum the MSE can be for the system and also help determine the SNR level at which breaklock or the threshold effect occurs. The two bounds to be considered are the Cramer-Rao and Ziv Zakai bounds [Refs 6; 12].

The Ziv-Zakai (ZZ) Bound

The ZZ bound as developed in references [8; 12] is stated as follows:

$$\varepsilon^2(\theta) \geq \max_{0 \leq \theta \leq \theta_p} \sin^2\theta \, P_e(-\theta,\theta) \qquad (25)$$

where $\theta$ is the target angle relative to boresite and $\theta_p$ is defined by

$$\sin \theta_p = \frac{\sin \theta_{max} + \sin \theta}{2}$$

The probability of error, $P_e(-\theta,\theta)$ is determined from detection theory and denotes the error probability of the best procedure for deciding whether a target is at $-\theta$ or $\theta$ when it is known that a target is at one of these positions and each has equal possibilities [Refs 6; 8].

The probability of error can be described as

$$P(\varepsilon) = P\{H_0\}P\{\ell>0/H_0\} + P\{H_1\}P\{\ell<0/H_1\} \qquad (26)$$

where $H_0$ and $H_1$ are two observation hypotheses and $\ell$ is the log-likelihood ratio as defined in reference [6]. For the minimum probability of error case, $P\{H_0\} = P\{H_1\}$ and therefore the detection threshold = 1 [Ref 6].

To begin with, the two hypotheses are

$$H_0: r_1 = A\sqrt{E}g_1(u_o)+n_1;\ r_2 = A\sqrt{E}g_2(u_o) + n_2 \qquad (27)$$

$$H_1: r_1 = A\sqrt{E}g_1(u_1)+n_1;\ r_2 = A\sqrt{E}g_2(u_1) + n_2 \qquad (28)$$

Recall that $u = k_o x \sin \theta$. The probability densities are

$$p(r_1 r_2/H_o) = \left(\frac{1}{\pi N_o}\right) \exp\left\{\frac{-1}{N_o}\left[(r_1 - A\sqrt{E}g_1(u_o))^2 + (r_2 - A\sqrt{E}g_2(u_o))^2\right]\right\} \qquad (29)$$

$$p(r_1 r_2/H_1) = \left(\frac{1}{\pi N_o}\right) \exp\left\{\frac{-1}{N_o}\left[(r_1 - A\sqrt{E}g_1(u_1))^2 + (r_2 - A\sqrt{E}g_2(u_1))^2\right]\right\} \quad (30)$$

The likelihood ratio is formed from the ratio of (30) to (29)

$$\ell(r) = \frac{\exp\left\{\frac{-1}{N_o}\left[(r_1 - A\sqrt{E}g_1(u_1))^2 + (r_2 - A\sqrt{E}g_2(u_1))^2\right]\right\}}{\exp\left\{\frac{-1}{N_o}\left[(r_1 - A\sqrt{E}g_1(u_o))^2 + (r_2 - A\sqrt{E}g_2(u_o))^2\right]\right\}} \underset{H_2}{\overset{H_1}{\gtrless}} 1$$

The log-likelihood ratio is

$$\ln\ell(r) = r_1[g_1(u_1) - g_1(u_o)] + r_2[g_2(u_1) - g_2(u_o)] + \frac{A\sqrt{E}}{2}[g_1^2(u_o) - g_1^2(u_1) + g_2^2(u_o) - g_2^2(u_1)] \underset{H_o}{\overset{H_1}{\gtrless}} 0 \quad (31)$$

The log-likelihood ratio, denoted $\ell$, has statistics as follows:

$$E\{\ell/H_o\} = A\sqrt{E}[g_1(u_1)g_1(u_o/-g_1^2(u_o) + g_2(u_o)g_2(u_1) - g_2^2(u_o)] + \frac{A\sqrt{E}}{2}[g_1^2(u_o) - g_1^2(u_1) + g_2^2(u_o) - g_2^2(u_1)]$$

$$= A\sqrt{E}[g_1(u_o)g_1(u_1) + g_2(u_o)g_2(u_1)] - \frac{A\sqrt{E}}{2}[g_1^2(u_o) + g_1^2(u_1) + g_2^2(u_o) + g_2^2(u_1)]$$

$$= \frac{-A\sqrt{E}}{2} E_o(1-\rho_o) \quad (32)$$

where

$$E_o = g_1^2(u_o) + g_1^2(u_1) + g_2^2(u_o) + g_2^2(u_1)$$

and

$$\rho_o = 2/E_o[g_1(u_o)g_1(u_1) + g_2(u_o)g_2(u_1)] \qquad (32a)$$

Similarly,

$$E\{\ell/H_1\} = \frac{A\sqrt{E}}{2} E_o(1-\rho_o) \qquad (33)$$

The variance of $\ell$ is

$$\text{Var}(\ell/H_o) = E\{(\ell-\bar{\ell})^2\}$$

$$= N_o/2[g_1^2(u_o)+g_1^2(u_1)+g_2^2(u_o)+g_2^2(u_1)$$

$$- 2(g_1(u_o)g_1(u_1)+g_2(u_o)g_2(u_1))]$$

$$= N_o/2\ E_o(1-\rho_o) \qquad (34)$$

From these statistics, the pdf's of $\ell$ given each observation hypothesis $H_0$ and $H_1$ are

$$p(\ell/H_0) = \left(\frac{1}{2\Pi\sigma_\ell^2}\right)^{\frac{1}{2}} \exp\left\{\frac{-1}{2\sigma_\ell^2}\left[\left(\ell + \frac{A\sqrt{E}}{2} E_o(1-\rho_o)\right)^2\right]\right\} \qquad (35)$$

$$p(\ell/H_1) = \left(\frac{1}{2\Pi\sigma_\ell^2}\right)^{\frac{1}{2}} \exp\left\{\frac{-1}{2\sigma_\ell^2}\left[\left(\ell - \frac{A\sqrt{E}}{2} E_o(1-\rho_o)\right)^2\right]\right\} \qquad (36)$$

where

$$\sigma_\ell^2 = N_o/2\ E_o(1-\rho_o)$$

For this situation, $P\{\ell>0/H_0\} = P\{\ell<0/H_1\}$ and the probability of error then becomes

$$P(\varepsilon) = 1/2P\{\ell>0/H_0\} + 1/2\ P\{\ell<0/H_1\} = P\{\ell>0/H_0\}$$

$$=\int_0^\infty p(\ell/H_0)\,d\ell$$

$$=\int_0^\infty \left(\frac{1}{2\Pi\sigma_\ell^2}\right)^{\frac{1}{2}} \exp\left\{\frac{-1}{2\sigma_\ell^2}\left[\left(\ell + \frac{A\sqrt{E}}{2}\ E_o(1-\rho_o)\right)^2\right]\right\}\ d\ell \quad (37)$$

This integral can be simplified with a change of variables by letting

$$x = \frac{(\ell + A\sqrt{E}/2\ E_o(1-\rho_o))}{\sigma_\ell}$$

Therefore

$$dx = \frac{d\ell}{\sigma_\ell}$$

Substituting back into (37) yields

$$P(\varepsilon) = \int_{x'}^\infty \frac{1}{\sqrt{2\Pi}}\ e^{-x^2/2}\ dx \quad (38)$$

where

$$x' = A\sqrt{E}[E_o/2N_o(1-\rho_o)]^{\frac{1}{2}}$$

Equation (38) can be recognized as the Q-function [Ref 6]. The probability of error is now

$$P(\varepsilon) = Q(x') = Q\left[A\left(\frac{E\,E_o}{2N_o}(1-\rho_o)\right)^{\frac{1}{2}}\right] \quad (39)$$

If symmetry in the error is assumed (i.e., $u_o = -u_1 = u$) then

$$E_o = \sin^2 u + \sin^2 u + \cos^2 u + \cos^2 u = 2$$

and from equation (32a) with $u_1 = -u = u_o$

$$\rho_o = (-\sin^2 u + \cos^2 u) = \cos 2u$$

The variable $\rho_o$ is known as the correlation coefficient [Ref 6] and its result is consistent since it must vary between ±1. Equation (39) becomes

$$P(\varepsilon) = Q[A(E/N_o(1 - \cos 2u))^{\frac{1}{2}}] \qquad (40)$$

Having determined the probability of error, the ZZ bound can now be derived for the MSE of the radar model. If we substitute $u = k_o \times \sin\theta$ and let $k_o \times = 1$, then for an MSE of $\varepsilon^2(\theta)$ the lower bound is [Ref 12]

$$\varepsilon^2(u) \geq u^2 \, Q[A(E/N_o(1-\cos 2u))^{\frac{1}{2}}]$$

and then

$$\varepsilon^2(\theta) \geq \sin^2\theta \, Q[A(E/N_o(1-\cos(2\sin\theta)))^{\frac{1}{2}}] \qquad (41)$$

Two properties can be seen from equation (41). First, for large SNR ($E_o/N_o$) the argument of the Q-function will be large, giving a small value for Q(x). This means a small probability of error and hence a smaller MSE. This is intuitively consistent since we would expect to track well at high SNR. As $\theta$ increases, $\varepsilon^2(\theta)$

increases, which tells us that the MSE becomes larger when we are not pointing at the target. So in order to keep the MSE small the boresite must be kept on the target.

The Cramer-Rao Bound

In reference [2], it was shown that for a one-dimensional Amplitude-Comparison Monopulse Radar, the CR bound for the variance of the estimated target position, $\mathrm{Var}(\hat{\theta})$, was

$$\mathrm{Var}(\hat{\theta}) \geq \frac{1}{A^2 \frac{2E}{N_o}(\dot{g}_1^2(u)+\dot{g}_2^2(u))} \tag{42}$$

For this case $\dot{g}_1^2(u) = \sin^2 u \cos^2 \theta$ and $\dot{g}_2^2(u) = \cos^2 u \cos^2 \theta$ so (41) becomes

$$\mathrm{Var}(\hat{\theta}) \geq \frac{1}{A^2 \frac{2E}{N_o} \cos^2 \hat{\theta}} = \frac{1}{A^2\ \mathrm{SNR} \cos^2 \hat{\theta}} \tag{42a}$$

The factor $(\dot{g}_1^2(u) + \dot{g}_2^2(u))$ can be shown to be the inverse of the beam-width [Ref 2].

The CR bound states that a narrow beam-width will ensure a small variance. But the CR bound does not account for the fact that when the threshold effect and breaklock occur, the target is outside of the radar beam-width and the variance of the error is very large. At this point (i.e., very low SNR) a narrow beam-width no longer guarantees a small error variance. The bound becomes

unreliable and cannot accurately lower bound the MSE at low SNR levels.

The Tracking Loop

To gain insight into where the breaklock point occurs it is necessary to design a tracking loop which uses equation (22) to steer the antenna boresite toward the target. Figure 8 shows a block diagram of the monopulse system which will be simulated.

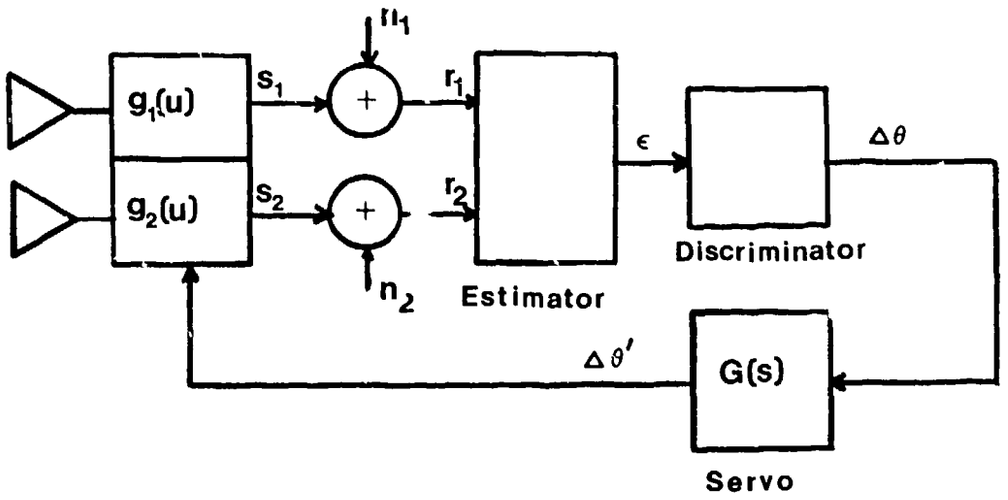


Fig. 8. Block Diagram of AC Monopulse Radar Showing the Estimator being used to Track a Target

In Figure 8, $s_1$, $s_2$, $n_1$ and $n_2$ are the representations of the signal and noise components respectively, where $s_1 = A\sqrt{E}g_1(u)$ and $s_2 = A\sqrt{E}g_2(u)$. The observation $r_1 = s_1 + n_1$ and $r_2 = s_2 + n_2$ are random numbers. For simulation purposes they are determined by using a random number generator to generate $n_1$ and $n_2$ which are then

added to $s_1$ and $s_2$ respectively. The antenna functions are determined by noting that equations (10) and (11) can be written as

$$g_1(u) = \cos (\sin \theta) \tag{10}$$

$$g_2(u) = \sin (\sin \theta) \tag{11}$$

where $k_o x_o = 1$ (this means that the distance between the two point sources is small and has been chosen so that $k_o x_o = 1$).

The target position relative to the boresite is $\theta$. Since this is a computer simulation, the actual target position is inserted into the antenna functions to provide the amplitude weighting. With this information, $r_1$ and $r_2$ are calculated and fed into the estimator. The estimator to be used is equation (23) which, restated, is

$$\varepsilon = r_1 \sin (\sin \hat{\theta}) - r_2 \cos (\sin \hat{\theta}) \tag{23}$$

The error, $\varepsilon$, is calculated using the estimated target position $\hat{\theta}$, and the random numbers $r_1$ and $r_2$ (which are calculated using the actual target position $\theta$). The target position, estimated and actual, is always relative to boresite. If we assume that the radar boresite is pointing to the estimated target position $\hat{\theta}$, then for each observation $\hat{\theta} = 0$ and the resulting error, $\varepsilon$, contains information pertaining to the actual target position.

The error $\varepsilon$, which now contains the target position $\theta$ and a noise component is fed to the discriminator. Recall that the mean of the error $\varepsilon$ is equation (22) rewritten here as

$$\bar{\varepsilon} = \sin(\hat{u} - u)$$

$$= \sin(\sin\hat{\theta} - \sin\theta) \qquad (43)$$

If a 3 dB beam-width of 3 degrees is assumed, $\Delta\theta$, or the difference between boresite and the target will be a maximum of $\pm 1.5$ degrees. For small values of $\theta$, $\sin\theta \approx \theta$, therefore

$$\varepsilon = \sin(\hat{\theta}-\theta) \qquad (44)$$

If we assume that the boresight is pointing at the estimated target position, then

$$\varepsilon = -\sin\theta \qquad (45)$$

Equation (45) can be further reduced to

$$\varepsilon = -\theta \qquad (46)$$

For the range of $\theta$ chosen, the actual discriminator curve is shown in Figure 9.

Because of the assumptions made, $\theta$ in equation (46) is the same as $\Delta\theta$, the distance in degrees the boresite must move to be pointing at the target.

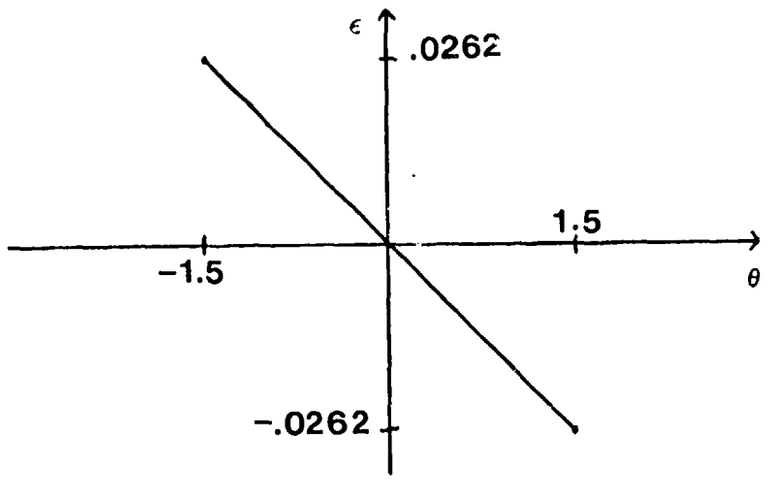


Fig. 9. Discriminator Curve Showing Maximum Values of $\varepsilon$ and $\theta$ or $\Delta\theta$

As stated before, the error is transformed into a corresponding $\Delta\theta$ by use of the discriminator curve. The error $\varepsilon$, fed to the discriminator is random due to the additive channel noise. The discriminator curve used represents the error without noise; therefore, the corresponding $\Delta\theta$ produced is also random.

The next step in the tracking loop is to input the target position $\theta$, or $\Delta\theta$, into the angle servo to steer the boresite to the target. The value used for $\Delta\theta$ will be constant during each observation interval; therefore, it can be modeled as a step input to the servo. The amplitude of the input to the servo after the next observation will reflect the change in the radar boresite as it moves closer to or away from the target. The input becomes a series of step functions whose amplitudes are proportional

to the distance the boresite must move (in either direction, $\pm\theta$) to the target.

The output of the servo will be delayed due to the inertia of the antenna and the drive motor, but it needs to be approximately equal to its input. The servo used should therefore provide a zero steady-state error for a step input.

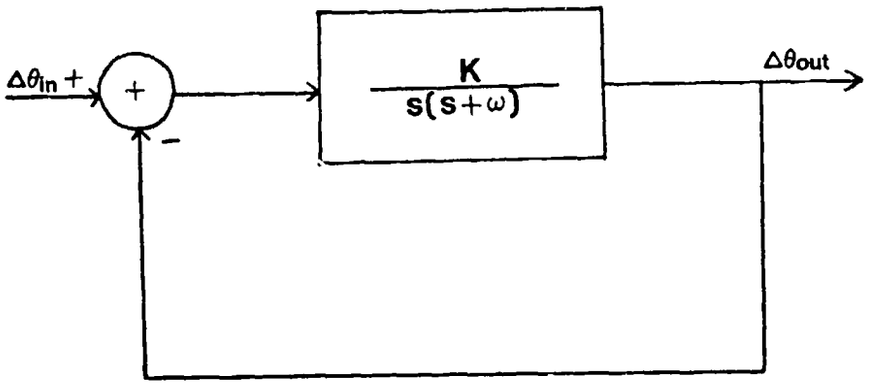


Fig. 10. Angle Servo Feedback Control Loop

Assume the angle servo has a feedback control loop as shown in Figure 10. The transfer function is

$$\frac{\Delta\theta_{out}}{\Delta\theta_{in}} = \frac{K}{s^2 + s\omega + K} \tag{47}$$

Equation (47) can be factored into

$$G(s) = \frac{K}{(s+\alpha)(s+\beta)} \tag{48}$$

Using (48) as the servo transfer function and assuming the input to the servo to be a step function $\Delta\theta(s) = \Delta\theta/s$, the servo output becomes

$$\Delta\theta/s \cdot G(s) = \frac{\Delta\theta K}{s(s+\alpha)(s+\beta)} \tag{49}$$

which has an inverse Laplace transform of

$$\frac{\Delta\theta K}{\alpha\beta} + \frac{\Delta\theta K(\beta e^{-\alpha t} - \alpha e^{-\beta t})}{\alpha\beta(\alpha-\beta)} \tag{50}$$

If we let $\alpha = -\sigma + j\omega$, $\beta = -\sigma - j\omega$ and $K = \alpha\beta$, then after some manupulation, equation (50) becomes

$$\Delta\theta'(t) = \Delta\theta[1-e^{-\sigma t}(\frac{\sigma}{\omega}\sin\omega t - \cos\omega t)] \tag{51}$$

The values of $\sigma$ and $\omega$ are obtained from the poles of the transfer function. The pole positions are chosen so that a value of $\sigma$ will damp the servo system response such that it will settle out without four system time constants. This settling time will give an output within 5 percent of the input value. The settling time is chosen to be a multitude of the PRI of the radar. The PRI used for the computer simulation is 1/200 pps or 5 ms.

Once an output $\Delta\theta'$ is obtained from the servo, it is used to steer the radar boresite. This is simulated by changing the antenna functions $g_1(u)$ and $g_2(u)$ to reflect the new target position. If there were no noise, the

boresite would point directly at the target after one pulse. Because of channel noise, however, the boresite will point close to the target after each pulse but never directly on it. The new (or adjusted) antenna functions produce a new error $\varepsilon$ which in turn produces a new $\Delta\theta$. This loop continues as the radar boresite tracks the target within some small error (MSE).

To begin the problem, a stationary target is tracked and the MSE is calculated. The stationary target is a simple case since in the routine the target position is initialized within the 3 dB beam-width and tracking it consists of maintaining the boresite on it.

To consider a moving target, a relationship between the target position, velocity, and range is needed. Figure 11 shows the geometry of the situation. The distance the target moves in the positive x direction is $V_T t$, where $V_T$ is the target velocity. $R_o$ is the range to the target at the point of acquisition and $R_T$ is the changing range to the target. Note that the target range $R_T$ and the SNR are inversely proportional. The changing SNR can be accounted for by using the radar range equation [Ref 1].

$$\text{SNR } R^4 = \frac{P_R G_R^2 \lambda^2 \sigma_T}{(4\Pi)^3 N} \qquad (52)$$

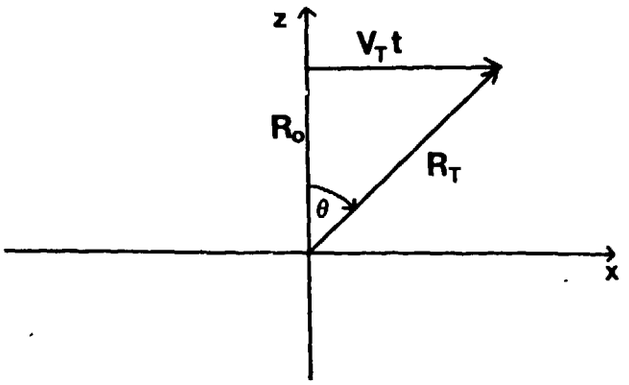


Fig. 11. Geometry Showing the Relationship Between Target Position, Velocity and Range

where $R$ = range to the target

$P_R$ = power received

$G_R$ = receiver gain

$\lambda$ = wavelength of carrier

$\sigma_T$ = target cross-section

$N$ = internal receiver noise power

For the problem at hand, the right side of equation (52) remains constant. If we let $SNR_o$ and $R_o$ be the initial SNR and target range and $SNR_T$ and $R_T$ be the new SNR and target range we have

$$SNR_o \, R_o^4 = \frac{P_R \, G_R^2 \, \lambda^2 \, \sigma_T}{(4\pi)^3 \, N} \tag{53}$$

and

$$SNR_T \, R_T^4 = \frac{P_R \, G_R^2 \, \lambda^2 \, \sigma_T}{(4\pi)^3 \, N} \tag{54}$$

Therefore

$$SNR_T \; R_T^4 = SNR_O \; R_O^4$$

and

$$SNR_T = SNR_O \left(\frac{R_O}{R_T}\right)^4 \tag{55}$$

Equation (55) can account for the changing SNR as the target range $R_T$ increases for a moving target.

$$\tan \theta_T = \frac{V_T t}{R_O}$$

$$\theta_T(t) = \tan^{-1}(V_T t / R_O) \tag{56}$$

With a relationship for $\theta_T$ as a function of velocity, time, and range, the target position can be accounted for in the computer simulation.

The Error

The tracking error for the stationary and non-stationary case is the difference between the radar bore-site and target position.

$$E_T = \theta_B - \theta_T \tag{57}$$

The simulation will take 50 observations which could consist of every pulse or every several pulses depending on the settling time chosen for the angle servo. Each set of 50 observations is considered a run. In each run a

"seed" is used to generate a vector of random numbers which are used to determine $n_1$ and $n_2$ which in turn are used to calculate $r_1$ and $r_2$. A different seed is used for each separate run and a new set of random data is generated. If equation (57) is squared for each observation and then averaged over the number of runs, an approximation of the MSE is obtained. For an example see Figure 12. In Figure 12a the value at observation 4 is summed over all the runs and then divided by the number of runs to obtain the MSE for that observation which is plotted in Figure 12b. If this is done for each observation, the approximate MSE is obtained for a single SNR level. Recall that an observation can be one pulse or a multiple of pulses.

The threshold or point of breaklock can be determined by observing when the MSE increases continually per observation. As the SNR is decreased, the plots of the MSE will look similar to Figure 13.

Since the beam-width is $\pm 1.5$ degree, an error $\varepsilon$ producing a $\Delta\theta$ greater or less than $\pm 1.5$ degrees will be automatically limited to $\pm 1.5$ degrees. The servo will then move the boresite its maximum limit and another observation will be made. If the error developed at this observation produces a $\Delta\theta$ again greater than the maximum, $\Delta\theta$ will automatically be limited again to $\pm 1.5$ degrees. The servo will not be able to keep up with the moving target to be able to track it. This is breaklock and can

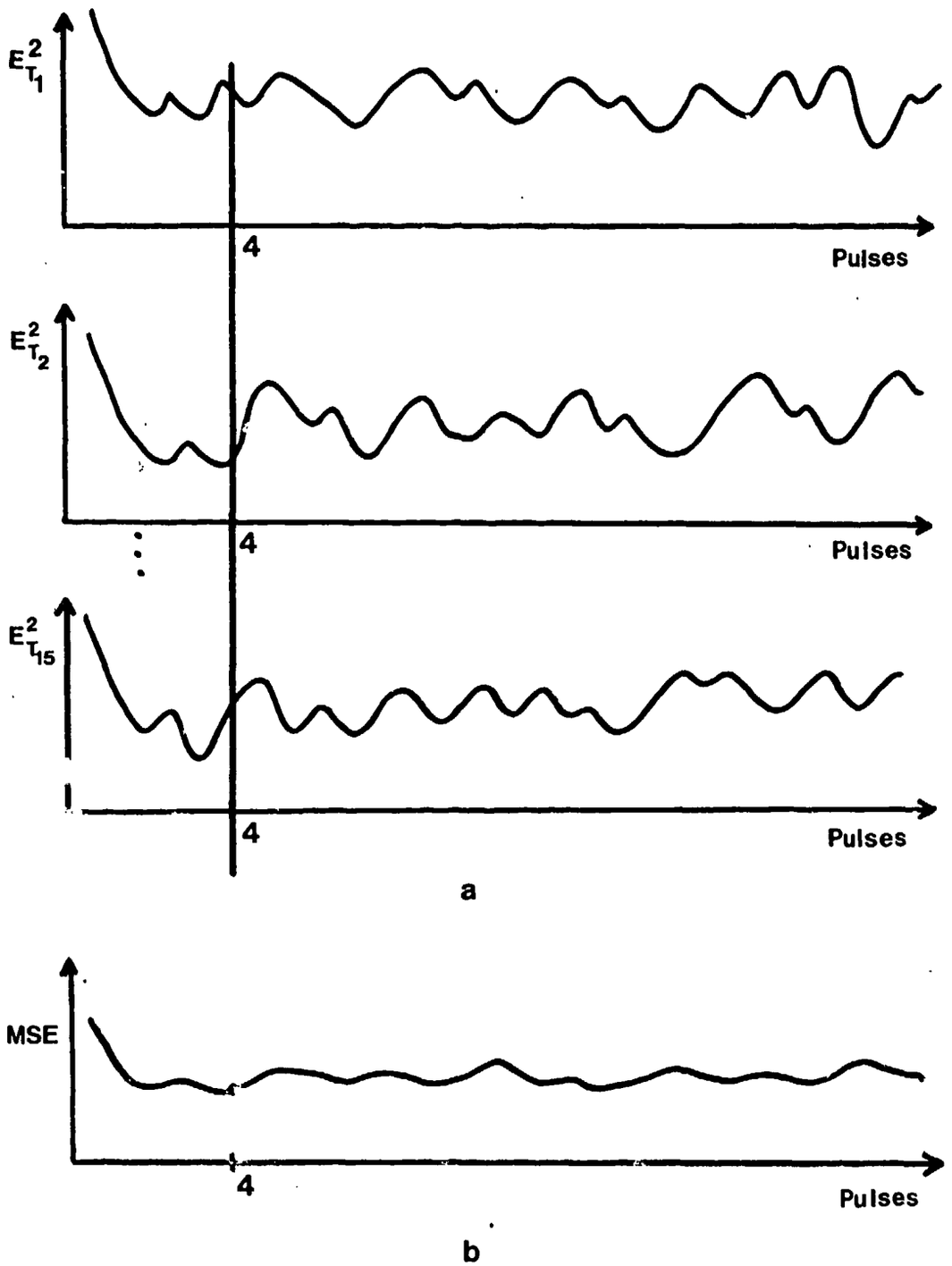


Fig. 12. (a) Example Plots of the Error Squared per Observation for One SNR Level; (b) Example Plot of the MSE per Observation for One SNR Level

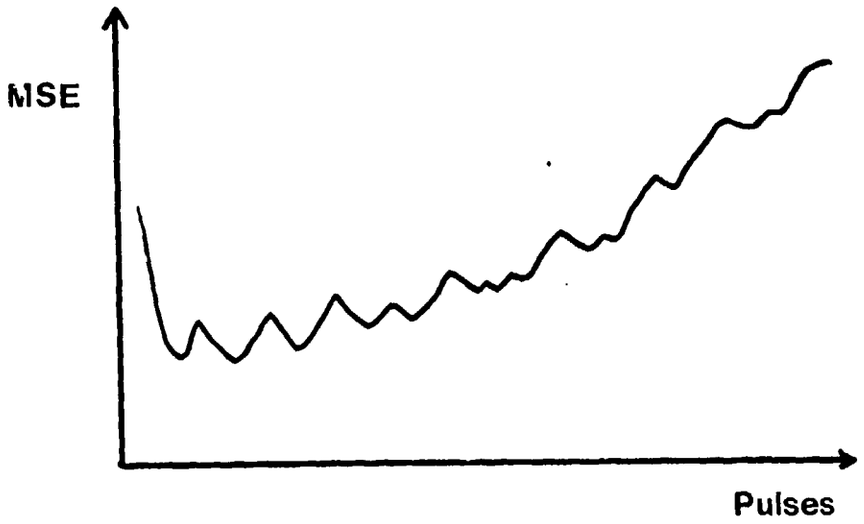


Fig. 13. Sketch of MSE Becoming Unbounded at Breaklock

be caused by a number of factors. The target velocity can be fast enough at a certain range to cause breaklock, the servo could be too slow to "catch up" to the target, or the SNR can degrade to a point where the threshold effect occurs. The velocity, range, and servo will be adjusted to prevent breaklock except at a low SNR.

## III. The Computer Program

The programs for the stationary and nonstationary target are straightforward. The only subroutines used were two IMSL subroutines, GGNML and MDNOR.

The program was designed so that the radar parameters such as PRI, servo settling time, and boresite position can be initiated at the beginning. The initial target position must be within ± 1.5 degrees of the boresite position.

The IMSL subroutine GGNML is called to generate a vector of random numbers to represent the noise components $n_1$ and $n_2$ of the observations $r_1$ and $r_2$. A vector of 100 random numbers is generated and two numbers are used for each observation. The program is set up for 50 observations but can be adjusted for any amount provided the random number vector is also adjusted. The random numbers $r_1$ and $r_2$ are then calculated using equations (14) and (15). The value for $\theta$ is calculated by subtracting the boresite position from the target position. It is then updated as the boresite is moved. Once an error is calculated from equation (23), it is converted to a $\Delta\theta$ by use of equation (24). This $\Delta\theta$ is used as input to the servo equation (51). The output of equation (51) is used to move the antenna.

This is simulated by changing $g_{\Sigma}(u)$ and $g_{\Delta}(u)$ to reflect the new difference between radar boresite and the target. For a moving target, equation (54) is used at this point to calculate the new target position. The SNR will change as the range from the radar to the target increases. This is accounted for in the program for the moving target. The boresite position is updated by adding the servo output to the old boresite position.

All of the above are accomplished for one observation. After this is done the tracking error is calculated by subtracting the target position from the boresite position. This value is squared and stored in a 50 column by 15 row array. The ZZ and CR bounds are also calculated at this point and stored in a similar array. After 15 runs, the columns of the array are summed and divided by the number of rows (15) to form the mean-square error per observation. The MSE is then plotted for 50 observations. The entire process is then repeated for a lower SNR level.

The SNR level was varied from 35 dB to -10 dB. The target velocity used was 609.6 meters/second. The servo settling time used was 100 milliseconds. The acquisition range was 6000 meters.

To calculate the ZZ bound, the IMSL subroutine MDNOR was called to evaluate the Q-function used to determine the probability of error.

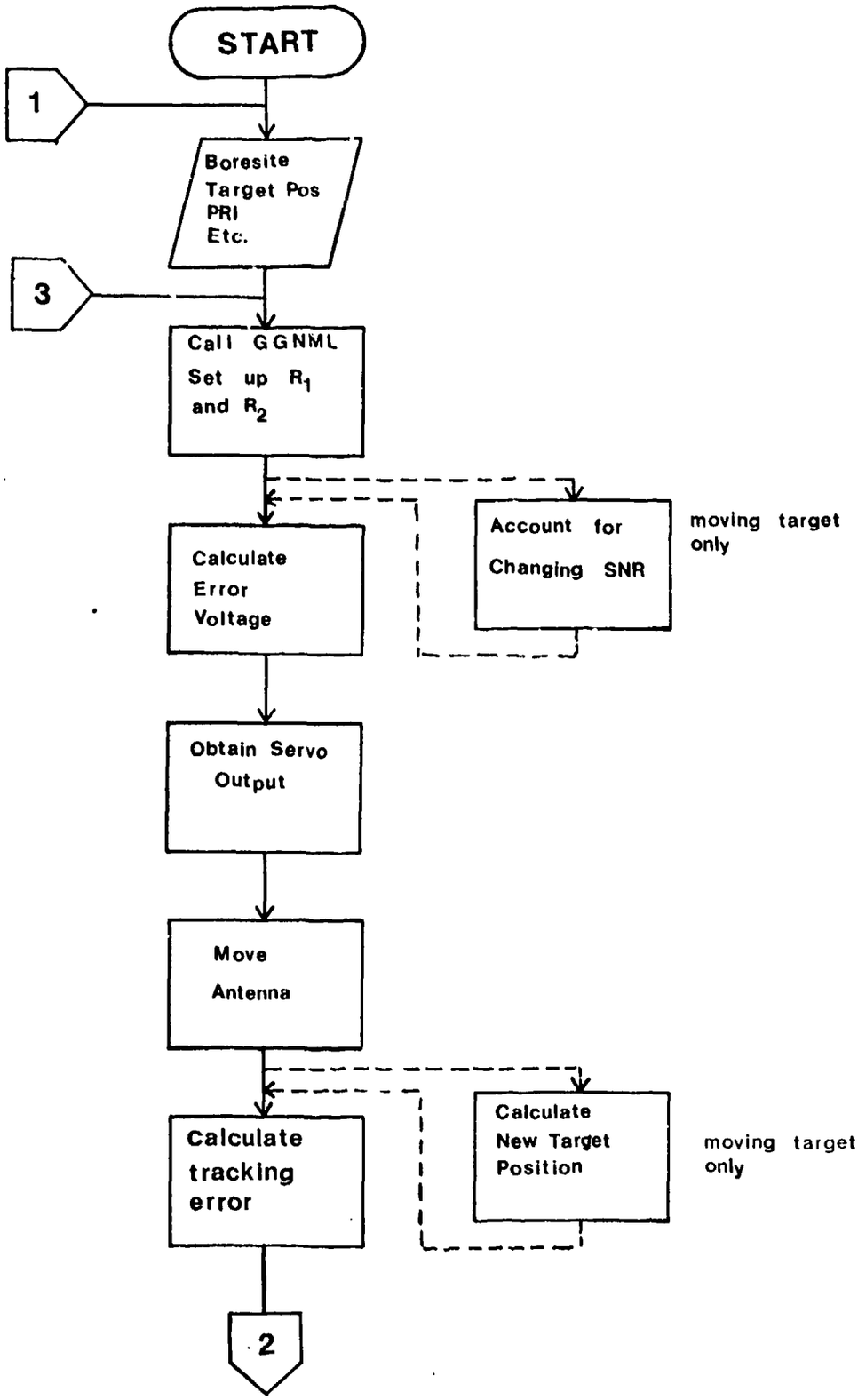


Fig. 14. Flow Diagram for Stationary/Nonstationary Target Tracking

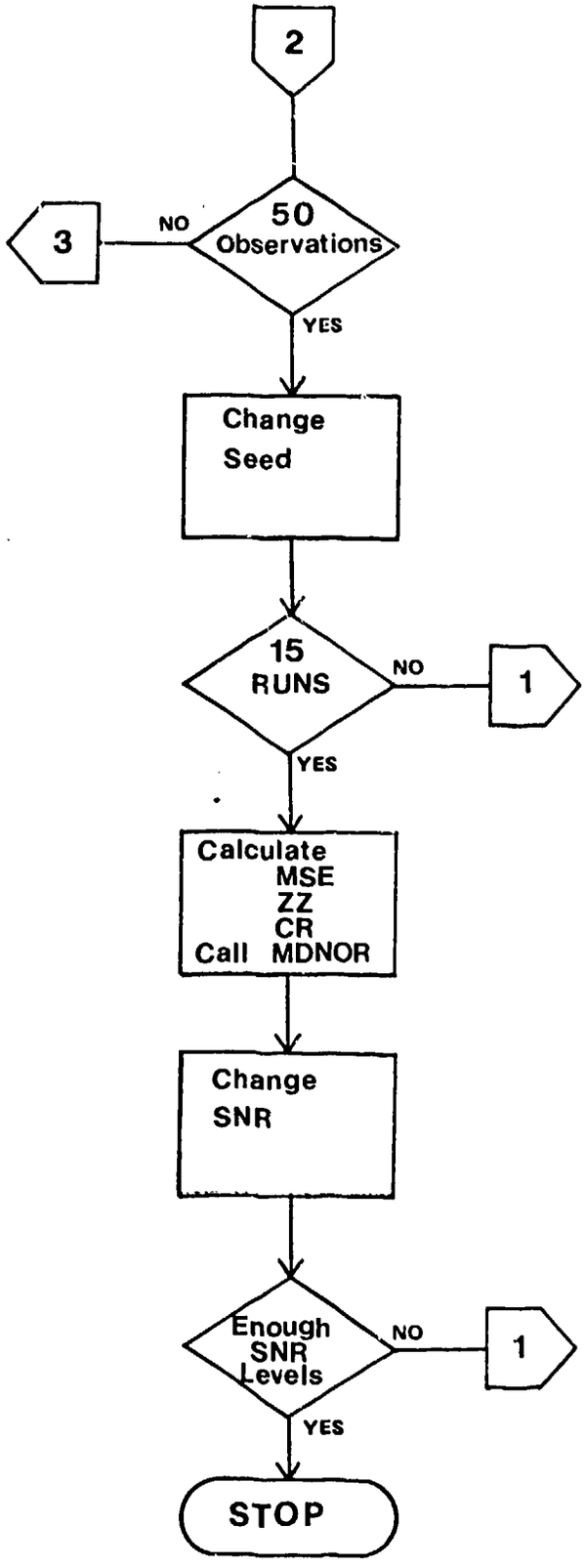


Fig. 14--Continued

# IV. Results and Conclusions

## General

The computer program was run for the stationary and the nonstationary target with the SNR varied from 35 dB to -10 db. For each SNR level, 15 runs were made taking 50 observations each. The MSE per observation was computed and plotted. In addition to the MSE, the Cramer-Rao and Ziv-Zakai bounds were calculated per observation and plotted (see Appendix B and C).

The object was to determine the point of breaklock and how the lower bounds can be used to quantify it.

## Stationary Target

As the SNR level was decreased, the MSE increased. It became increasingly difficult for the boresite to stay on target. The MSE became unbounded between -7 dB and -10 dB. Breaklock is assumed to have occurred here.

## Cramer-Rao Bound

As Figure 15 shows, the MSE at 7 dB is greater than the constant level of the CR bound. As the SNR was decreased the CR bound became very inaccurate. In Figure 16 the MSE is below the CR bound in some places. It appears that the CR bound is the average of the actual

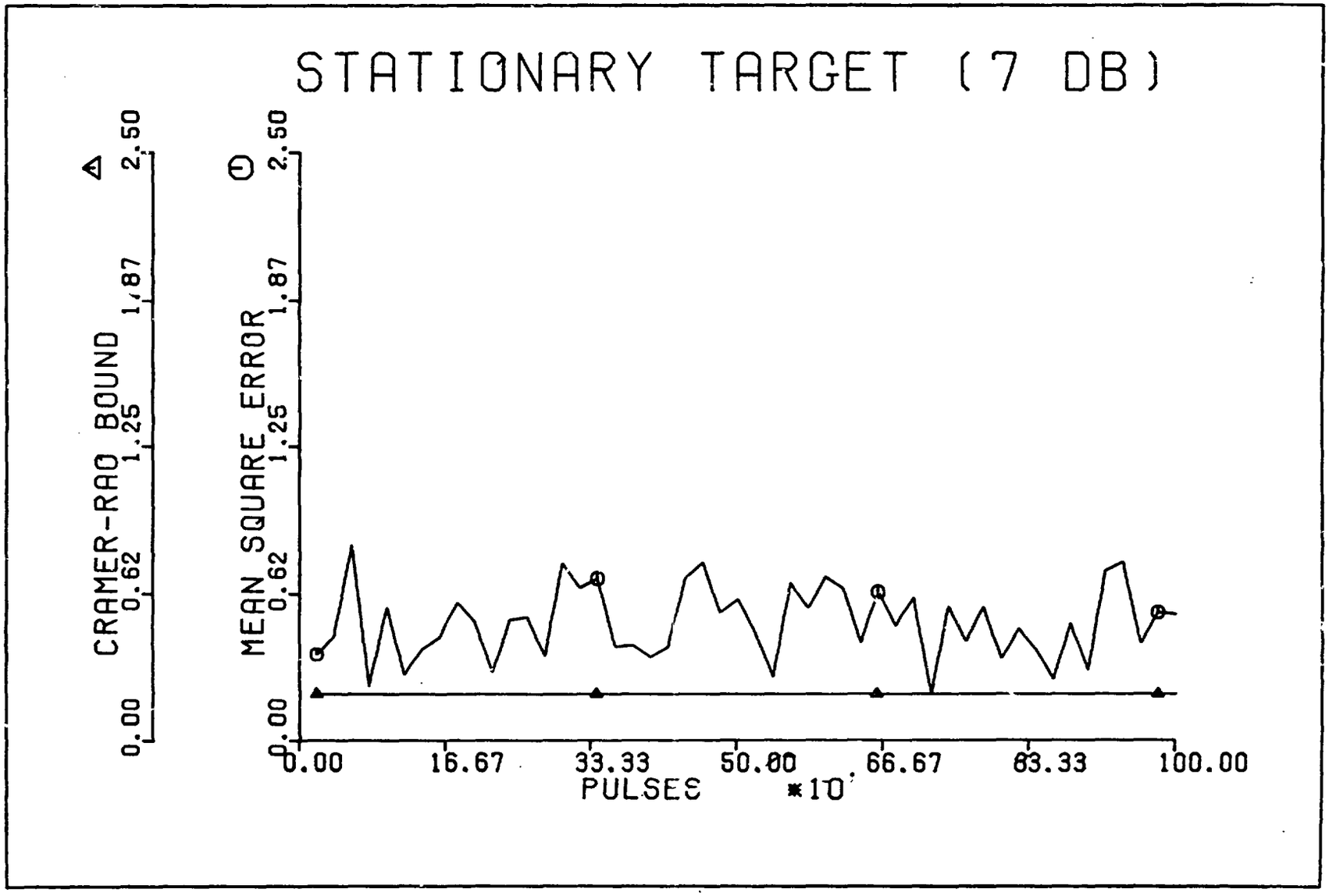


Fig. 15. Stationary Target (7 dB)

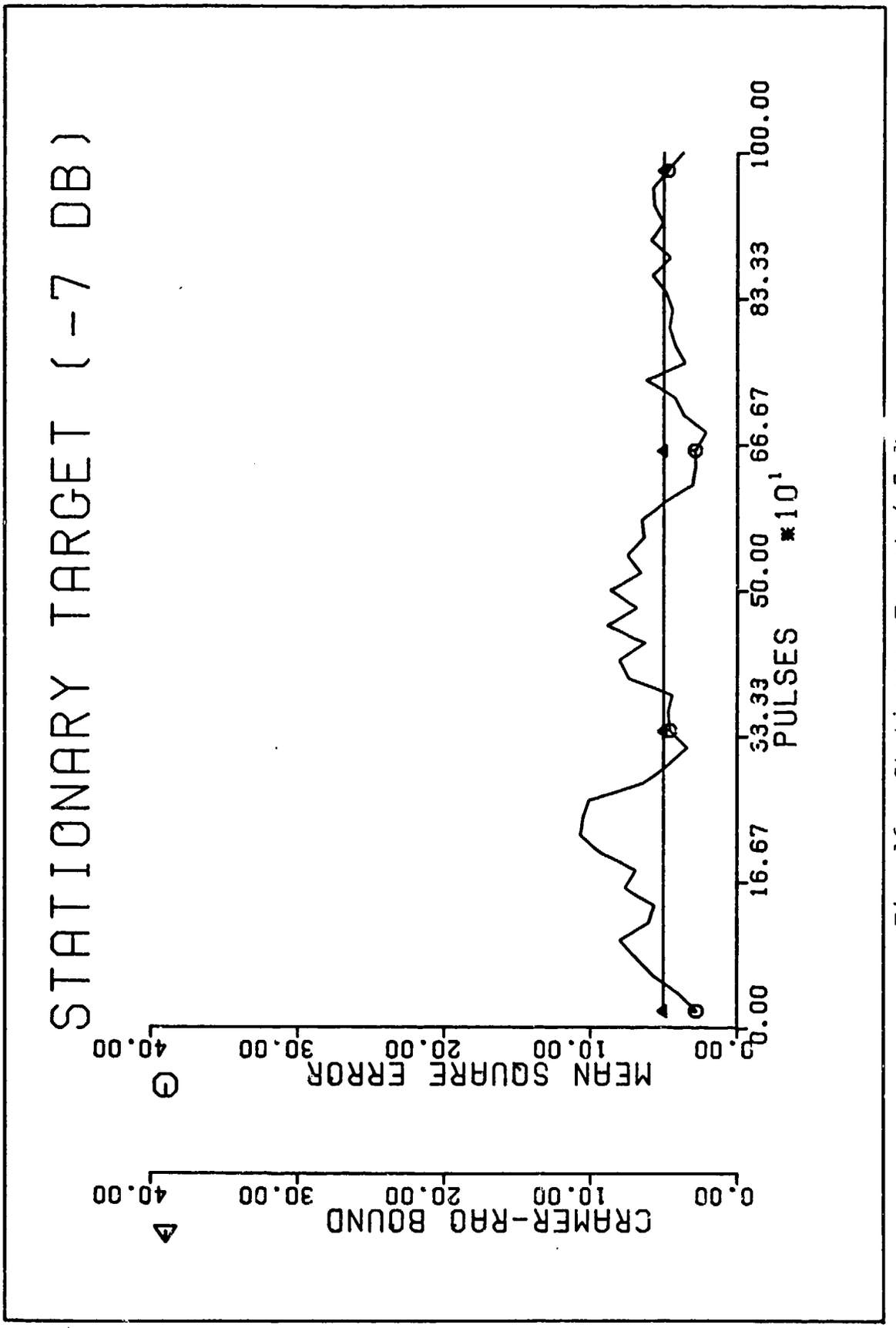


Fig. 16. Stationary Target (-7 d

MSE. But according to the definition of the lower bound, the MSE must always be greater than or equal to the lower bound. Figure 17 shows the MSE compared to the CR bound at -20 dB. The MSE is completely below the CR bound.

The Ziv-Zakai Bound

The ZZ bound for the stationary target tends to follow the general trend of the MSE. Note the large magnitude difference between the ZZ bound and the MSE (see Figure 18). The ZZ bound is the product of the $\sin^2 \theta$ and the $P(\varepsilon)$. Neither is ever greater than 1; therefore, the ZZ bound is never greater than 1. The importance of the ZZ bound in this case therefore is that it shows the trend of the MSE. Note in Figure 18 that the ZZ bound at many points has the same peaks and valleys as the MSE. In Figure 19 the MSE becomes unbounded. This trend is also shown in the ZZ bound.

Moving Target--Cramer-Rao Bound

Figures 20 and 21 show the MSE as compared to the CR bound. Breaklock occurs below 5 dB when the MSE becomes unbounded. The CR bound does not show any trend toward breaklock even at a very low SNR (Figure 21). The CR bound is generally constant with a slight upward trend toward the end of the run. This is due to the SNR decreasing as the target moves horizontally past the radar. The upward movement of the bound is not related to the actual MSE.

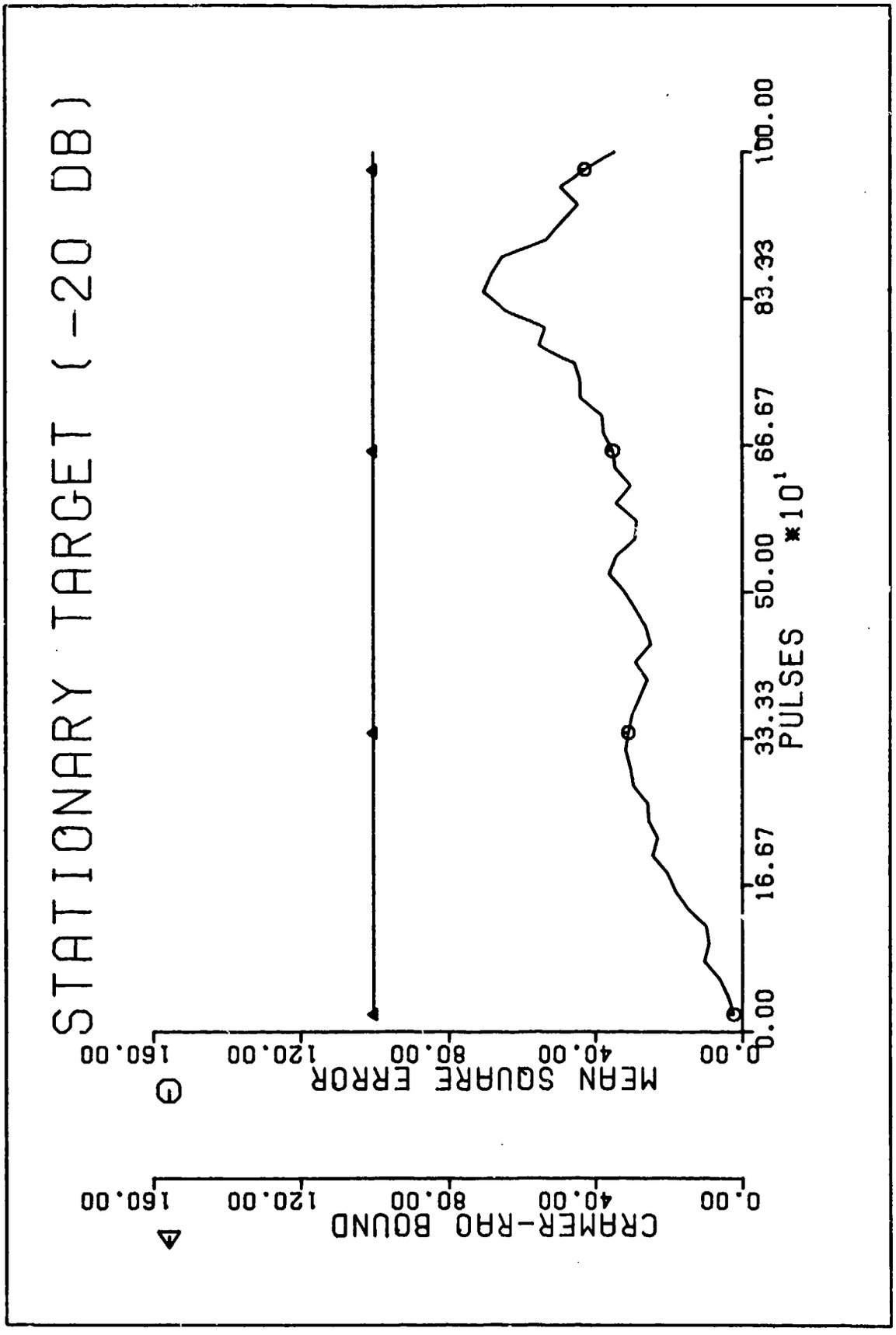


Fig. 17. Stationary Target (-20 dB)

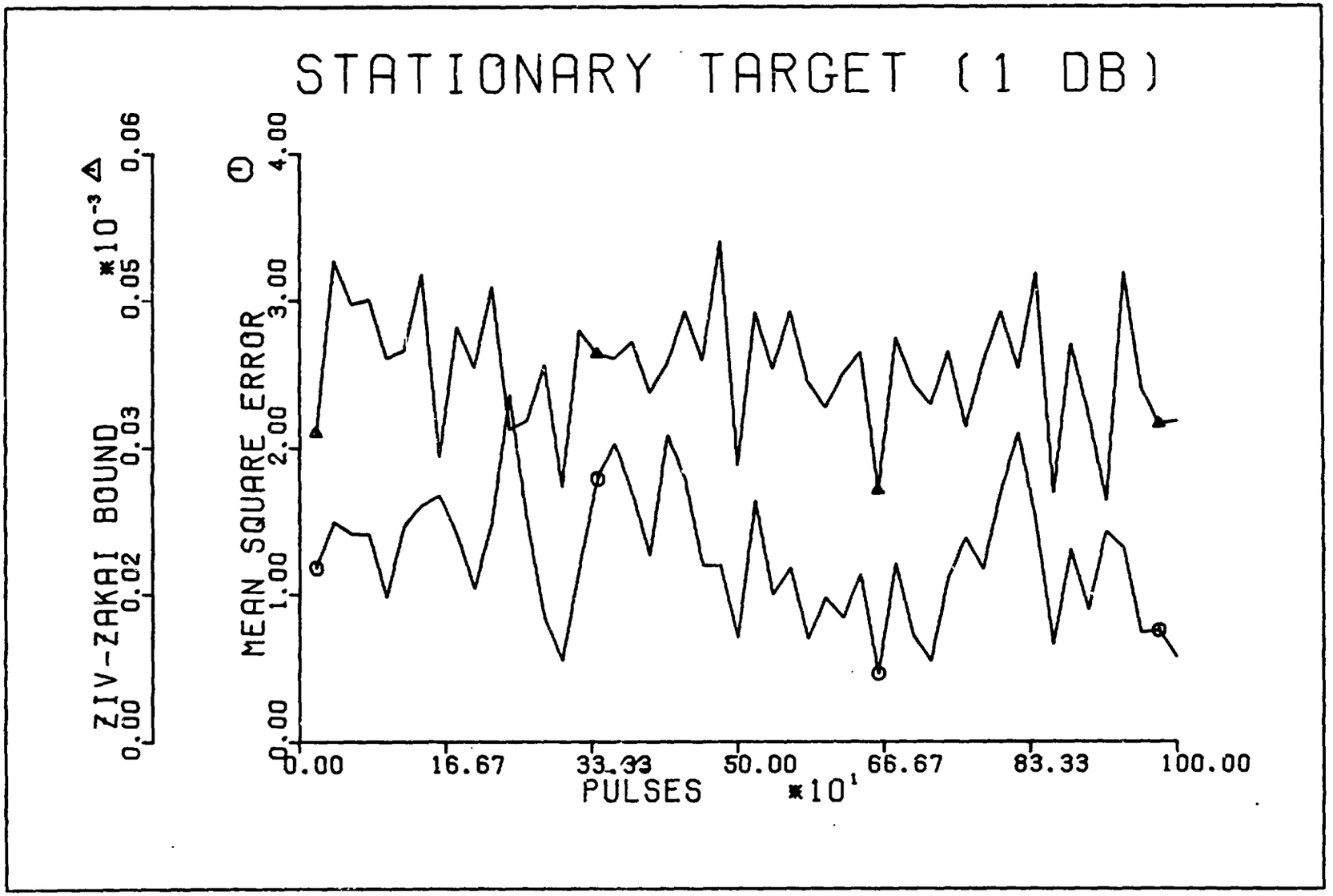


Fig. 18. Stationary Target (1 dB)

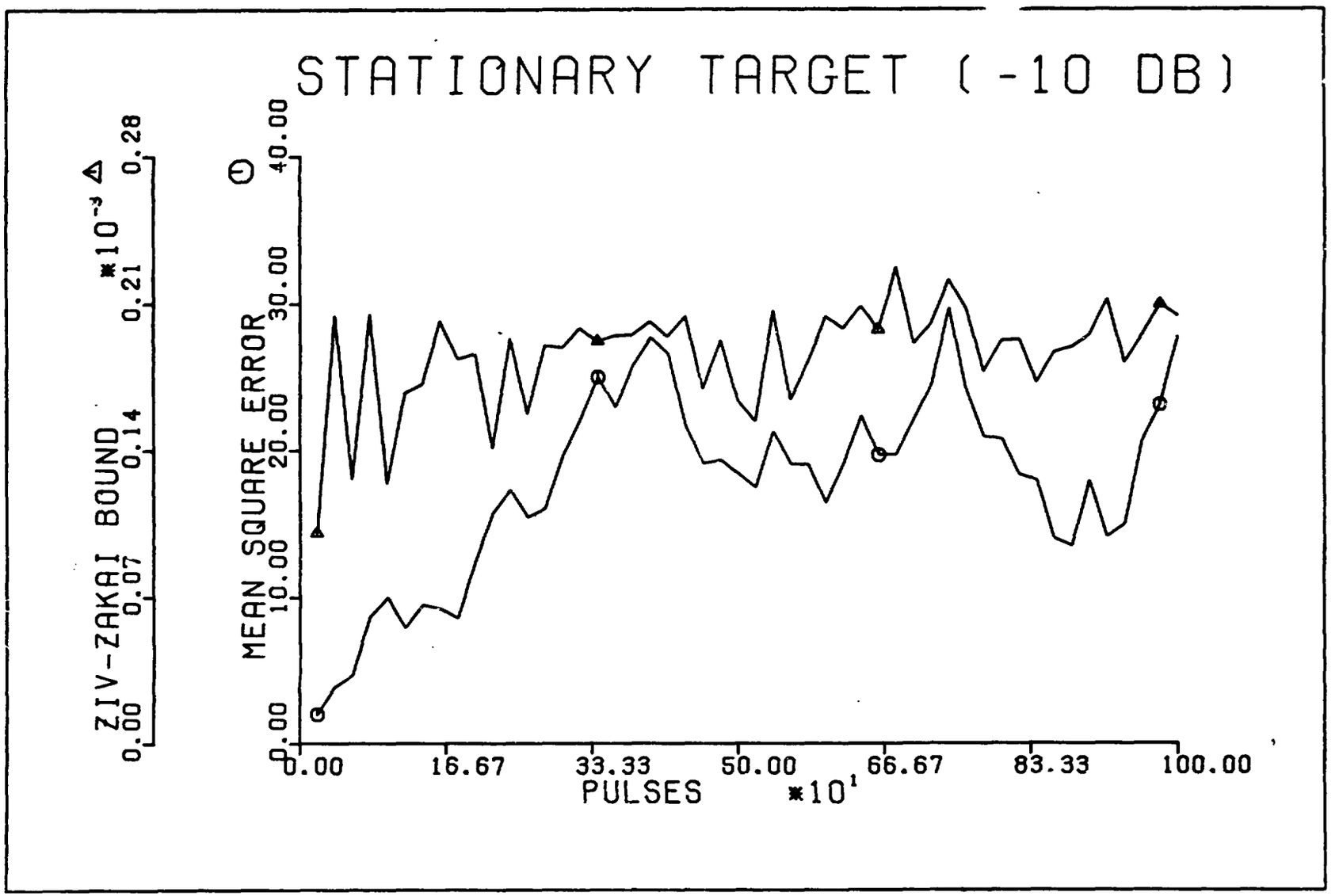


Fig. 19. Stationary Target (-10 dB)

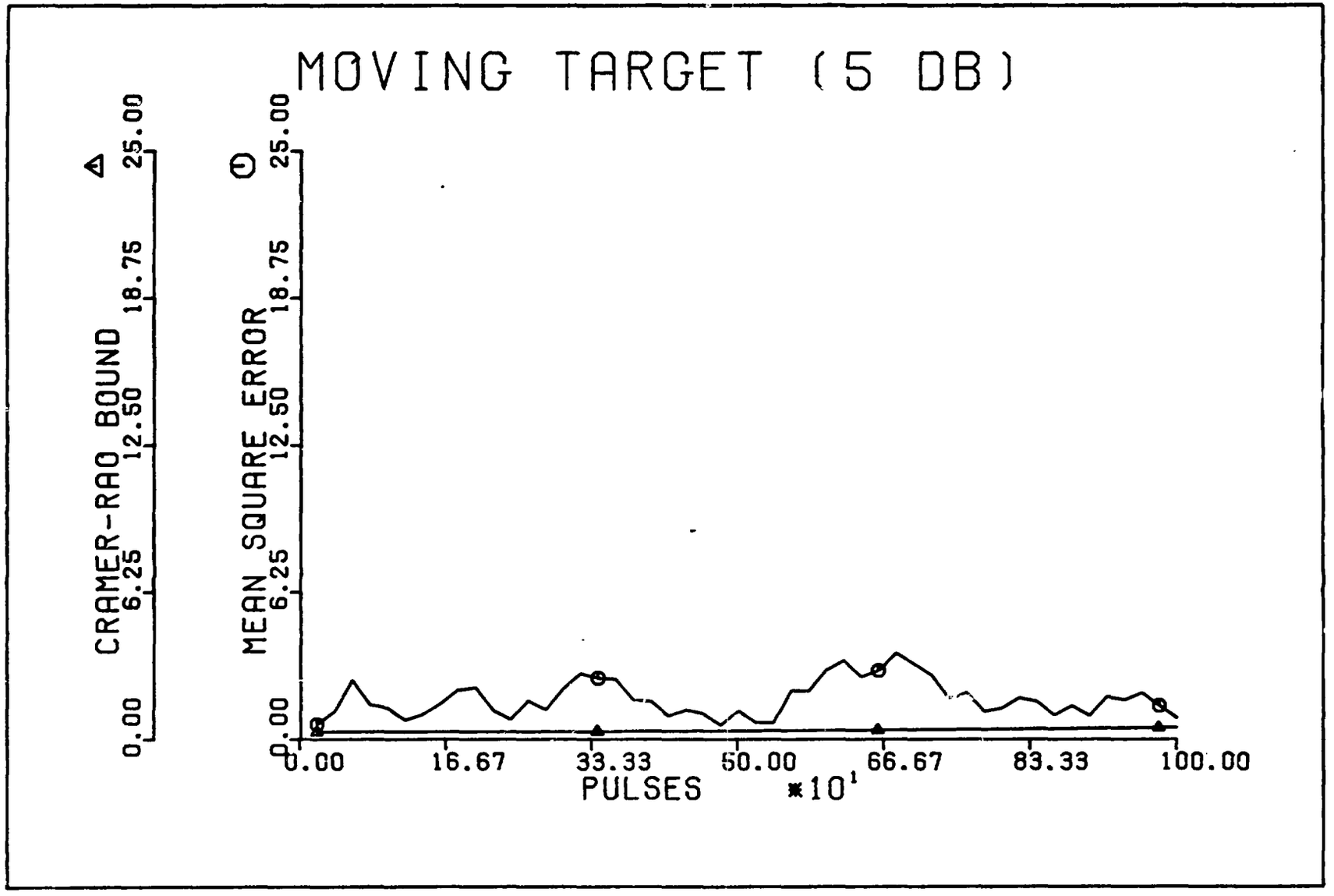


Fig. 20. Moving Target (5 dB)

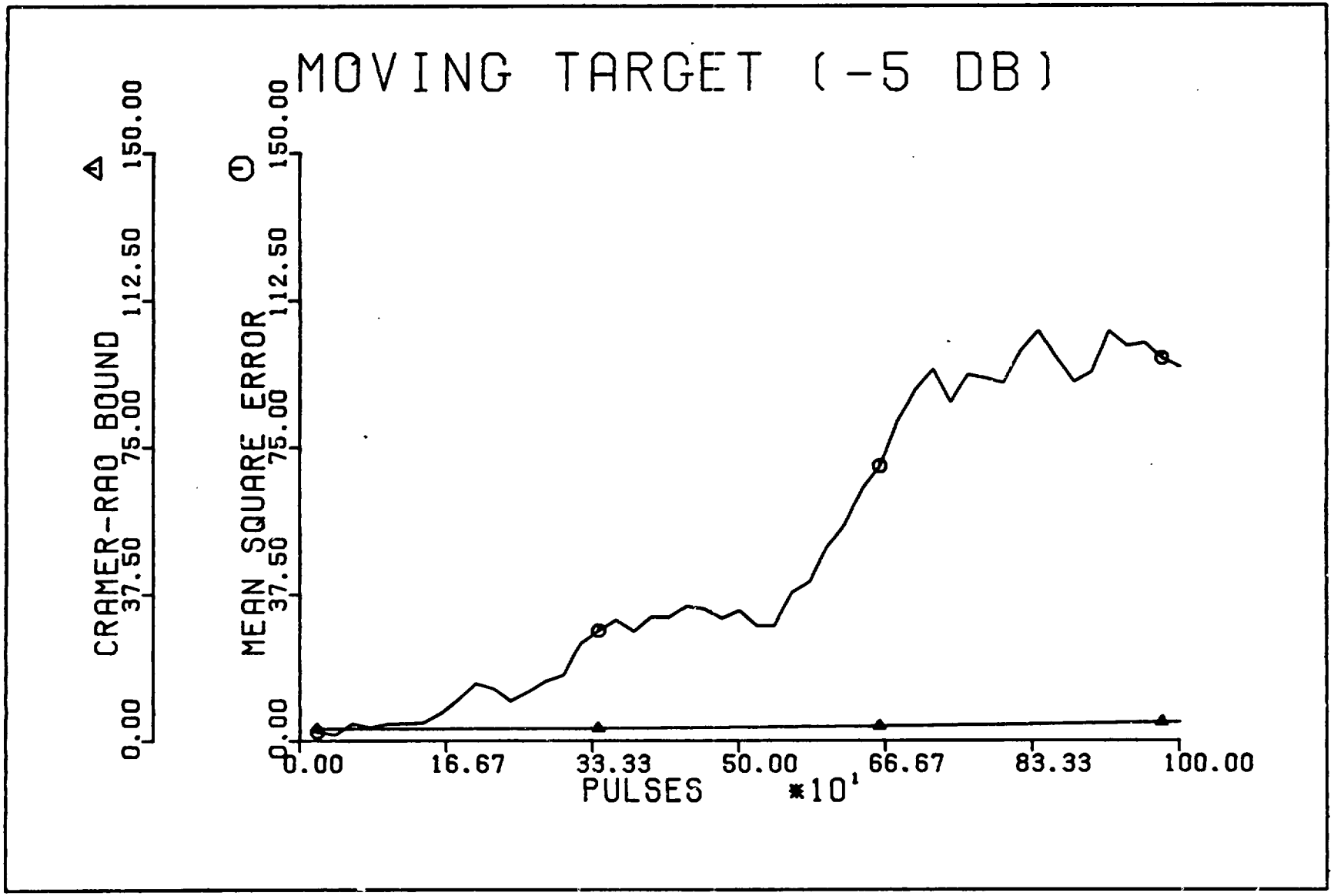


Fig. 21. Moving Target (-5 dB)

As the SNR is decreased, the CR bound tells us that the MSE is increasing but gives no indication when breaklock occurs.

Ziv-Zakai Bound

As in the stationary case, the ZZ bound follows the trend of the actual MSE. The ZZ bound becomes unbounded as the MSE becomes unbounded (Figures 22 and 23).

Among other reasons, the breaklock point occurs because of SNR level, the target range and speed, and the angle servo response time. The exact level of SNR for breaklock is not important here since it would depend on the parameters of an actual (not simulated) random system. What is important is that if these parameters were taken into account, the breaklock or threshold of an actual system could be predicted by the ZZ bound.

Ziv-Zakai Bound Compared to Cramer-Rao Bound

It is interesting to observe why the ZZ bound follows the actual MSE closer than the CR bound. The CR bound as stated in Chapter II is

$$\mathrm{Var}(\hat{\theta}) \geq \frac{1}{\mathrm{SNR}\cos^2\theta} \qquad (42)$$

The angle $\theta$ is the difference between the boresite and target position on the radar beam (i.e., the error). It is limited to $\pm 1.5$ degrees since the 3 dB

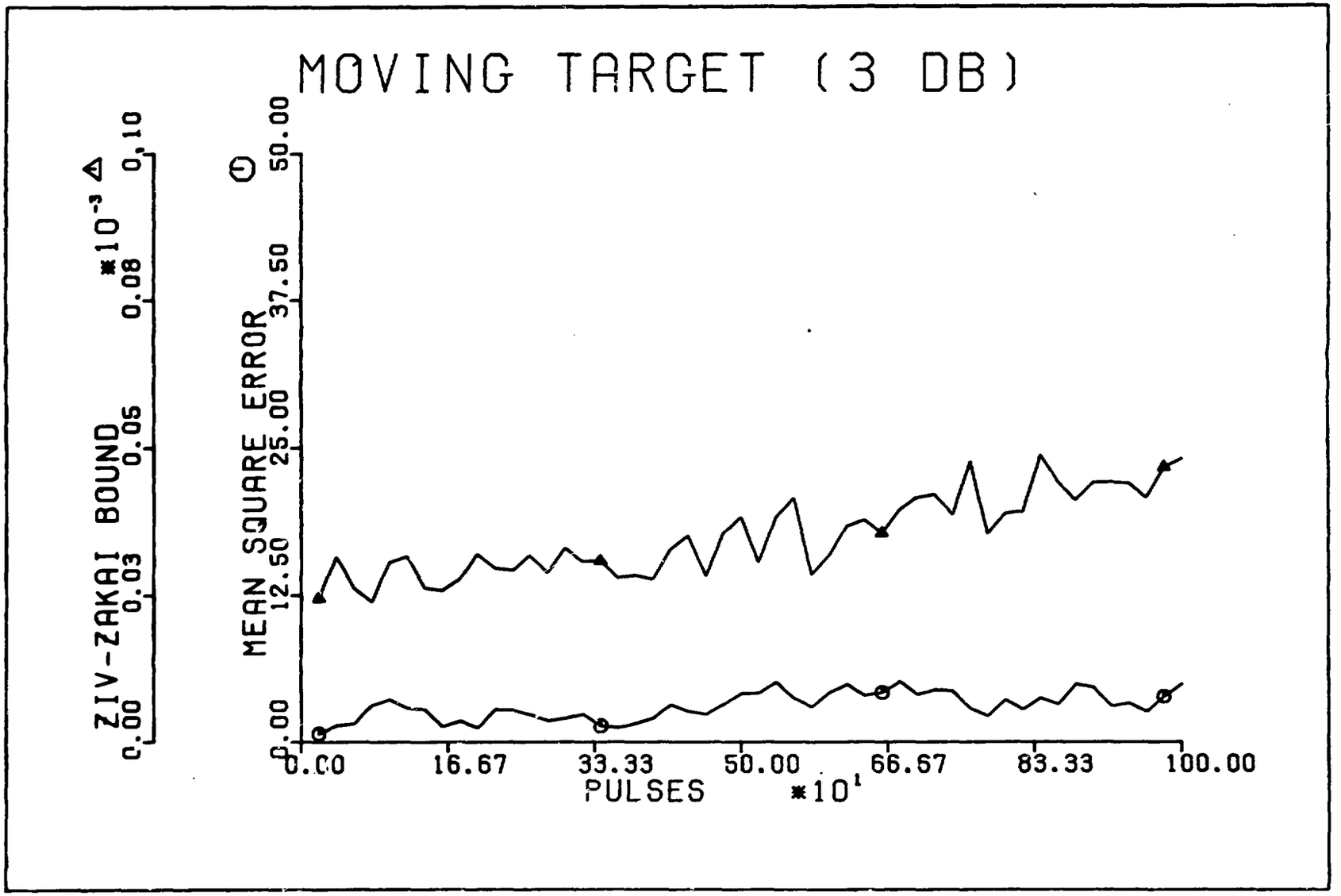


Fig. 22. Moving Target (3 dB)

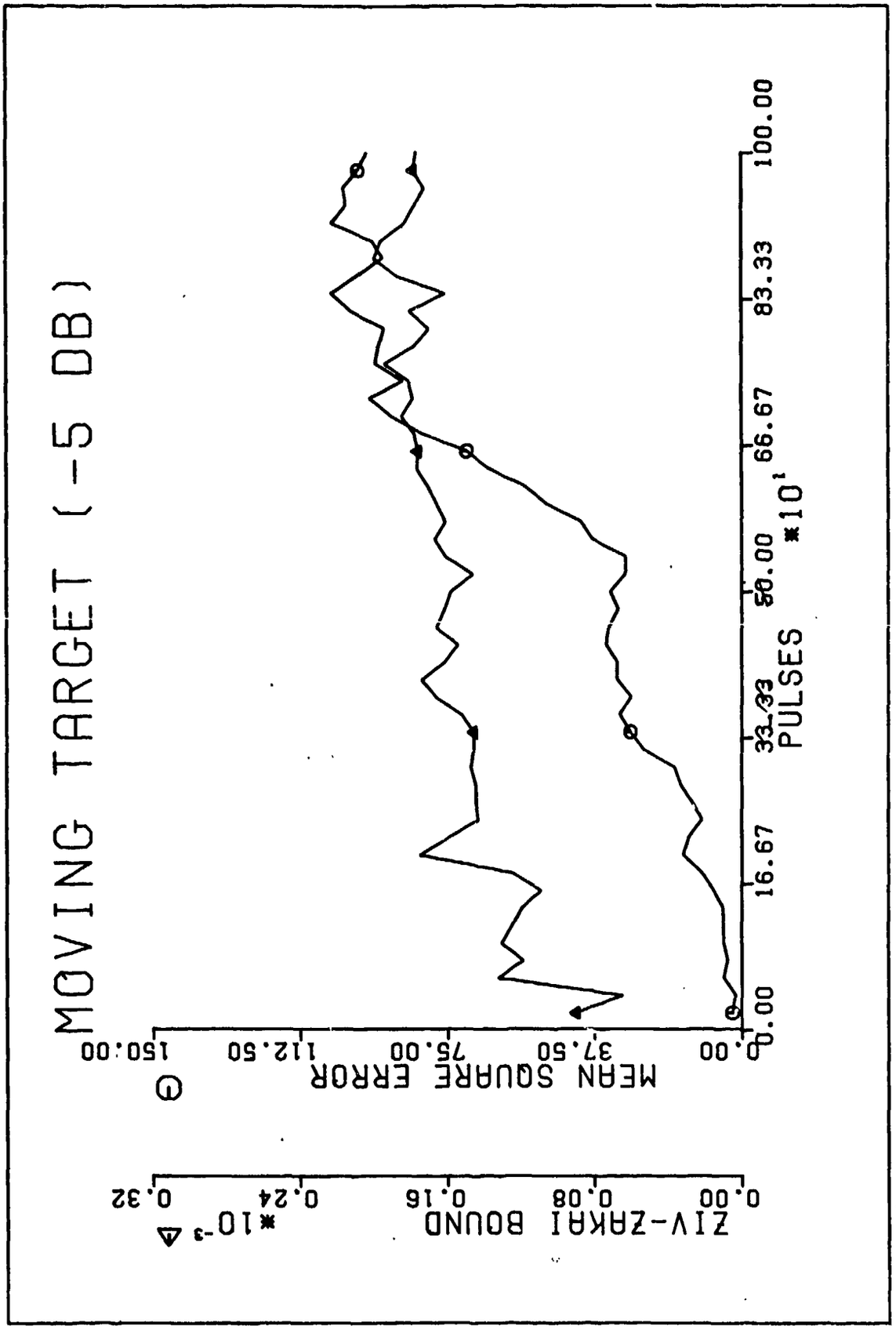


Fig. 23. Moving Target (-5 dB)

beam-width is 3 degrees. The cosine of a very small angle is approximately 1 so the CR bound is essentially constant for each SNR level (i.e., it is not influenced heavily by the error). On the other hand, the ZZ bound is

$$\varepsilon^2(\theta) \geq \sin^2 \theta Q[A(E/N_o(1-\cos 2u))^{\frac{1}{2}}] \qquad (41)$$

where $u = \sin \theta$ and $\theta$ is the target position relative to boresite.

The probability of error is related to the SNR level and is small for lage SNR and approaches 1 for small SNR. The factor that allows the ZZ bound to follow the general trend of the actual MSE is $\sin^2 \theta$ or $\theta^2$.

Since $\theta$ is the error between the boresite and target and is limited to $\pm 1.5$ degrees, $\sin^2 \theta = \theta^2$ which can be related to the mean-square error. Hence the ZZ bound is more prone to follow the actual MSE. Because of the tremendous magnitude difference between the ZZ bound and MSE, the ZZ bound does not give a good indication for a lower bound on the MSE. It could be possible, however, to scale the ZZ bound to the actual MSE and not only be able to predict its trend but a more accurate and realistic lower bound. More research would be required to develop a scaling factor.

The reason that $\theta$ is limited to $\pm 1.5$ degrees is because it has been assumed that there are no side lobes to the radar or that they are being neglected. Once the

target leaves the 3 dB beam-width it can no longer be tracked. However, if there exists a significant level of sidelobes, then $\theta$ could be limited to the angle of these sidelobes.

As a final conclusion it is necessary to observe what information the two bounds give as to how to keep the MSE small. In reference [2] it was concluded that the CR bound states that the variance is small for large SNR and narrow beam-width. It is smallest when the boresite is kept on the target. This can be seen from equation (42).

The $\cos^2\theta$ term is 1 when $\theta = 0$ which means the boresite is on the target. The $\cos^2\theta$ decreases as $\theta$ becomes larger, therefore increasing the variance. The ZZ bound has the same characteristics. The smaller $\theta$ is the smaller the MSE. The contribution of the probability of error is mainly due to the SNR level.

In communication theory, the correlation coefficient, $\rho$, is used to measure the similarities between two signals. If both signals are exactly the same, $\rho = 1$ and if they are opposite, $\rho = -1$ [Ref 11]. In this thesis the correlation coefficient is used in a slightly different manner. The correlation coefficient was determined to be $\rho = \cos 2u$ from equation (32a). The variable u is equal to $\sin\theta$ and for a small $\theta$, $\sin\theta \tilde{} \theta$ ; therefore, $\rho = \cos 2\theta$ . The angle $\theta$ is the target angle relative to the boresite. When the boresite is directly on the target, $\theta = 0$ and $\rho = 1$. As $\theta$

increases the correlation coefficient decreases. This means that for two targets symmetrically located on the radar beam, the resolution ability increases respectively with the separation angle $2\theta$. For the problem presented in this thesis there is only one target; however, there exists the possibility of a false target at its symmetrical opposite. By using the correlation coefficient, the error associated with detecting the target or its symmetrical opposite is accounted for in the error probability in equation (41).

Recommendations

The application of the ZZ bound to the mean-square tracking error has proven fruitful. It is well worth recommending an investigation of the two-dimensional case. Once the probability of error is determined, and a suitable two-dimensional inequality of the tchebycheff type is found, the ZZ bound for the covariance of the tracking error can be determined.

It is also recommended that an additional noise source be considered in the one- or two-dimensional case. The noise source can be a repeater jammer or chaff cloud. As the radar is tracking the target the noise source will expedite breaklock. The question of what noise power is needed to cause breaklock and how can the ZZ bound help in quantifying the MSE should be addressed.

Further recommendations are to consider actual servo parameters for the radar system and incorporate random target motion to simulate evasive action. Also an investigation of sidelobe structure for a typical monopulse radar would be an interesting addition to the tracking error.

## Bibliography


1. Barton, David K. Radar Systems Analysis. Englewood Cliffs, N.J.: Prentice Hall, 1964.

2. Cronk, Peter M. Model of a Tracking Radar in Terms of Non-Linear Second Order Phase Lock Loop. MS Thesis. Wright-Patterson AFB, Ohio: School of Engineering, Air Force Institute of Technology, December 1981.

3. D'Azzo, John J. and Constantine H. Houpis. Feedback Control System Analysis and Synthesis (second edition). New York: McGraw-Hill Book Company, 1966.

4. Helstrom, C. W. "The Resolution of Signals in White, Gaussian Noise," Proceedings of the IRE. 1111-1118. September 1955.

5. Hofstetter, Edward M. and Darrol F. Delong, Jr. "Detection and Parameter Estimation in an Amplitude-Comparison Monopulse Radar," IEEE Transactions on Information Theory, IT-15 (1): 22-30 (January 1969).

6. Melsa, James J. and David L. Cohn. Decision and Estimation Theory. New York: McGraw-Hill, 1978.

7. Savage, I. R. "Probability Inequalities of the Tchebycheff Type," Journal of Research NBS, Vol. 65-B: 211-222 (July-September 1961).

8. Seidman, Lawrence P. "Bearing Estimating Error with a Linear Array," IEEE Transactions on Audio and Electroacoustic, AU-19 (2): 147-157 (June 1971).

9. Seidman, Lawrence P. "Performance Limitations and Error Calculations for Parameter Estimation," Proceedings of the IEEE 58(5): 644-652 (May 1970).

10. Van Trees, Harry L. Detection, Estimation, and Modulation Theory. New York: Wiley, 1968-71.

11. Ziemer, R. E. and W. H. Trantor. Principles of Communications. Boston: Houghton Mifflin, 1976.

12. Ziv, Jacob and Moshe Zakai. "Some Lower Bounds on Signal Parameter Estimation," IEEE Transactions on Information Theory, ITT 15(3): 386-391 (May 1969).

## Appendix A

## The Two-Dimensional Monopulse Radar Model and the Two-Dimensional Ziv-Zakai Bound

### Introduction

An attempt was made to model the two-dimensional (2-D) Amplitude-Comparison monopulse radar and derive a 2-D ZZ bound. The ZZ bound used in this thesis was derived for a one-dimensional (azimuth) situation. To expand the bound to 2-D is not a simple task and, as will be shown, its complexity increases four-fold. The 2-D radar model is slightly more complex but not difficult.

Since it is simpler, the 2-D radar model is developed first with its resulting antenna functions. The antenna functions derived could be the source of some of the difficulties encountered in developing this approach. For example, they are no longer independent of each other. Each beam (sum and difference) in each dimension, contains both azimuth and elevation information. This result seems consistent with what would be expected from a two-dimensional system. The problem could arise from using the Gram-Schmidt orthogonalization procedure to describe the observations.

After the 2-D model is developed, the 2-D ZZ bound is discussed. The attempt to derive this bound was

abandoned due to two main obstacles encountered. Recommendations are also included as to what directions may be taken to overcome the obstacles.

The Two-Dimensional Radar Model

A 2-D Amplitude-Comparison monopulse radar consists of four antennas placed symmetrically in the x-z plane. As in the one-dimensional case, the antennas are considered point sources in an array. Figure A-1 shows a simple model of the 2-D case where antennas A and B are split into a sum and difference and likewise antennas C and D. This configuration produces one sum beam and two difference beams.

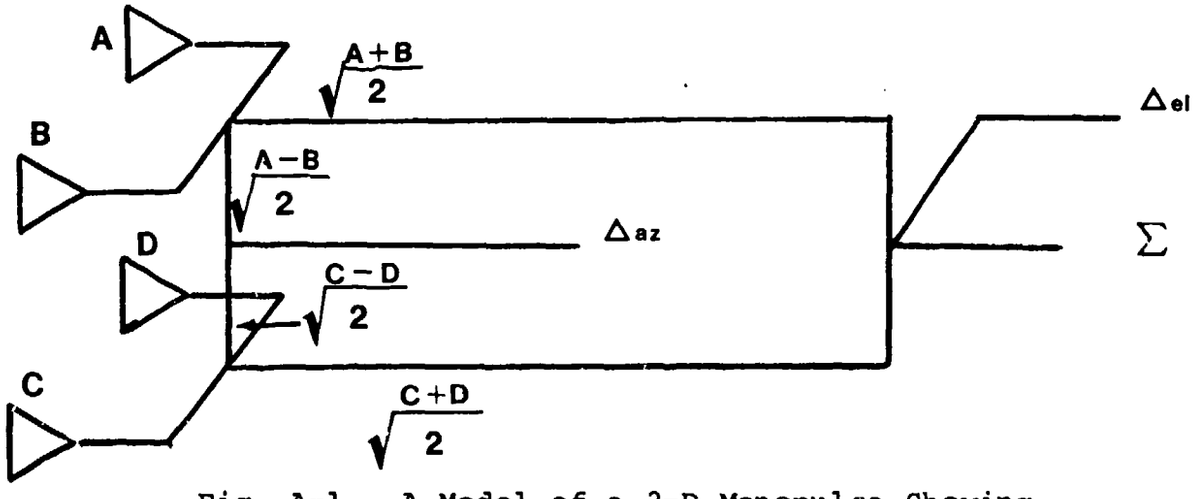


Fig. A-1. A Model of a 2-D Monopulse Showing Four Antennas and the Sum and Difference Beams

The azimuth difference beam is obtained by subtracting the difference of the four antennas and the elevation difference beam is obtained by subtracting their sums. The difference beams are

$$\Delta_{az} = \frac{A-B}{\sqrt{2}} - \frac{C-D}{\sqrt{2}}$$

$$= \frac{(A+D) - (B+C)}{\sqrt{2}} \qquad \text{(A-1)}$$

$$\Delta_{el} = \frac{(A+B) - (C+D)}{\sqrt{2}} \qquad \text{(A-2)}$$

The sum beam is obtained by adding the antenna sums.

$$\Sigma = \frac{(A+B) + (C+D)}{\sqrt{2}} \qquad \text{(A-3)}$$

The sum and difference beams can be used to derive the antenna functions. Assuming that the monopulse can be modeled as a 2-D array with four point sources, the approaching plane waves can be described as (see Figure A-2)

$$E_A = E_o e^{j\bar{K}_A \cdot \hat{r}} \qquad \text{(A-4)}$$

$$E_B = E_o e^{j\bar{K}_B \cdot \hat{r}} \qquad \text{(A-5)}$$

$$E_C = E_o e^{j\bar{K}_C \cdot \hat{r}} \qquad \text{(A-6)}$$

$$E_D = E_o e^{j\bar{K}_D \cdot \hat{r}} \qquad \text{(A-7)}$$

where $E_o$ is a constant.

$$\bar{K}_A = k_o(x\hat{x}+z\hat{z}) \qquad \bar{K}_B = k_o(-x\hat{x}+z\hat{z})$$

$$\bar{K}_C = k_o(-x\hat{x}-z\hat{z}) \qquad \bar{K}_D = k_o(x\hat{x}-z\hat{z})$$

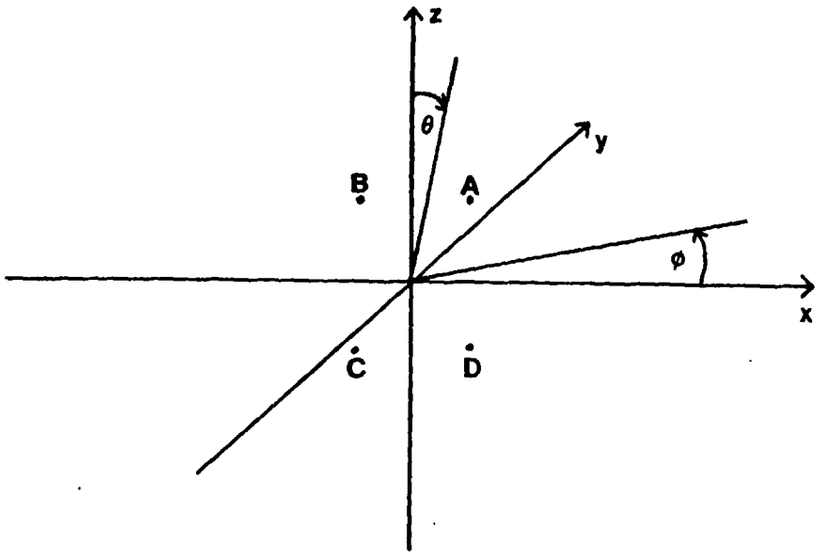


Fig. A-2. Coordinate System Showing Four Point Sources in an Array

and

$$\hat{r} = \hat{x} \sin\theta \cos\phi + \hat{y} \sin\theta \sin\phi + \hat{z} \cos\theta$$

Performing the dot product $\bar{K}\cdot\hat{r}$ in equations (A-4) through (A-7) gives

$$E_A = E_o \exp[jk_o(x \sin\theta \cos\phi + z \cos\theta)] \qquad (A-8)$$

$$E_B = E_o \exp[jk_o(-x \sin\theta \cos\phi + z \cos\theta)] \qquad (A-9)$$

$$E_C = E_o \exp[-jk_o(x \sin\theta \cos\phi + z \cos\theta)] \qquad (A-10)$$

$$E_D = E_o \exp[jk_o(x \sin\theta \cos\phi - z \cos\theta)] \qquad (A-11)$$

If we let $u = k_o x \sin\theta \cos\phi$ and $v = k_o z \cos\theta$ and use Euler's equation, the antenna functions can be

obtained by substituting equations (A-8) through (A-11) into (A-1) through (A-3). If the magnitude of the result is taken, the antenna functions are [Ref 8]

$$\Delta_{el} = 2\sqrt{2}\ E_o \cos u \sin v \qquad \text{(A-12)}$$

$$\Delta_{az} = 2\sqrt{2}\ E_o \sin u \cos v \qquad \text{(A-13)}$$

$$\Sigma = 2\sqrt{2}\ E_o \cos u \cos v \qquad \text{(A-14)}$$

By normalizing these functions, the final form of the antenna functions becomes

$$g_1(u,v) = \sin u \cos v \qquad \text{(A-15)}$$

$$g_2(u,v) = \cos u \sin v \qquad \text{(A-16)}$$

$$g_3(u,v) = \cos u \cos v \qquad \text{(A-17)}$$

A block diagram of the model can now be shown. Figure A-3 shows the output of the four antennas (target return) being weighted by the three antenna functions. White gaussian channel noise is added to the weighted target returns to form the observations $r_1(t)$, $r_2(t)$, and $r_3(t)$. The same assumptions apply to the WGN as did in the one-dimensional case.

In order to use the observations to obtain a maximum likelihood estimate of the azimuth and elevation angles, the Gram-Schmidt orthogonalization procedure is used as before with the one-dimensional case. The vector observations are therefore

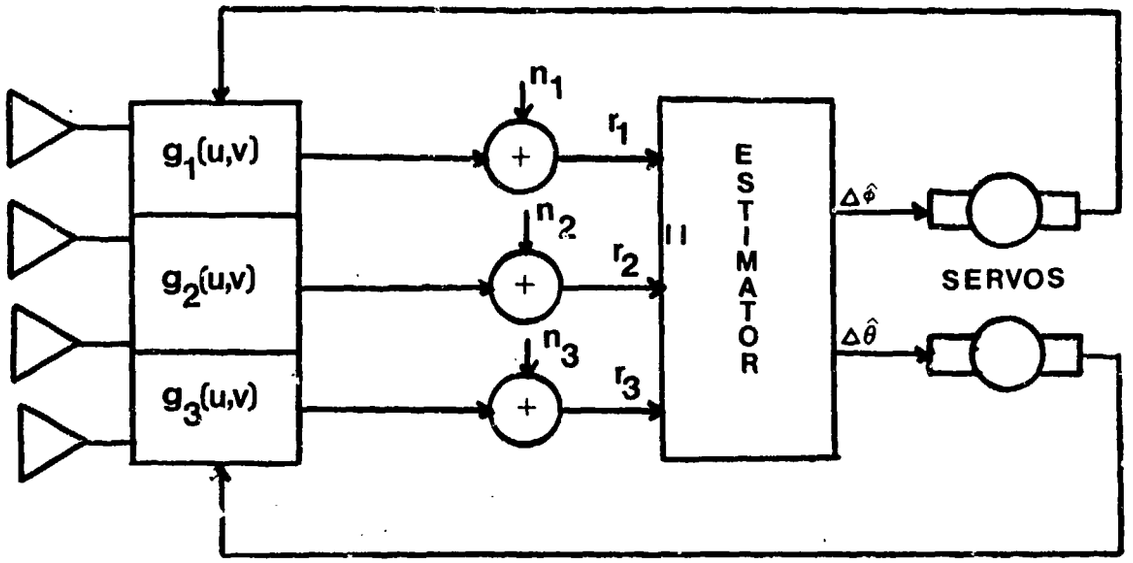


Fig. A-3. Block Diagram of the Two-Dimensional Radar Model

$$r_1 = A\sqrt{E}\, g_1(u,v) + n_1 \qquad \text{(A-18)}$$

$$r_2 = A\sqrt{E}\, g_2(u,v) + n_2 \qquad \text{(A-19)}$$

$$r_3 = A\sqrt{E}\, g_3(u,v) + n_3 \qquad \text{(A-20)}$$

The mean and variance of these vectors are

$$E\{r_1/A,u,v\} = A\sqrt{E}\, g_1(u,v);\ \mathrm{Var}(r_1/A,u,v) = N_o/2 \qquad \text{(A-21)}$$

$$E\{r_2/A,u,v\} = A\sqrt{E}\, g_2(u,v);\ \mathrm{Var}(r_2/A,u,v) = N_o/2 \qquad \text{(A-22)}$$

$$E\{r_3/A,u,v\} = A\sqrt{E}\, g_3(u,v);\ \mathrm{Var}(r_3/A,u,v) = N_o/2 \qquad \text{(A-23)}$$

The joint pdf is again the product of the individual pdfs.

$$p(r_1 r_2/A,u,v) = \left(\frac{1}{2\pi\, N_o/2}\right)^{3/2}$$

$$\exp\left\{\frac{-1}{2(N_o/2)}\left[(r_1 - A\sqrt{E}g_1)^2 + (r_2 - A\sqrt{E}g_2)^2 + (r_3 - A\sqrt{E}g_3)^2\right]\right\} \qquad \text{(A-24)}$$

The maximum likelihood estimate is obtained by finding [Ref 6]

$$\frac{\partial \ell n}{\partial A} p(r_1 r_2 r_3 / A, u, v) = 0$$

$$\frac{\partial \ell n}{\partial u} p(r_1 r_2 r_3 / A, u, v) = 0$$

$$\frac{\partial \ell n}{\partial v} p(r_1 r_2 r_3 / A, u, v) = 0$$

Let $$\frac{\partial g_i}{\partial u}(u,v) = \dot{g}_i = \frac{\partial g_i}{\partial v}(u,v)$$

for notational purposes.

The steps to obtain the maximum likelihood estimate are the same as in the one-dimensional case. The result for the A estimate is

$$\hat{A} = \frac{r_1 g_1 + r_2 g_2 + r_3 g_3}{\sqrt{E}(g_1^2 + g_2^2 + g_3^2)} \qquad \text{(A-25)}$$

The general error equation is

$$\begin{aligned} & r_1(g_1 g_2 \dot{g}_2 + g_1 g_3 \dot{g}_3 - g_2^2 \dot{g}_1 - g_3^2 \dot{g}_1) \\ + & r_2(g_1 g_2 \dot{g}_1 + g_2 g_3 \dot{g}_3 - g_1^2 \dot{g}_2 - g_3^2 \dot{g}_2) \\ + & r_3(g_1 g_3 \dot{g}_1 + g_2 g_3 \dot{g}_2 - g_1^2 \dot{g}_3 - g_2^2 \dot{g}_3) = 0 \end{aligned} \qquad \text{(A-26)}$$

The partial derivatives of the antenna functions are

$$\frac{\partial g_1}{\partial u} = -\sin u \sin v\, du \text{ and } \frac{\partial g_1}{\partial v} = \cos u \cos v\, dv \quad \text{(A-27 a,b)}$$

$$\frac{\partial g_2}{\partial u} = \cos u \cos v\, du \text{ and } \frac{\partial g_2}{\partial v} = -\sin u \sin v\, dv \quad \text{(A-28 a,b)}$$

$$\frac{\partial g_3}{\partial u} = -\sin u \cos v\, du \text{ and } \frac{\partial g_3}{\partial v} = -\cos u \sin v\, dv \quad \text{(A-29 a,b)}$$

Substituting these into equation (A-26) yields

$$\varepsilon_1 = \sin \hat{u} \cos^2 v(r_1 \sin v + r_3 \cos v) - r_2 \cos \hat{u} \cos v \quad \text{(A-30)}$$

$$\varepsilon_2 = \sin \hat{v} \cos^2 u(r_2 \sin u + r_3 \cos u) - r_1 \cos u \cos \hat{v} \quad \text{(A-31)}$$

$\varepsilon_1$ and $\varepsilon_2$ represent the error equations for azimuth and elevation. Note that both equations contain azimuth and elevation information.

The expected values of $\varepsilon_1$ and $\varepsilon_2$ are

$$\bar{\varepsilon}_1 = A\sqrt{E} \cos^2 v \sin(\hat{u} - u) \quad \text{(A-32)}$$

$$\bar{\varepsilon}_2 = A\sqrt{E} \cos^2 u \sin(\hat{v} - v) \quad \text{(A-33)}$$

With these results it can be seen that if $\hat{u} = u$ then $\bar{\varepsilon}_1 = 0$ and if $\hat{v} = v$, $\bar{\varepsilon}_2 = 0$. If u represented an azimuth bearing and v represented an elevation bearing, these two equations could be used separately to steer the radar in

each dimension. However, recall that $u = k_o x \sin\theta \cos\phi$ and $v = k_o z \cos\theta$. A change in u will effect v and vice versa.

From this point on it becomes clear that the 2-D case is not simple and straightforward. Equations (A-32) and (A-33) are not independent of each other. Not only will there be a variance of $\varepsilon_1$ and $\varepsilon_2$ but also a covariance.

The error equation for the one-dimensional case described a two-dimensional discriminator curve (i.e., for an error $\varepsilon$ a $\Delta\theta$ was obtained). The error equations in the 2-D case describe a three-dimensional discriminator curve. For each value of v in equation (A-32), there is a 2-D discriminator curve which yields a $\Delta u$ for every $\varepsilon_1$. Likewise, in equation (A-33), for each value of u there is a 2-D curve that yields a $\Delta v$ for every $\varepsilon_2$.

The variables u and v represent the actual target position, whereas $\hat{u}$ and $\hat{v}$ represent an estimate of the target position. For computer simulation purposes, the values of u and v are known and will therefore determine what curve in (A-32) and (A-33) to use. The actual error, however, will be derived from equations (A-30) and (A-31) and the resulting $\varepsilon_1$ and $\varepsilon_2$ are applied to (A-32) and (A-33) to obtain $\Delta u$ and $\Delta v$. The $\Delta u$ and $\Delta v$ obtained will theoretically drive the boresite to the target. Because of WGN, the boresite will not point directly at the target.

Instead it will be within some variance (or covariance) of the actual position. A new error will develop for each observation which results in steering the boresite closer to the target.

The input to the azimuth and elevation servo must be in the form of $\Delta\phi$ and $\Delta\theta$. To derive these values note that

$$\Delta u = k_o \, x \, \sin\theta \cos\phi \tag{A-34}$$

and

$$\Delta v = k_o \, z \cos\theta \tag{A-35}$$

If we let $k_o x = k_o z = 1$ we have two equations and two unknowns. $\Delta u$ and $\Delta v$ are known quantities obtained from the discriminator curves. The values for $\Delta\theta$ and $\Delta\phi$ are

$$\Delta\theta = \cos^{-1}(\Delta v) \tag{A-36}$$

$$\Delta v = \cos^{-1}(\Delta u / \sin(\cos^{-1}(\Delta v))) \tag{A-37}$$

Since $\theta$ and $\phi$ are the difference between boresite and target, $\theta = \Delta\theta$ and $\phi = \Delta\phi$.

With this information a tracking loop can be implemented. The tracking error in azimuth and elevation can be computed. Recall that both error equations contain azimuth and elevation information. It should also be noted that the results for $\Delta\theta$ and $\Delta\phi$ are dependent. Besides a separate error for azimuth and elevation, a combined error needs to be developed.

This appears to be intuitively consistent with what one would expect from a two-dimensional Amplitude-Comparison monopulse. In Figure A-4 the 2-D beam is pictured with a target (x) shown off boresite. The antenna functions would weight such a target return in both azimuth and elevation.

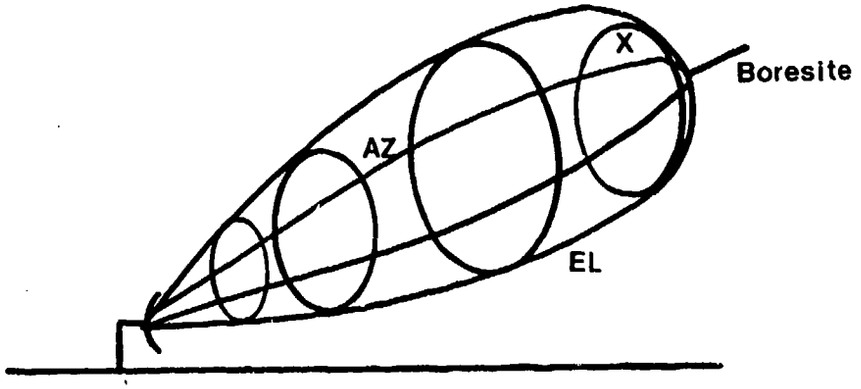


Fig. A-4. A Two-Dimensional Beam Showing a Target (x) Off Boresite

In order to move the boresite quickly and most efficiently, a combined azimuth-elevation error would be necessary.

Steps to implement a two-dimensional tracking loop were not taken. In order to find the threshold of such a system and quantify it, a 2-D ZZ and CR bound is necessary. This is the obstacle that prevented the 2-D case from being pursued further.

The Two-Dimensional Lower Bounds

The Cramer-Rao (CR) bound is defined as [Ref 6]

$$\mathrm{Var}(\hat{u}) \geq \left[\frac{-1}{E\{\frac{\partial^2 \ell n}{\partial u^2}\, p(r_1 r_2/A,u)\}}\right] \qquad \text{(A-38)}$$

for the one-dimensional case. It can be shown that for the 2-D case [Ref 6]

$$\mathrm{Cov}(\hat{u},\hat{v}) \geq \left[\frac{-1}{E\{\frac{\partial^2 \ell n}{\partial u \partial v}\, p(r_1 r_2 r_3/A,u,v)\}}\right] \qquad \text{(A-39)}$$

The Ziv-Zakai (ZZ) bound is not so easily transformed into two dimensions. The one-dimensional ZZ bound is stated here as [Ref 3]

$$\varepsilon^2(\theta) \geq \max_{0 \leq \theta \leq \theta_p} \sin^2(\theta) P_e(-0,\theta) \qquad \text{(A-40)}$$

where $\theta_p$ is defined by

$$\sin \theta_p = \frac{\sin \theta_{max} + \sin \theta}{2}$$

To develop a two-dimensional bound, the same steps as outlined by Ziv and Zakai must be taken [Ref 12].

The first obstacle to overcome in developing a 2-D bound is finding the probability of error $P(\varepsilon)$. The $P(\varepsilon)$ as used in the ZZ bound is the error probability of

the best procedure for deciding whether a target is at $-\theta$ or $\theta$ when it is known that it is at one of these positions and each has equal possibilities [Ref 8]. If we want to expand the $P(\varepsilon)$ to two dimensions, four regions must be considered.

Instead of just the case where a target is at $u_1$ or $u_2$, there are now four cases shown in Figure A-5. Instead of a binary detection problem we now have an M-ary detection problem where M = 4 [Ref 6].

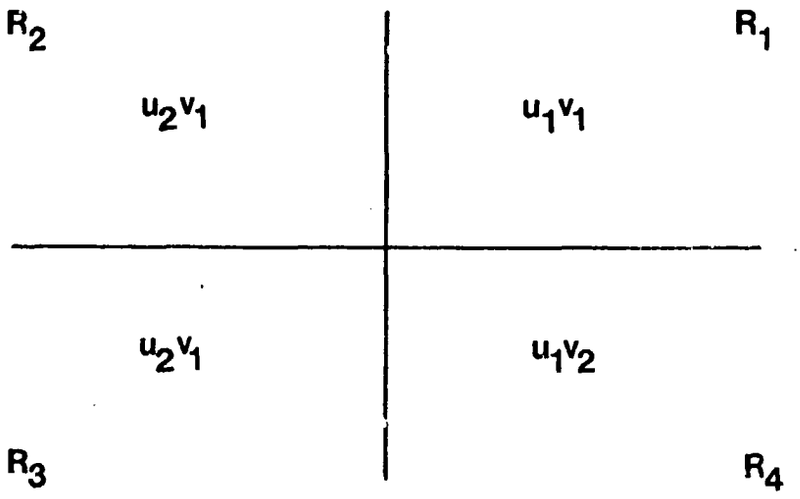


Fig. A-5. Decision Regions for a Two-Dimensional Case

The four hypotheses are

$$H_1: \quad r_1 = A\sqrt{E}\, g_1(u_1 v_1) + n_1 \qquad \text{(A-41)}$$

$$r_2 = A\sqrt{E}\, g_2(u_1 v_1) + n_2$$

$$r_3 = A\sqrt{E}\, g_3(u_1 v_1) + n_3$$

$$H_2: \quad r_1 = A\sqrt{E}\, g_1(u_2 v_1) + n_1 \tag{A-42}$$

$$r_2 = A\sqrt{E}\, g_2(u_2 v_1) + n_2$$

$$r_3 = A\sqrt{E}\, g_3(u_2 v_1) + n_3$$

$$H_3: \quad r_1 = A\sqrt{E}\, g_1(u_2 v_2) + n_1 \tag{A-43}$$

$$r_2 = A\sqrt{E}\, g_2(u_2 v_2) + n_2$$

$$r_3 = A\sqrt{E}\, g_3(u_2 v_2) + n_3$$

$$H_4: \quad r_1 = A\sqrt{E}\, g_1(u_1 v_2) + n_1 \tag{A-44}$$

$$r_2 = A\sqrt{E}\, g_2(u_1 v_2) + n_2$$

$$r_3 = A\sqrt{E}\, g_3(u_1 v_2) + n_3$$

From detection theory, with probability of error costs the decision region $R_j$ is given as the values of $r_j$ for which [Ref 6:Ch. 5]

$$P\{H_j\}p(r/A_j) > P\{H_k\}p(r/H_k) \quad \text{for } j \neq k \tag{A-45}$$

Equal probability of hypotheses is assumed so equation (A-45) becomes

$$p(r/H_j) > p(r/H_k) \tag{A-46}$$

where $p(r/H_j) = p(r_1 r_2 r_3/H_j)$ etc.

For decision region $R_1$ we have

$$p(r/H_1) > p(r/H_2) \tag{A-47a}$$

$$p(r/H_1) > p(r/H_3) \tag{A-47b}$$

$$p(r/H_1) > p(r/H_4) \tag{A-47c}$$

Similarly, for regions $R_2$, $R_3$, and $R_4$

$$R_2: \; p(r/H_2) > p(r/H_1) \tag{A-48a}$$

$$p(r/H_2) > p(r/H_3) \tag{A-48b}$$

$$p(r/H_2) > p(r/H_4) \tag{A-48c}$$

$$R_3: \; p(r/H_3) > p(r/H_1) \tag{A-49a}$$

$$p(r/H_3) > p(r/H_2) \tag{A-49b}$$

$$p(r/H_3) > p(r/H_4) \tag{A-49c}$$

$$R_4: \; p(r/H_4) > p(r/H_1) \tag{A-50a}$$

$$p(r/H_4) > p(r/H_2) \tag{A-50b}$$

$$p(r/H_4) > p(R/H_3) \tag{A-50c}$$

The next step is to find the likelihood ratios for each decision region. For notational purposes, let

$$\ell_j(r) = \frac{p(r/H_j)}{p(r/H_1)}$$

$$\ell_{jk}(r) = \frac{p(r/H_j)}{p(r/H_k)}$$

Using this notation, for the four regions we have

$R_1$: $\ell_2(r) < 0$ $\quad$ $R_2$: $\ell_2(r) > 0$

$\ell_3(r) < 0$ $\quad$ $\ell_{23}(r) > 0$

$\ell_4(r) < 0$ $\quad$ $\ell_{24}(r) > 0$

$R_3$: $\ell_3(r) > 0$ $\quad$ $R_4$: $\ell_4(r) > 0$

$\ell_{32}(r) > 0$ $\quad$ $\ell_{42}(r) > 0$

$\ell_{34}(r) > 0$ $\quad$ $\ell_{43}(r) > 0$

As in Chapter II of this thesis, symmetry will be assumed in the error. The probability of error will therefore be the same in each decision region. The total $P(\varepsilon)$ will be the sum of the $P(\varepsilon)$'s in each region. This result is shown as

$$P(\varepsilon) = p\{H_1\}P_\varepsilon(R_1) + P\{H_2\}P_\varepsilon(R_2) + P\{H_3\}P_\varepsilon(R_3) + P\{H_4\}P_\varepsilon(R_4) \qquad \text{(A-51)}$$

Since $P\{H_j\} = 1/4$ and $P_\varepsilon(R_1) = P_\varepsilon(R_2) = P_\varepsilon(R_3) = P_\varepsilon(R_4)$ then

$$P(\varepsilon) = P_\varepsilon(R_1) \qquad \text{(A-52)}$$

The statistics for the likelihood ratios for region 1 will be determined and used to describe the $P(\varepsilon)$.

By following the same steps outlined in Chapter II we get

$$E\{\ell_2(r)/H_1\} = \frac{A\sqrt{E}}{2} E_o(1-\rho_2) \tag{A-53}$$

where

$$E_o = [g_1^2(u_1v_1) + g_1^2(u_2v_1) + g_2^2(u_1v_1) + g_2^2(u_2v_1) + g_3^2(u_1v_1) + g_3^2(u_2v_1)]$$

and

$$\rho_2 = \frac{2}{E_o}[g_1(u_1v_1)g_1(u_2v_1) + g_2(u_1v_1)g_2(u_2v_1) + g_3(u_1v_1)g_3(u_2v_1)]$$

$$E\{\ell_2(r)/H_2\} = -\frac{A\sqrt{E}}{2} E_o(1-\rho_2) \tag{A-54}$$

$$\text{Var}(\ell_2(r)/H_1) = \text{Var}(\ell_2(r)/H_2) = N_o/2\ E_o(1-\rho_2) \tag{A-55}$$

Also

$$E\{\ell_3(r)/H_1\} = \frac{A\sqrt{E}}{2} E_o(1-\rho_3) \tag{A-56}$$

$$E\{\ell_3(r)/H_3)\} = -\frac{A\sqrt{E}}{2} E_o(1-\rho_3) \tag{A-57}$$

$$\text{Var}(\ell_3(r)/H_3) = \text{Var}(\ell_3(r)/H_3) = N_o/2\ E_o(1-\rho_3) \tag{A-58}$$

and

$$E\{\ell_4(r)/H_1\} = \frac{A\sqrt{E}}{2} E_o(1-\rho_4) \tag{A-59}$$

$$E\{\ell_4(r)/H_4\} = -\frac{A\sqrt{E}}{2} E_o(1-\rho_4) \tag{A-60}$$

$$\mathrm{Var}(\ell_4(r)/H_1) = \mathrm{Var}(\ell_4(r)/H_4) = N_o/2\,E_o(1-\rho_4) \quad \text{(A-61)}$$

The $P(\varepsilon)$ is

$$P(\ell_2>0/H_2)P\{H_2\} + P(\ell_3>0/H_3)P\{H_3\}$$

$$+ P(\ell_4>0/H_4)P\{H_4\} \quad \text{(A-62)}$$

Since $P\{H_2\} = P\{H_3\} = P\{H_4\} = 1/4$, equation (A-62) becomes

$$P(\varepsilon) = 1/4P(\ell_2>0/H_2) + 1/4P(\ell_3>0/H_3)$$

$$+ 1/4P(\ell_4>0/H_4) \quad \text{(A-63)}$$

Each term in equation (A-63) can be expressed as a Q-function.

$$P(\varepsilon) = 1/4\{(1-Q[A(\frac{EE_o}{2N_o}(1-\rho_2))^{\frac{1}{2}}])$$

$$+ (1-Q[A(\frac{EE_o}{2N_o}(1-\rho_3))^{\frac{1}{2}}])$$

$$+ (1-Q[A(\frac{EE_o}{2N_o}(1-\rho_4))^{\frac{1}{2}}])\} \quad \text{(A-64)}$$

Since symmetry is assumed, $\rho_2 = \rho_3 = \rho_4 = \rho$

$$P(\varepsilon) = 3/4\{(1-Q[A(\frac{EE_o}{2N_o}(1-\rho))^{\frac{1}{2}}])\} \quad \text{(A-65)}$$

Now that a probability of error has been determined the next step is to derive the ZZ bound. Ziv and Zakai used the Tchebycheff inequality to transform their probability of error into a form including a mean-square

error. Since this is a two-dimensional case a two-dimensional inequality of the Tchebycheff type is needed. Reference [7] shows several probability inequalities of the Tchebycheff type. A two-dimensional one called the Berge inequality is stated as

$$P\left(\max\left\{\frac{|x_1-u_1|}{\sigma_1}\ ,\ \frac{|x_2-u_2|}{\sigma_2}\right\} \geq \lambda\right) \leq \frac{1+\sqrt{1-\rho^2}}{\lambda^2} \qquad \text{(A-70)}$$

where $x_1$ and $x_2$ are random variables

$$u_i = E\{x_i\}$$

$$\sigma_i^2 = E\{(x_i-u_i)^2\}$$

$$\sigma_{12} = E\{(x_1-u_1)(x_2-u_2)\}$$

$$\rho = \frac{\sigma_{12}}{\sigma_1\sigma_2}$$

and $\lambda > 0$

As can be seen from the definition of $\rho$, the lower bound on the covariance could possibly be obtained from this inequality; however, attempts to do so were unsuccessful. It is recommended that the Berge inequality be investigated further as to its possible use in determining the ZZ bound in two dimensions. A search for other two-dimensional inequalities may prove worthwhile also. Once a suitable inequality is found the 2-D ZZ bound

can be derived and the 2-1 monopulse radar model can be simulated and its threshold quantified.

## Appendix B

## Plots of Stationary Target MSE Compared to the Cramer-Rao and Ziv-Zakai Bounds from 35 dB to -10 dB

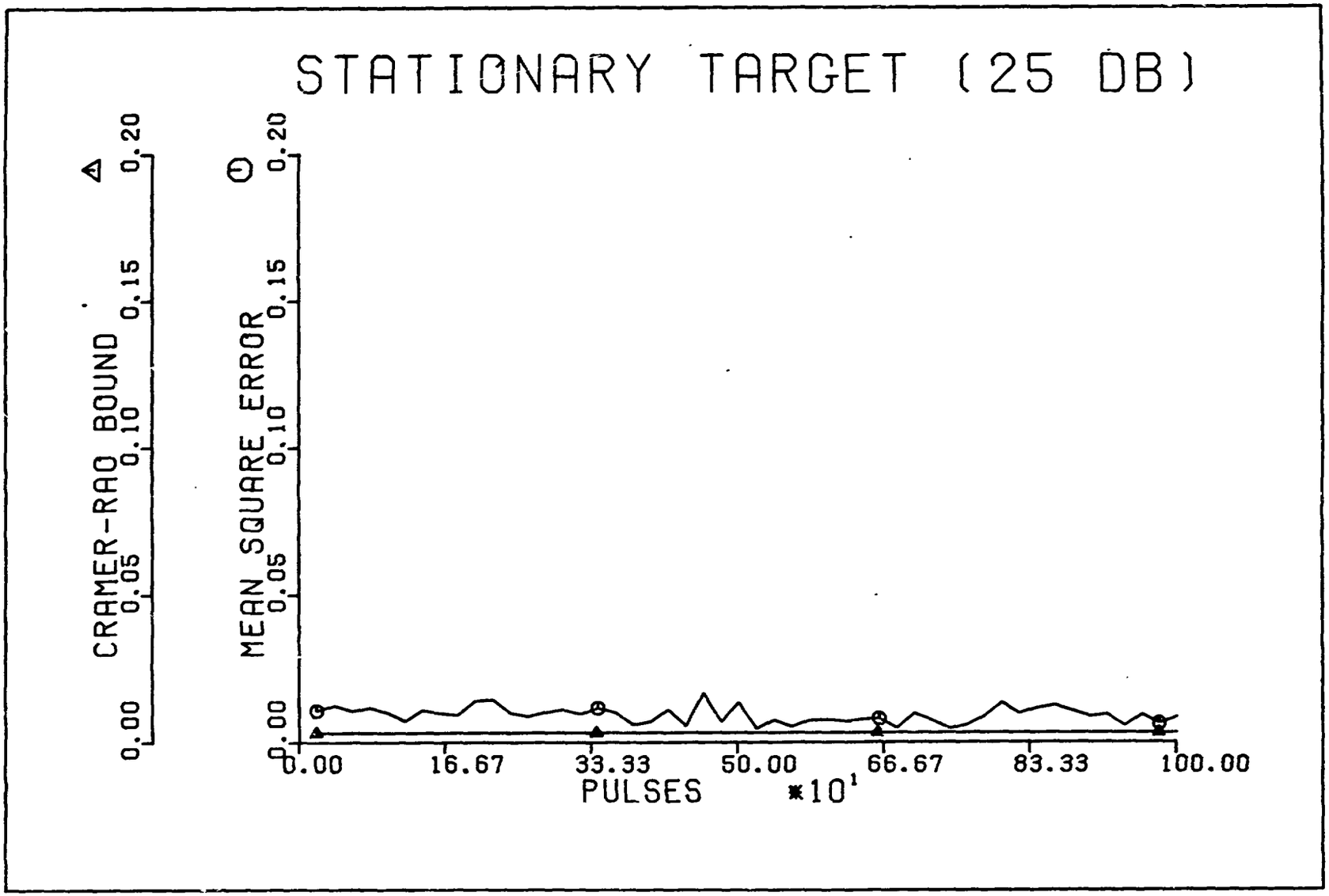
STATIONARY TARGET (25 DB)
CRAMER-RAO BOUND
MEAN SQUARE ERROR
0.00
0.05
0.10
0.15
0.20
0.00
16.67
33.33
50.00
66.67
83.33
100.00
PULSES
*10¹

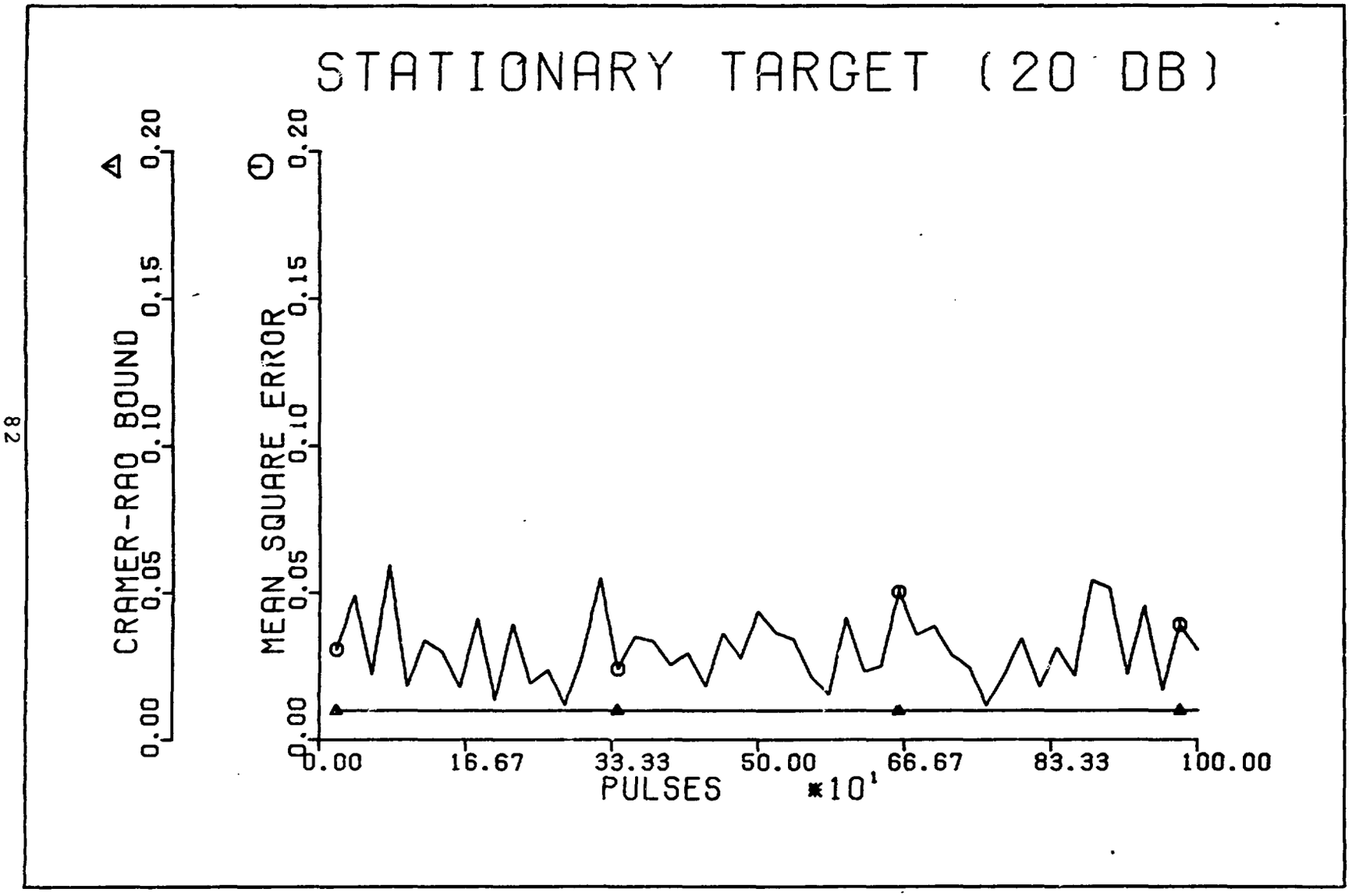
STATIONARY TARGET (20 DB)
CRAMER-RAO BOUND
MEAN SQUARE ERROR
0.00
0.05
0.10
0.15
0.20
0.00
16.67
33.33
50.00
66.67
83.33
100.00
PULSES
*10¹

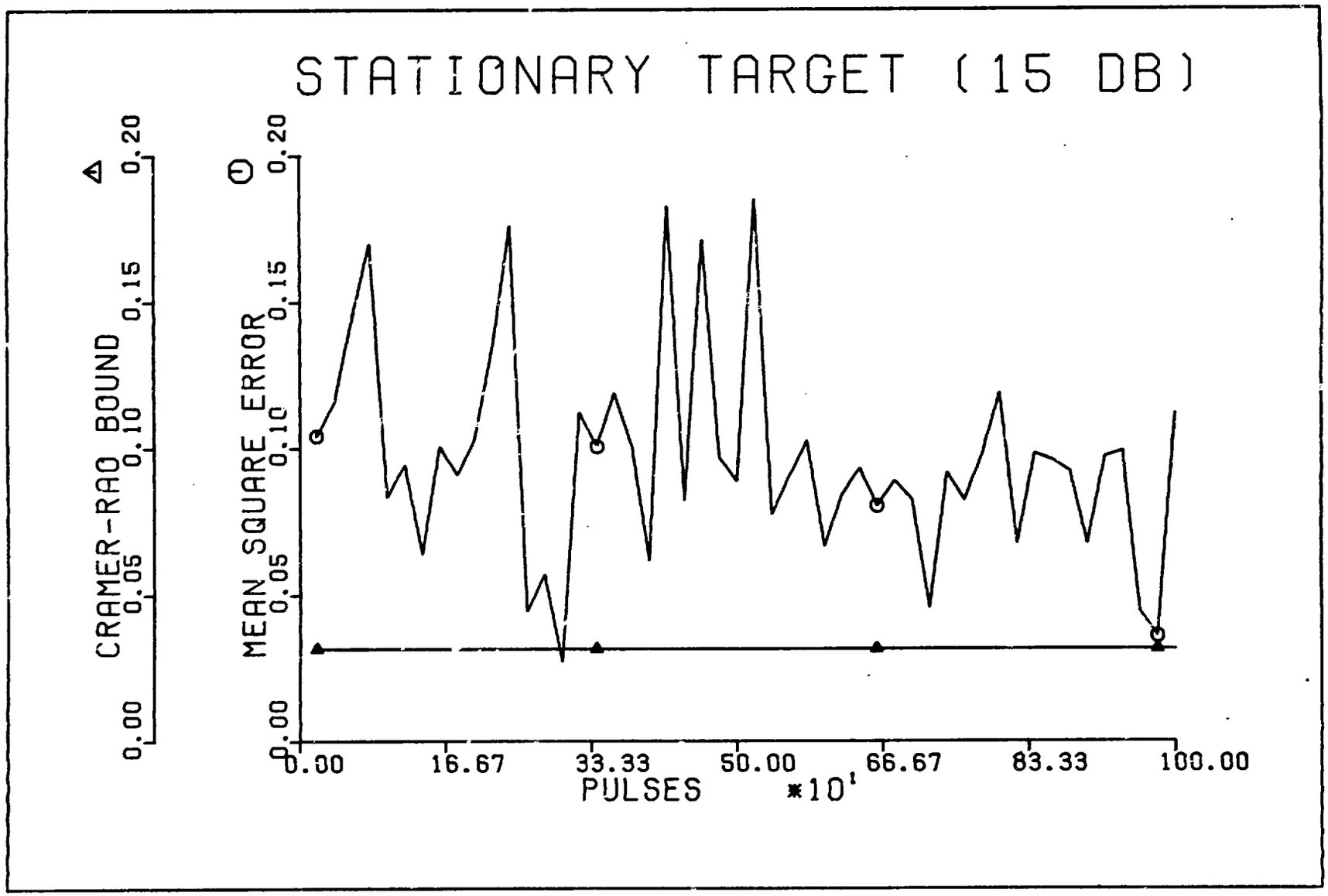
STATIONARY TARGET (15 DB)
CRAMER-RAO BOUND
MEAN SQUARE ERROR
0.00
0.05
0.10
0.15
0.20
0.00
16.67
33.33
50.00
66.67
83.33
100.00
PULSES
*10¹

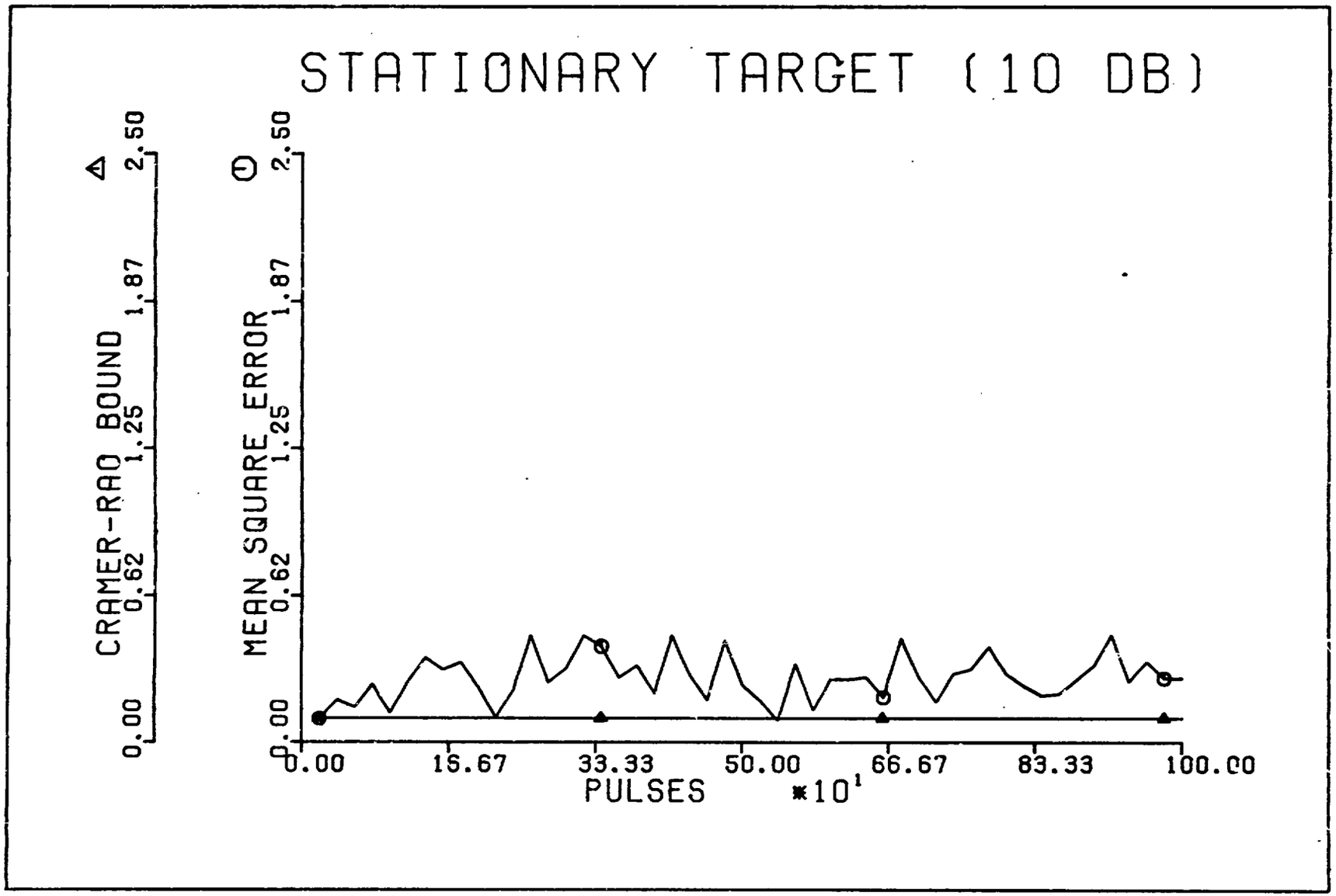
STATIONARY TARGET (10 DB)
CRAMER-RAO BOUND
Δ
0.00
0.62
1.25
1.87
2.50
MEAN SQUARE ERROR
Θ
0.00
0.62
1.25
1.87
2.50
0.00
16.67
33.33
50.00
66.67
83.33
100.00
PULSES
*10¹

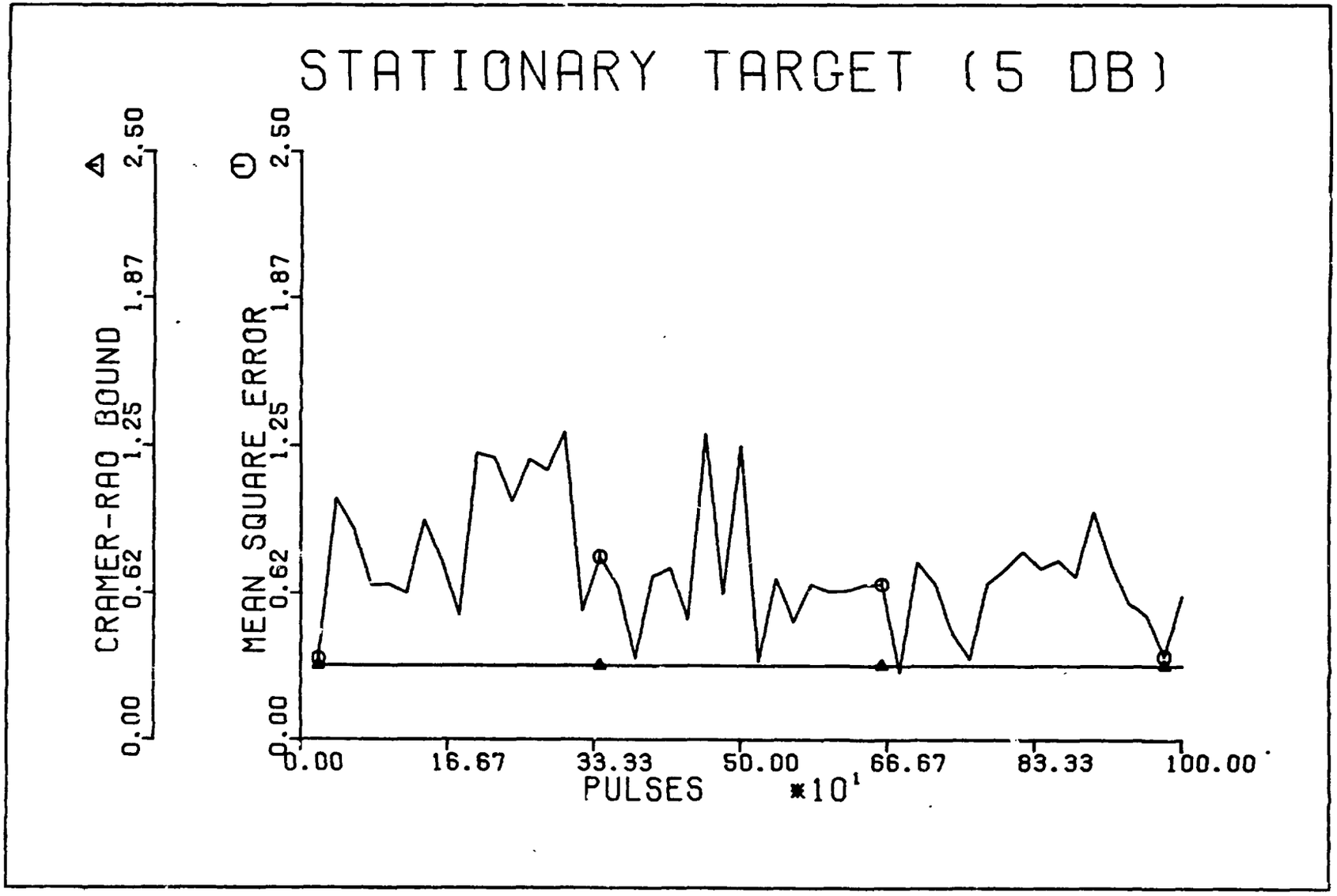
STATIONARY TARGET (5 DB)
CRAMER-RAO BOUND
MEAN SQUARE ERROR
0.00
0.62
1.25
1.87
2.50
0.00
16.67
33.33
50.00
66.67
83.33
100.00
PULSES
*10¹

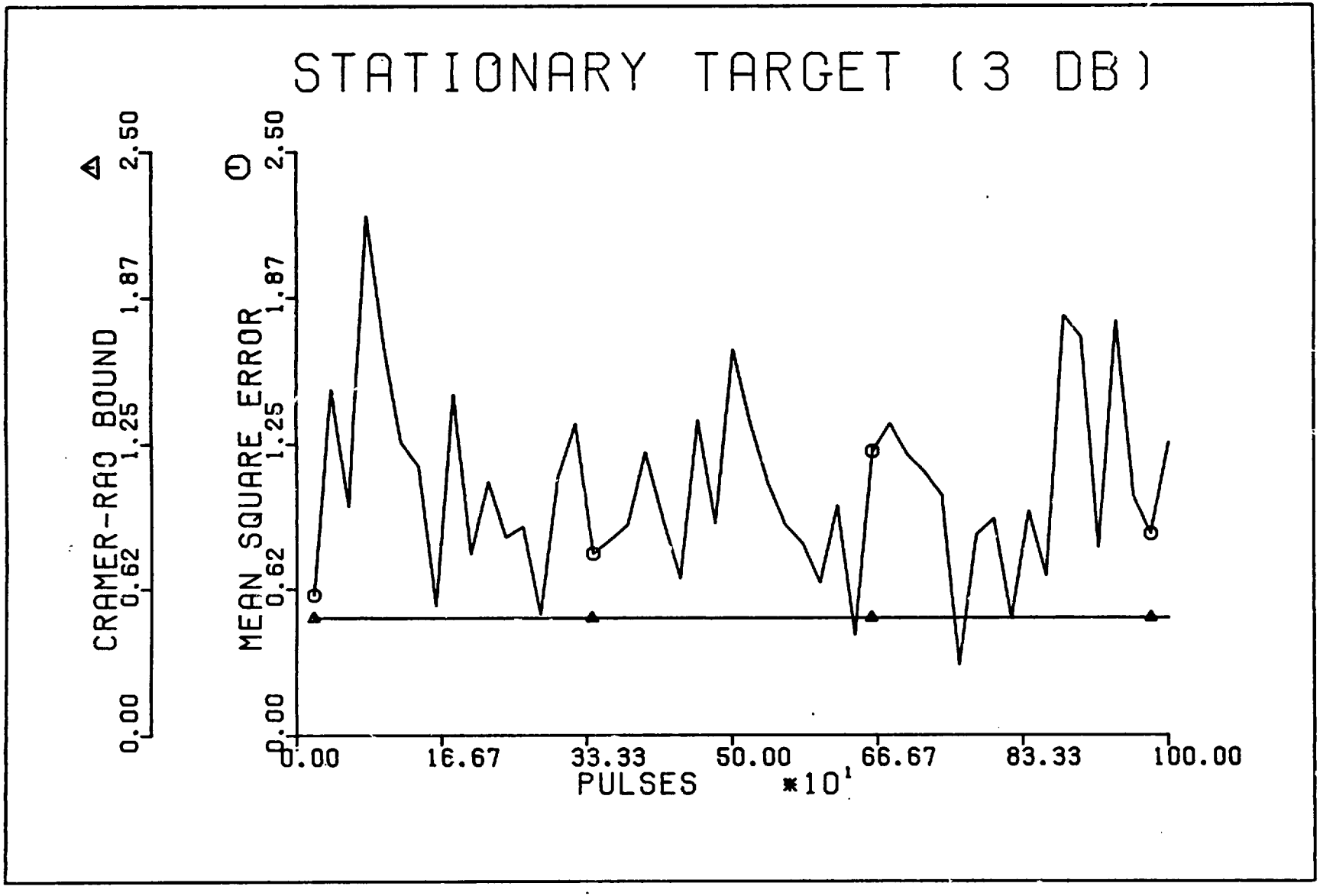
STATIONARY TARGET (3 DB)
CRAMER-RAO BOUND
Δ
0.00
0.62
1.25
1.87
2.50
MEAN SQUARE ERROR
O
0.00
0.62
1.25
1.87
2.50
0.00
16.67
33.33
50.00
66.67
83.33
100.00
PULSES
*10¹

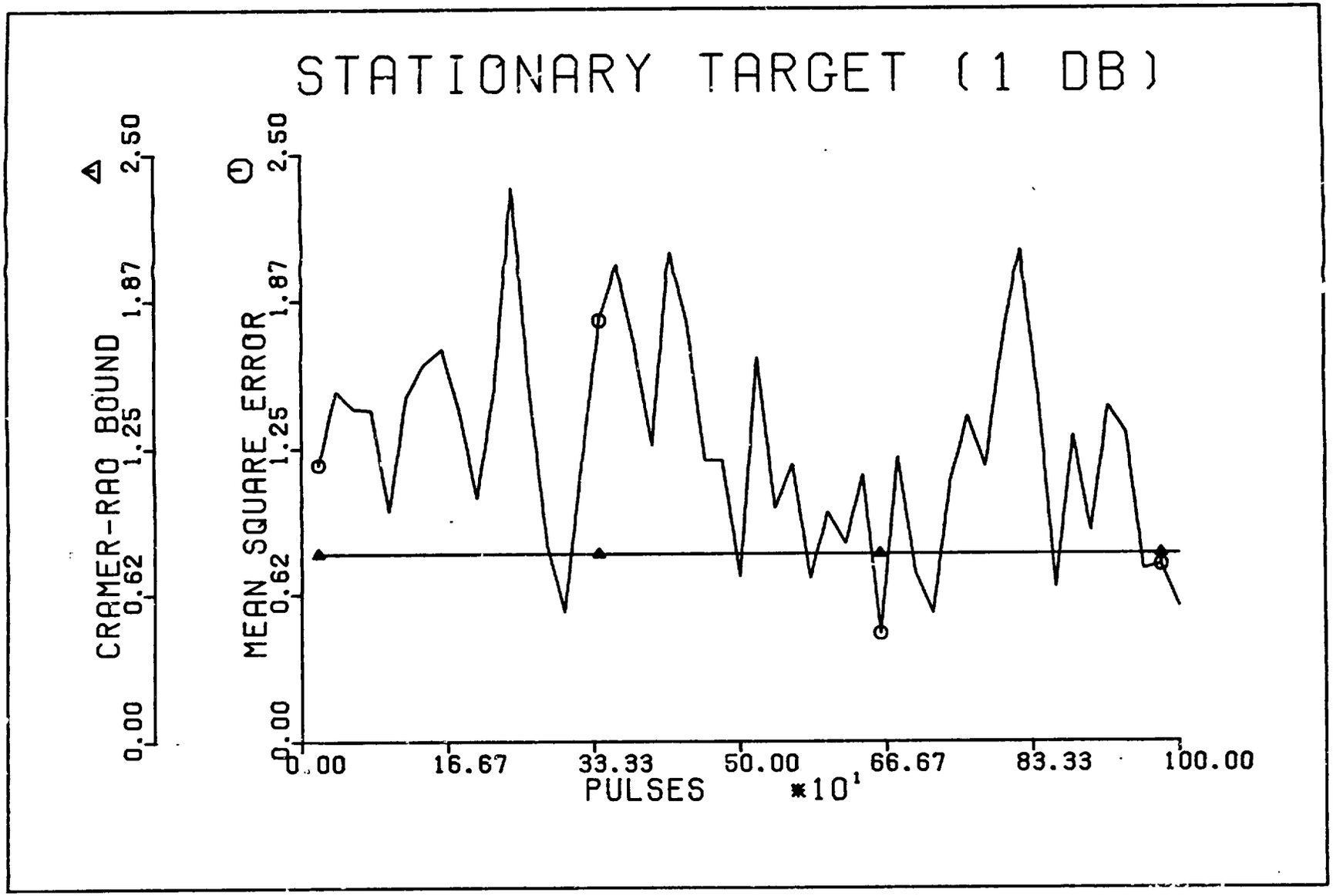
STATIONARY TARGET (1 DB)
CRAMER-RAO BOUND
MEAN SQUARE ERROR
0.00
0.62
1.25
1.87
2.50
0.00
16.67
33.33
50.00
66.67
83.33
100.00
PULSES
*10¹

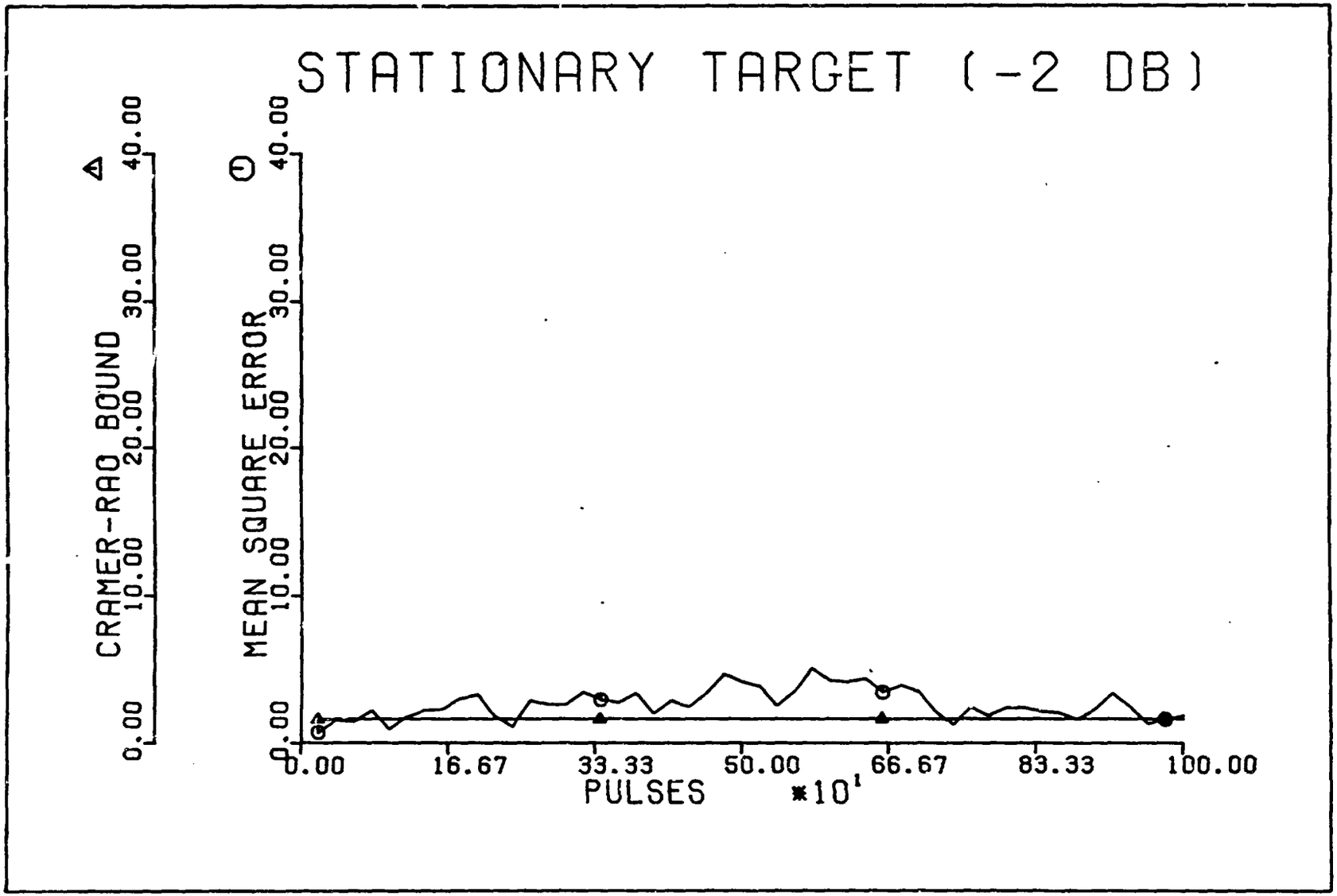
STATIONARY TARGET (-2 DB)
CRAMER-RAO BOUND
MEAN SQUARE ERROR
0.00
10.00
20.00
30.00
40.00
0.00
16.67
33.33
50.00
66.67
83.33
100.00
PULSES
*10¹

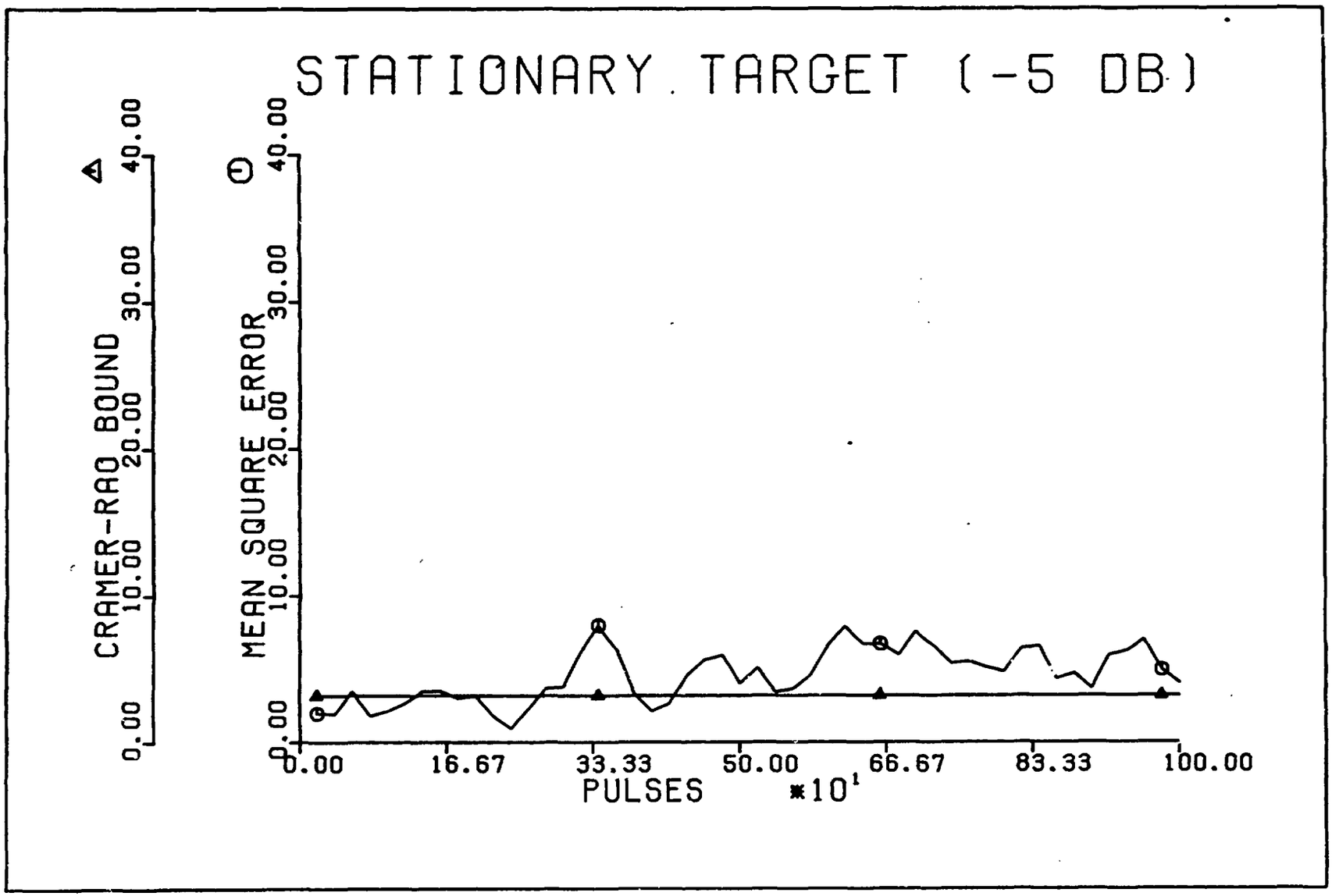
STATIONARY TARGET (-5 DB)
CRAMER-RAO BOUND
MEAN SQUARE ERROR
0.00
10.00
20.00
30.00
40.00
0.00
16.67
33.33
50.00
66.67
83.33
100.00
PULSES
*10¹

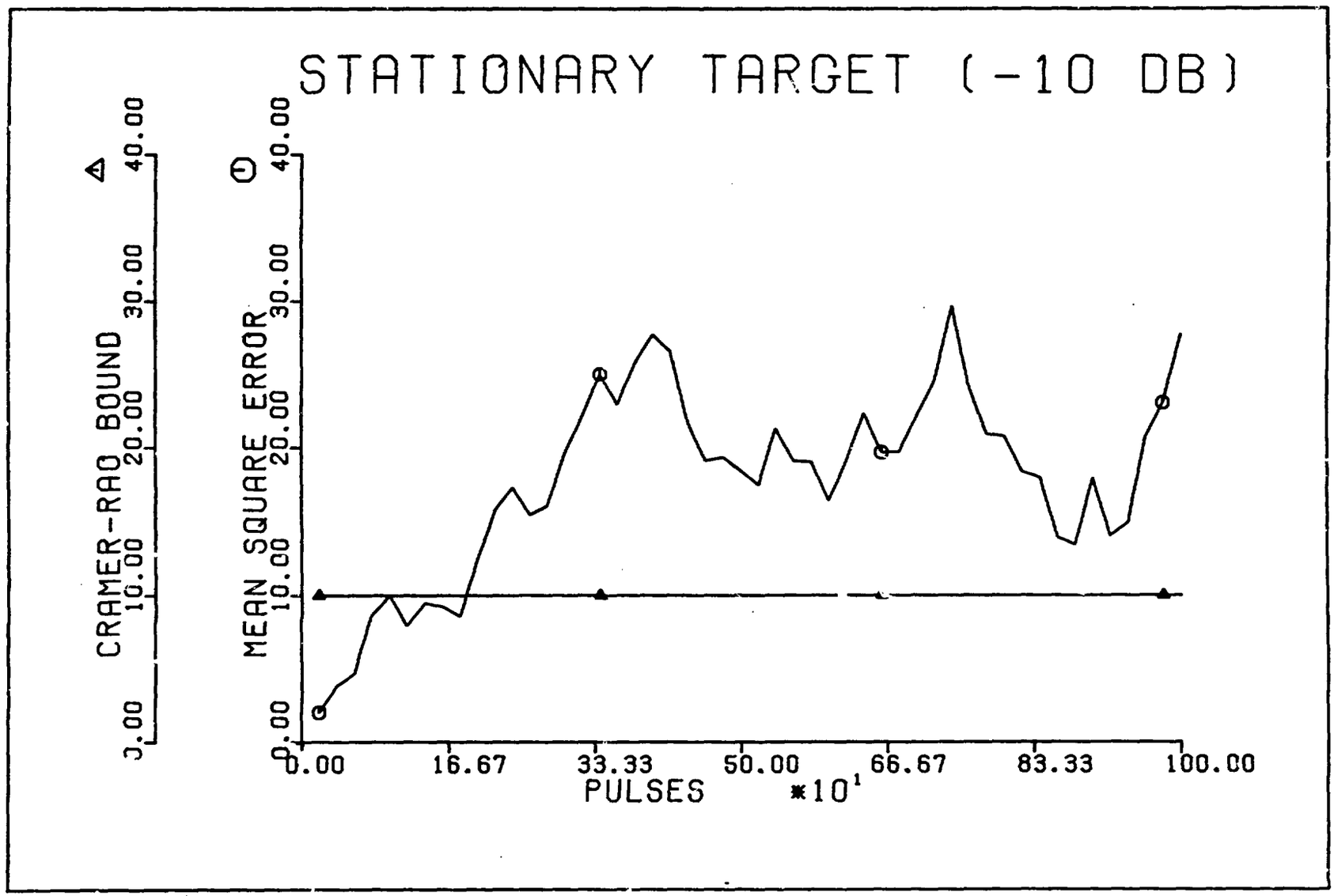
STATIONARY TARGET (-10 DB)
CRAMER-RAO BOUND
MEAN SQUARE ERROR
0.00
10.00
20.00
30.00
40.00
0.00
16.67
33.33
50.00
66.67
83.33
100.00
PULSES
*10¹

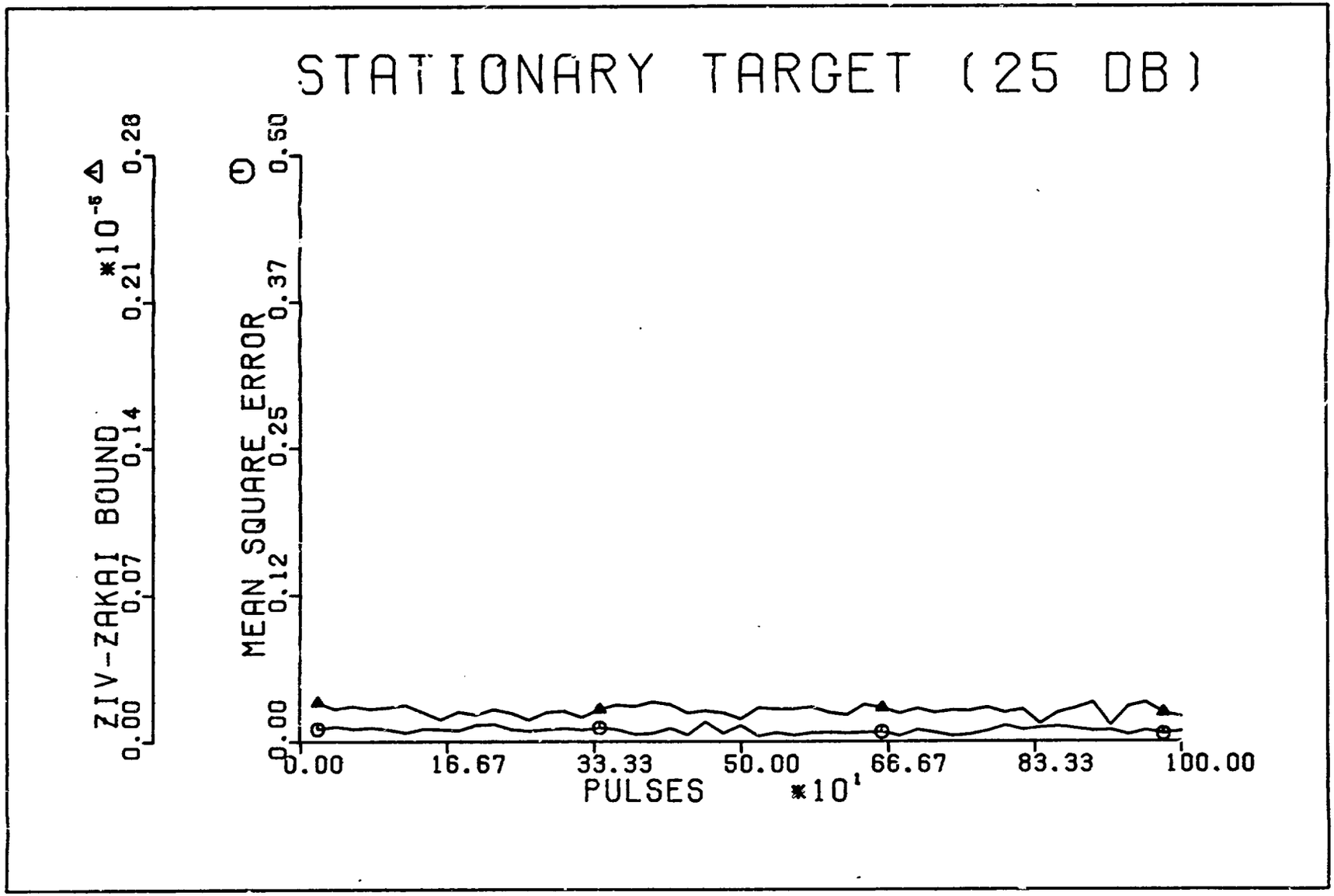
STATIONARY TARGET (25 DB)
ZIV-ZAKAI BOUND
*10^-5
0.00
0.07
0.14
0.21
0.28
MEAN SQUARE ERROR
0.00
0.12
0.25
0.37
0.50
0.00
16.67
33.33
50.00
66.67
83.33
100.00
PULSES
*10^1

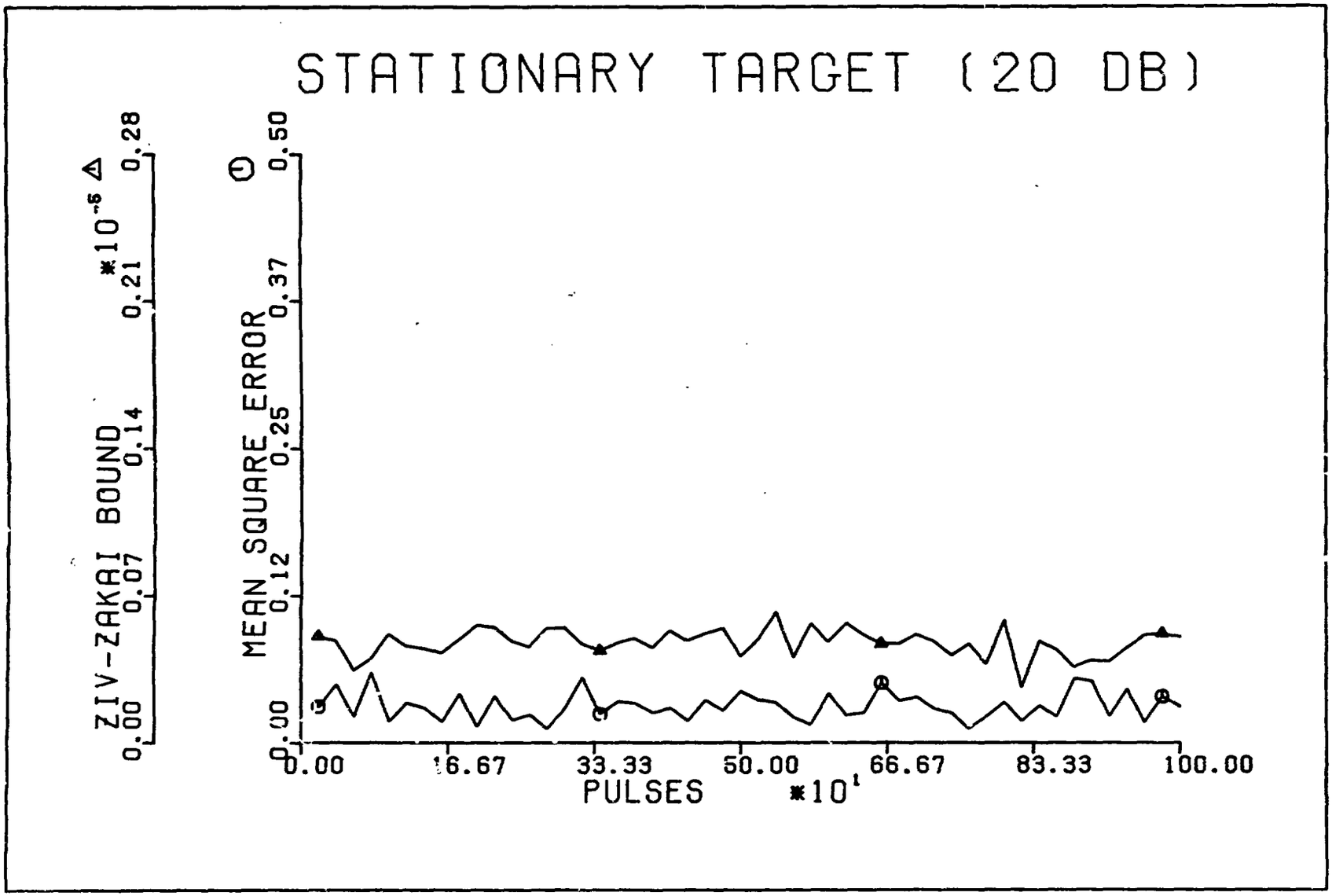
STATIONARY TARGET (20 DB)
ZIV-ZAKAI BOUND
0.00
0.07
0.14
0.21
*10^-6
0.28
MEAN SQUARE ERROR
0.00
0.12
0.25
0.37
0.50
0.00
16.67
33.33
50.00
66.67
83.33
100.00
PULSES *10^1

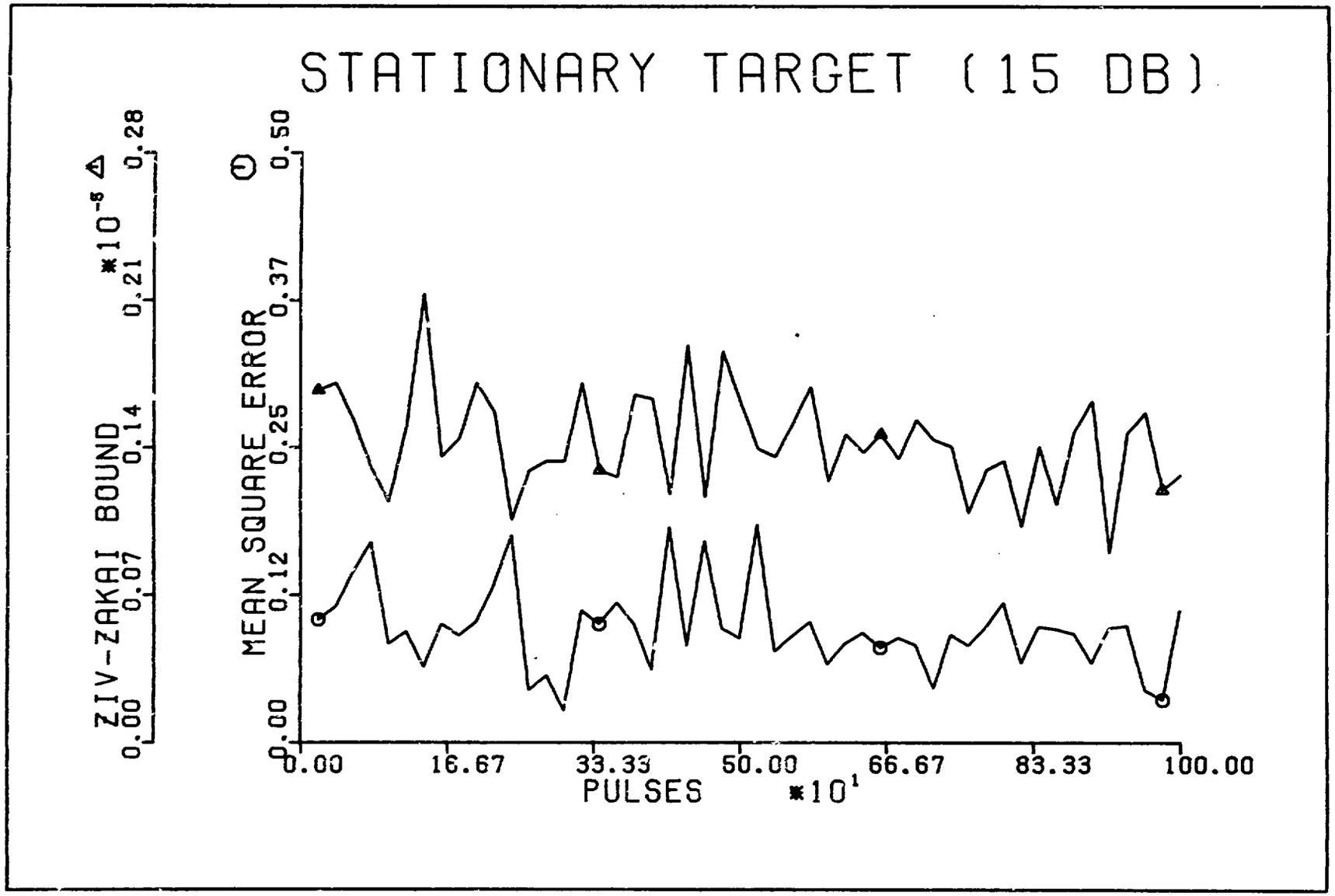
STATIONARY TARGET (15 DB)
MEAN SQUARE ERROR
0.00
0.12
0.25
0.37
0.50
ZIV-ZAKAI BOUND
*10^-5
0.00
0.07
0.14
0.21
0.28
0.00
16.67
33.33
50.00
66.67
83.33
100.00
PULSES
*10^1

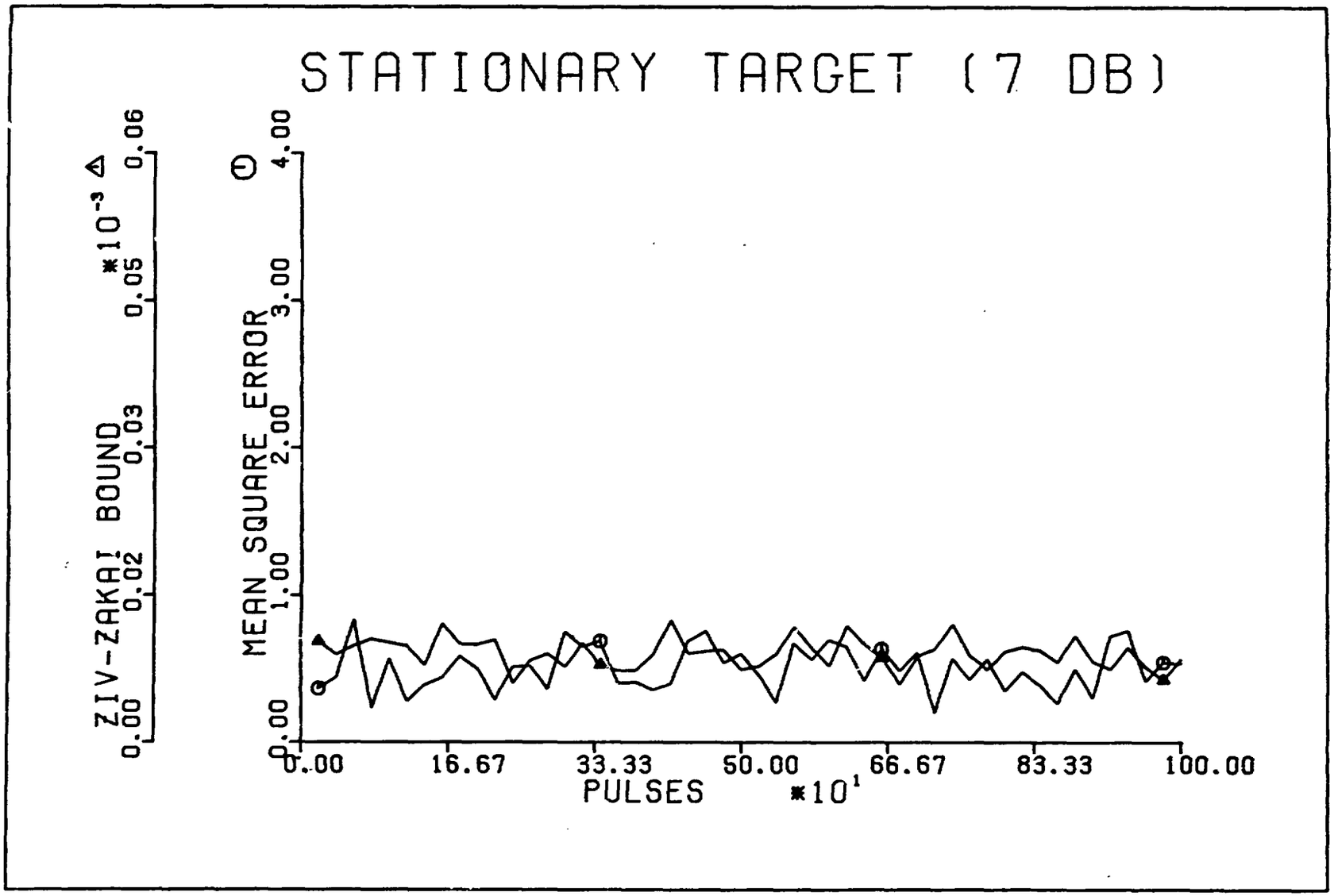
STATIONARY TARGET (7 DB)
ZIV-ZAKAI BOUND
0.00
0.02
0.03
0.05
0.06
*10⁻³ Δ
MEAN SQUARE ERROR
0.00
1.00
2.00
3.00
4.00
Θ
0.00
16.67
33.33
50.00
66.67
83.33
100.00
PULSES
*10¹

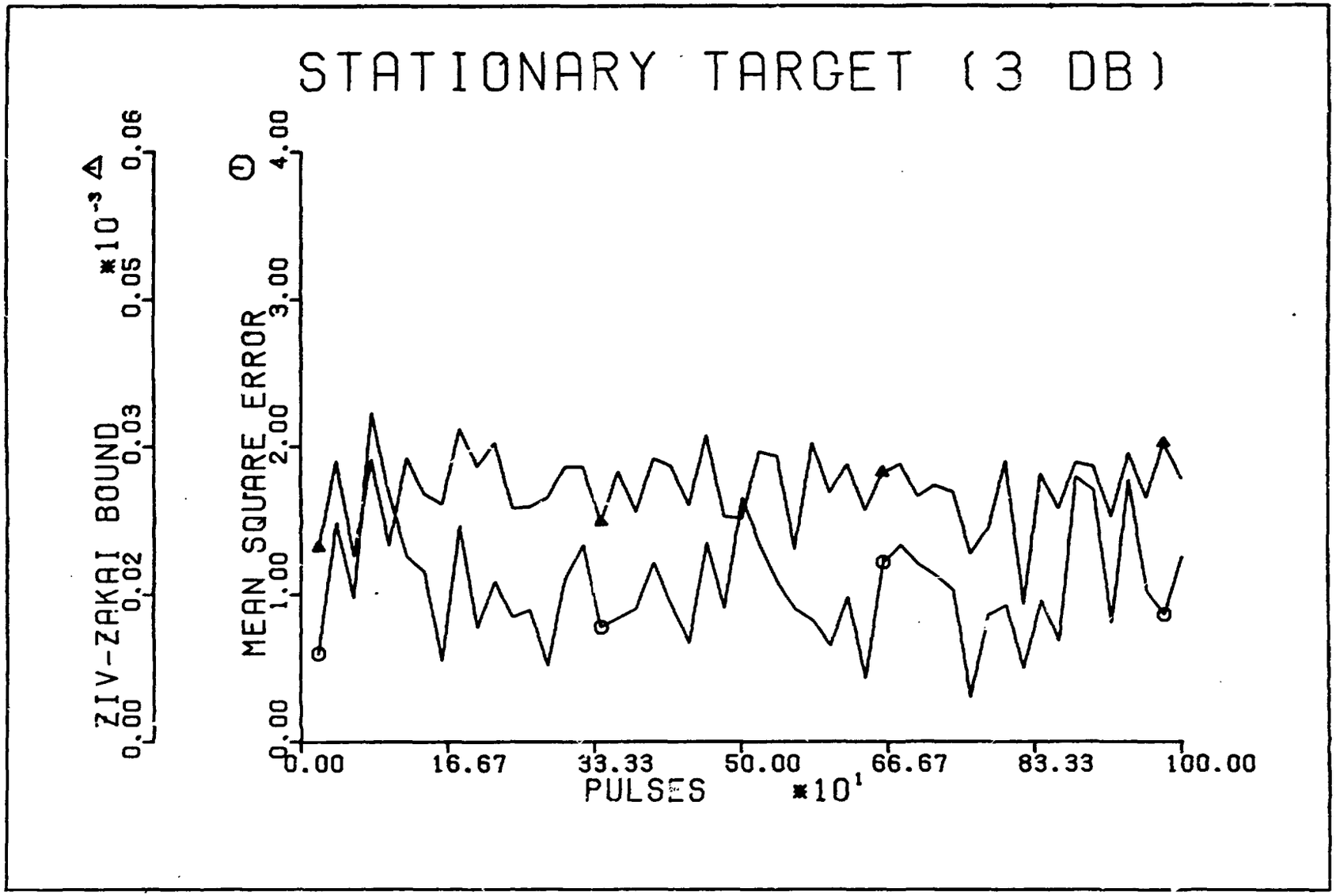
STATIONARY TARGET (3 DB)
ZIV-ZAKAI BOUND Δ
*10^-3
0.00
0.02
0.03
0.05
0.06
MEAN SQUARE ERROR Θ
0.00
1.00
2.00
3.00
4.00
0.00
16.67
33.33
50.00
66.67
83.33
100.00
PULSES *10^1

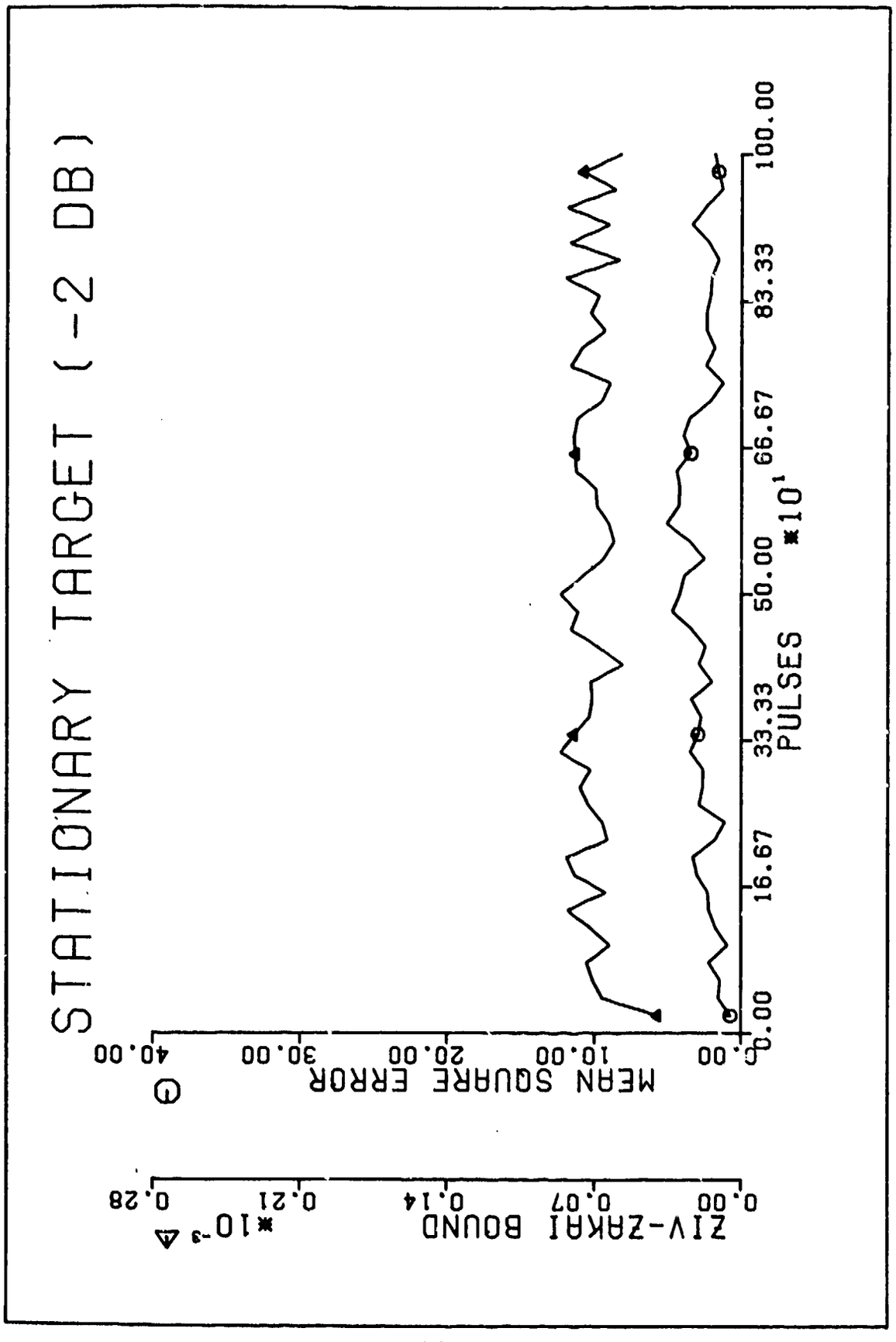
STATIONARY TARGET (-2 DB)
MEAN SQUARE ERROR
0.00
10.00
20.00
30.00
40.00
PULSES
0.00
16.67
33.33
50.00
66.67
83.33
100.00
*10¹
ZIV-ZAKAI BOUND
0.00
0.07
0.14
0.21
0.28
*10⁻³

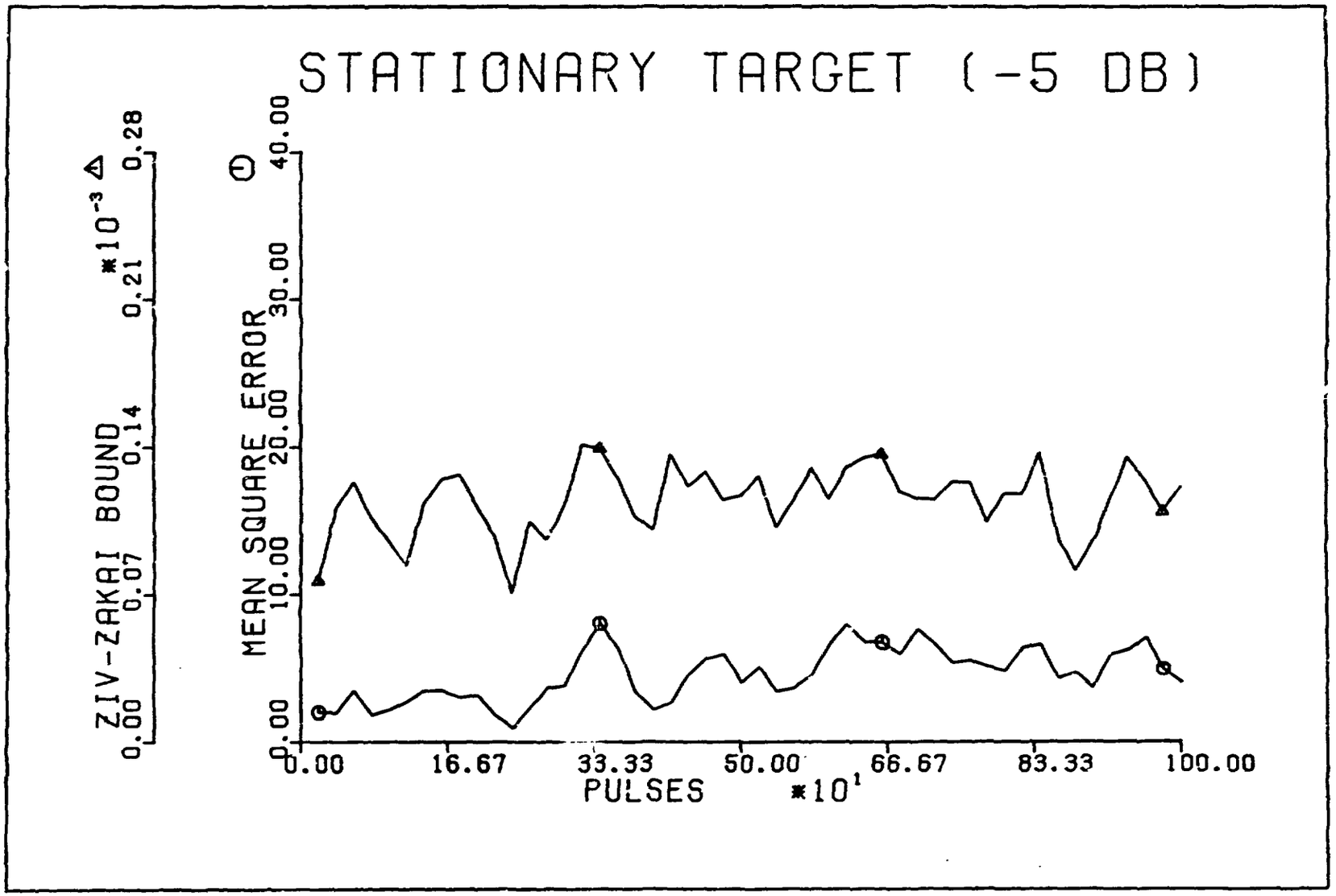
STATIONARY TARGET (-5 DB)
ZIV-ZAKAI BOUND
0.00
0.07
0.14
0.21
0.28
*10^-3
Δ
MEAN SQUARE ERROR
0.00
10.00
20.00
30.00
40.00
Θ
0.00
16.67
33.33
50.00
66.67
83.33
100.00
PULSES
*10^1

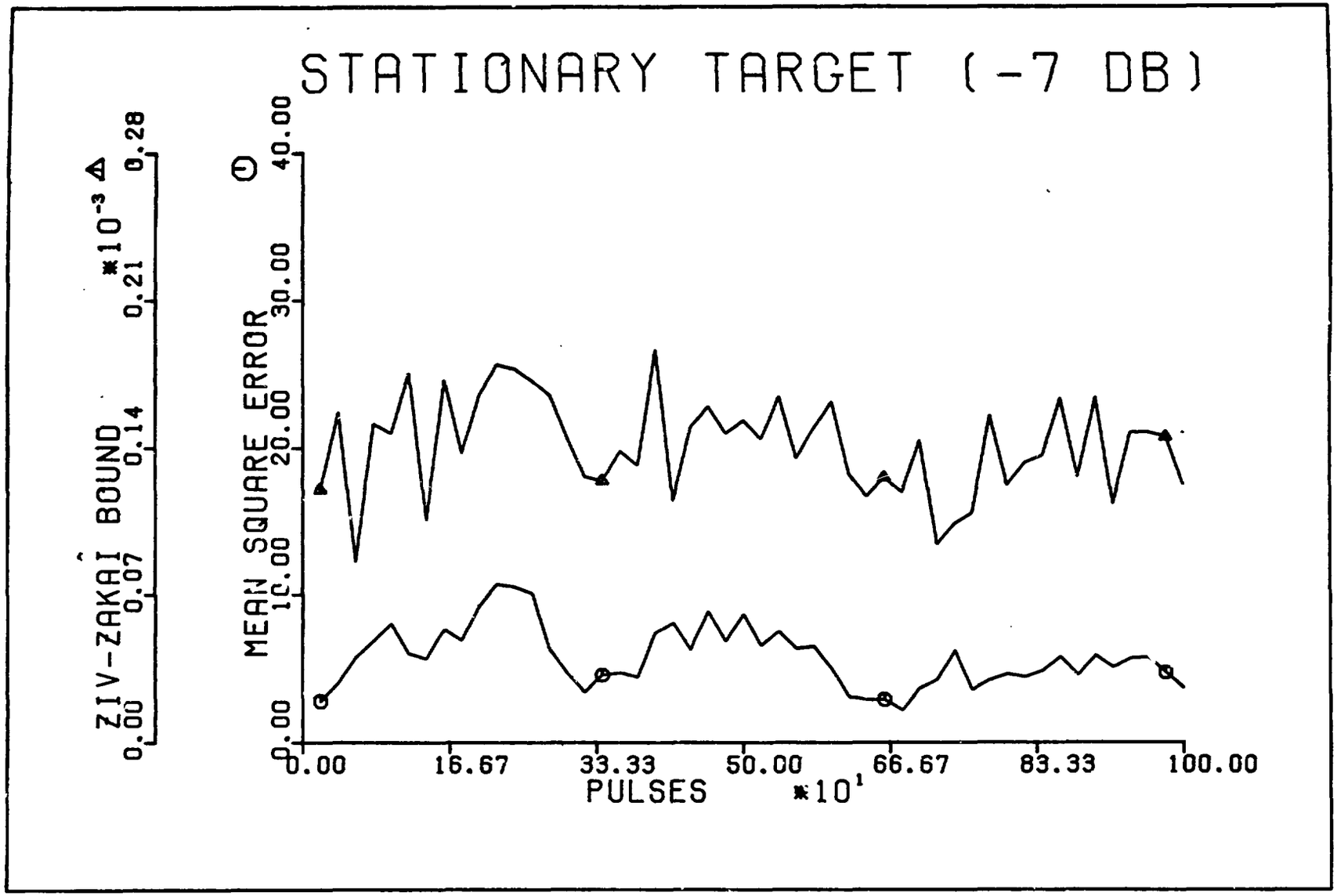
STATIONARY TARGET (-7 DB)
ZIV-ZAKAI BOUND
0.00
0.07
0.14
0.21
0.28
*10^-3
Δ
MEAN SQUARE ERROR
0.00
10.00
20.00
30.00
40.00
Θ
0.00
16.67
33.33
50.00
66.67
83.33
100.00
PULSES
*10^1

# Appendix C

## Plots of Moving Target MSE Compared to the Cramer-Rao and Ziv-Zakai Bounds from 35 dB to -10 dB

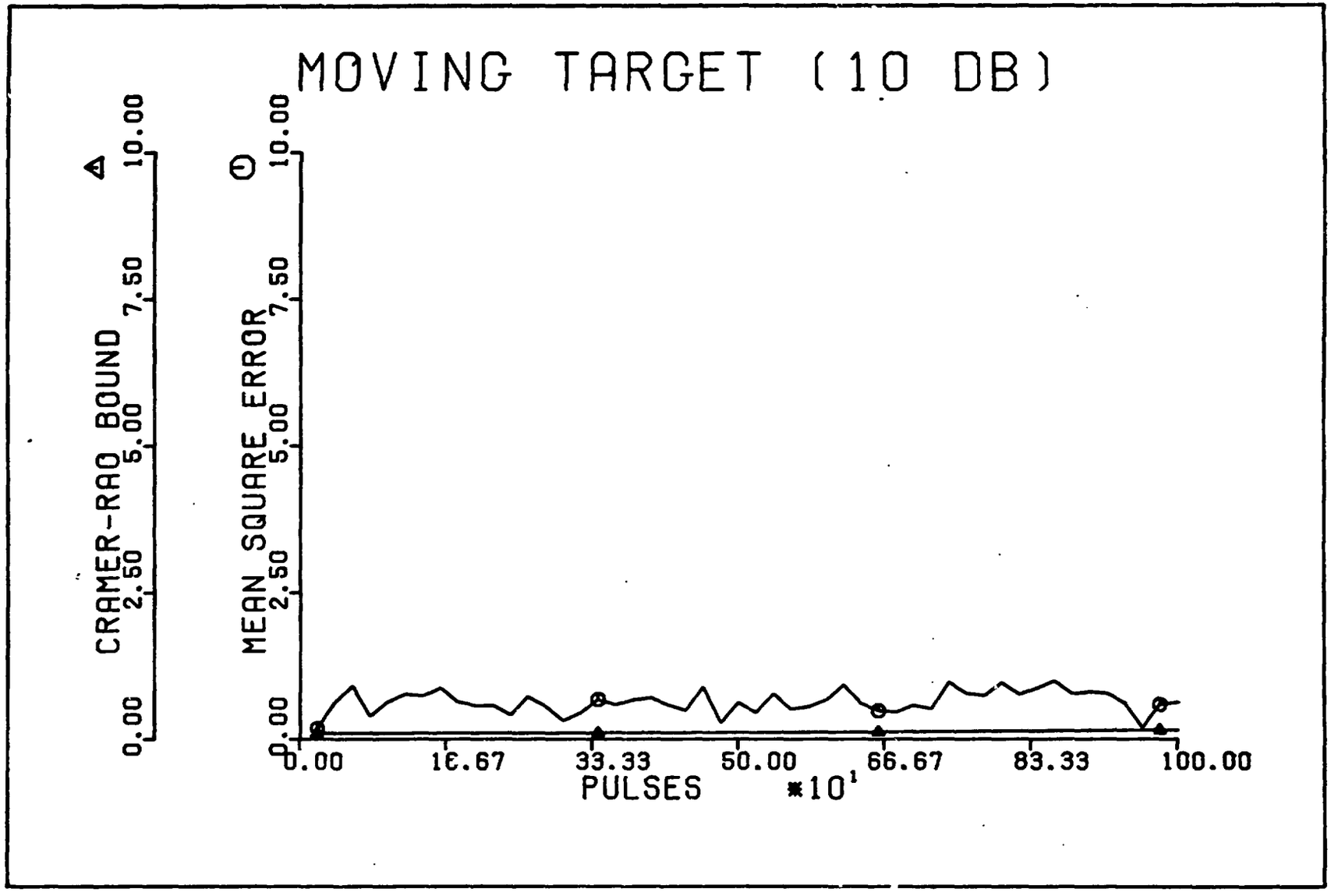
MOVING TARGET (10 DB)
CRAMER-RAO BOUND
MEAN SQUARE ERROR
0.00
2.50
5.00
7.50
10.00
0.00
16.67
33.33
50.00
66.67
83.33
100.00
PULSES
*10¹

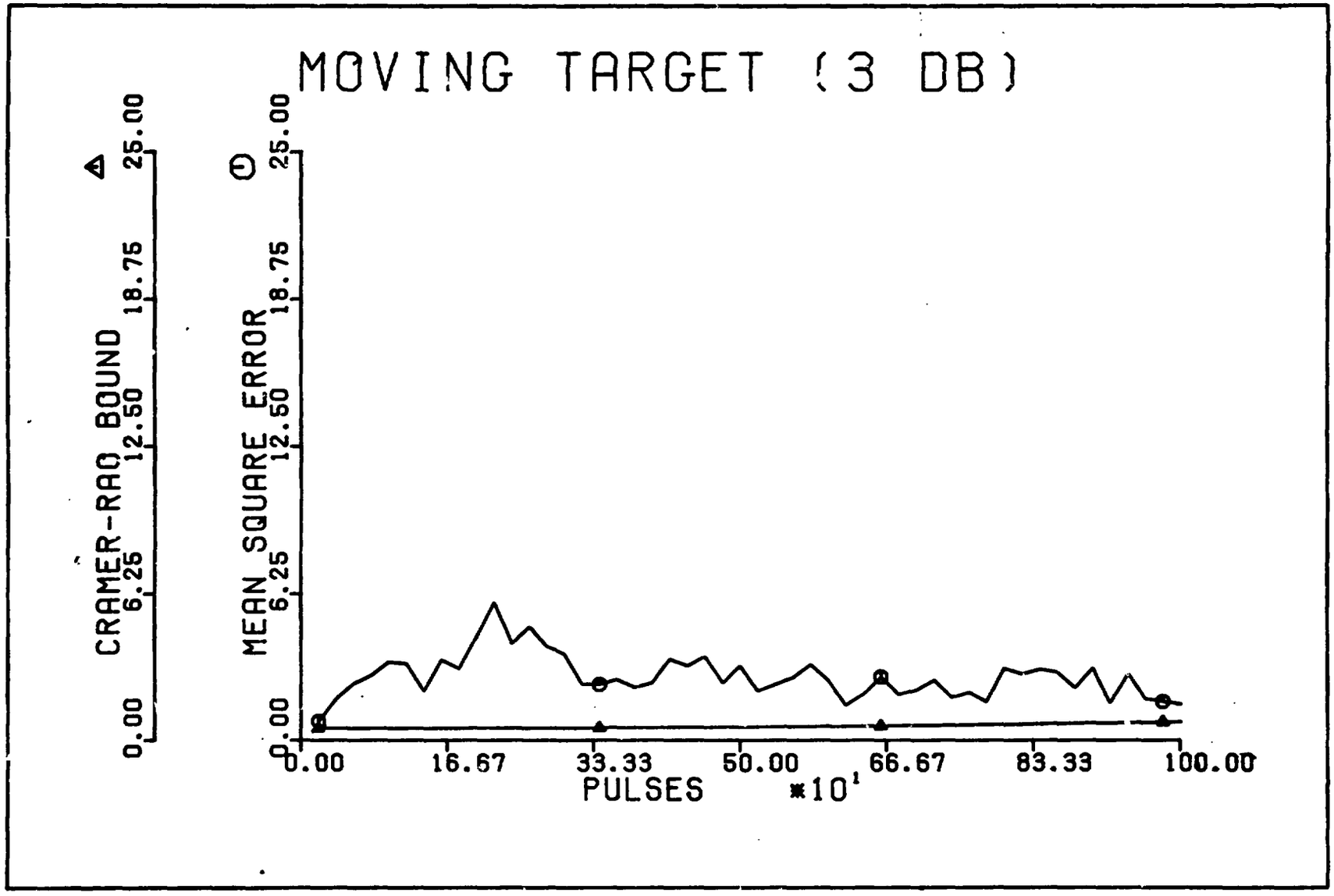
MOVING TARGET (3 DB)
CRAMER-RAO BOUND
MEAN SQUARE ERROR
0.00
6.25
12.50
18.75
25.00
0.00
16.67
33.33
50.00
66.67
83.33
100.00
PULSES
*10¹

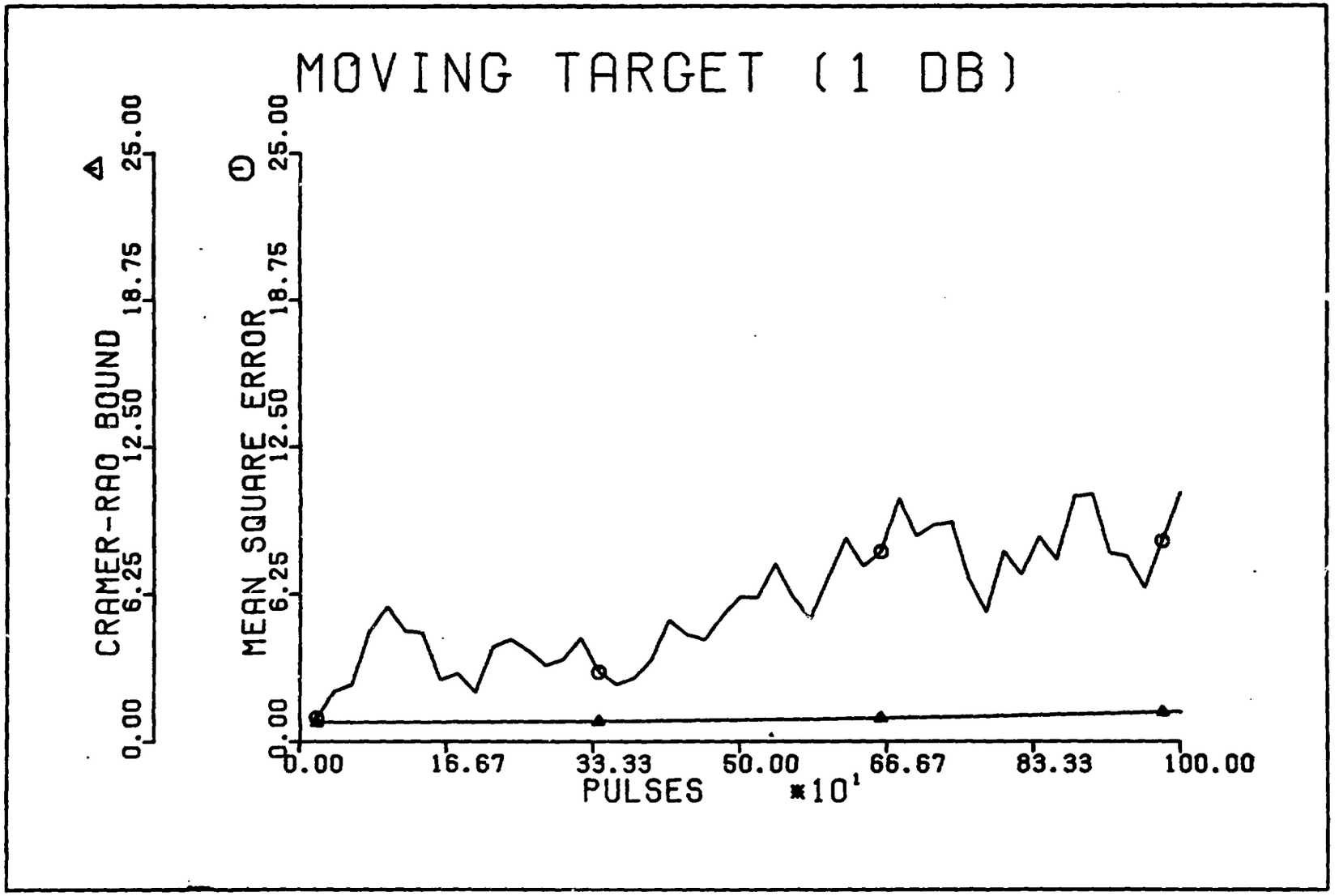
MOVING TARGET (1 DB)
CRAMER-RAO BOUND
MEAN SQUARE ERROR
0.00
6.25
12.50
18.75
25.00
0.00
16.67
33.33
50.00
66.67
83.33
100.00
PULSES
*10¹

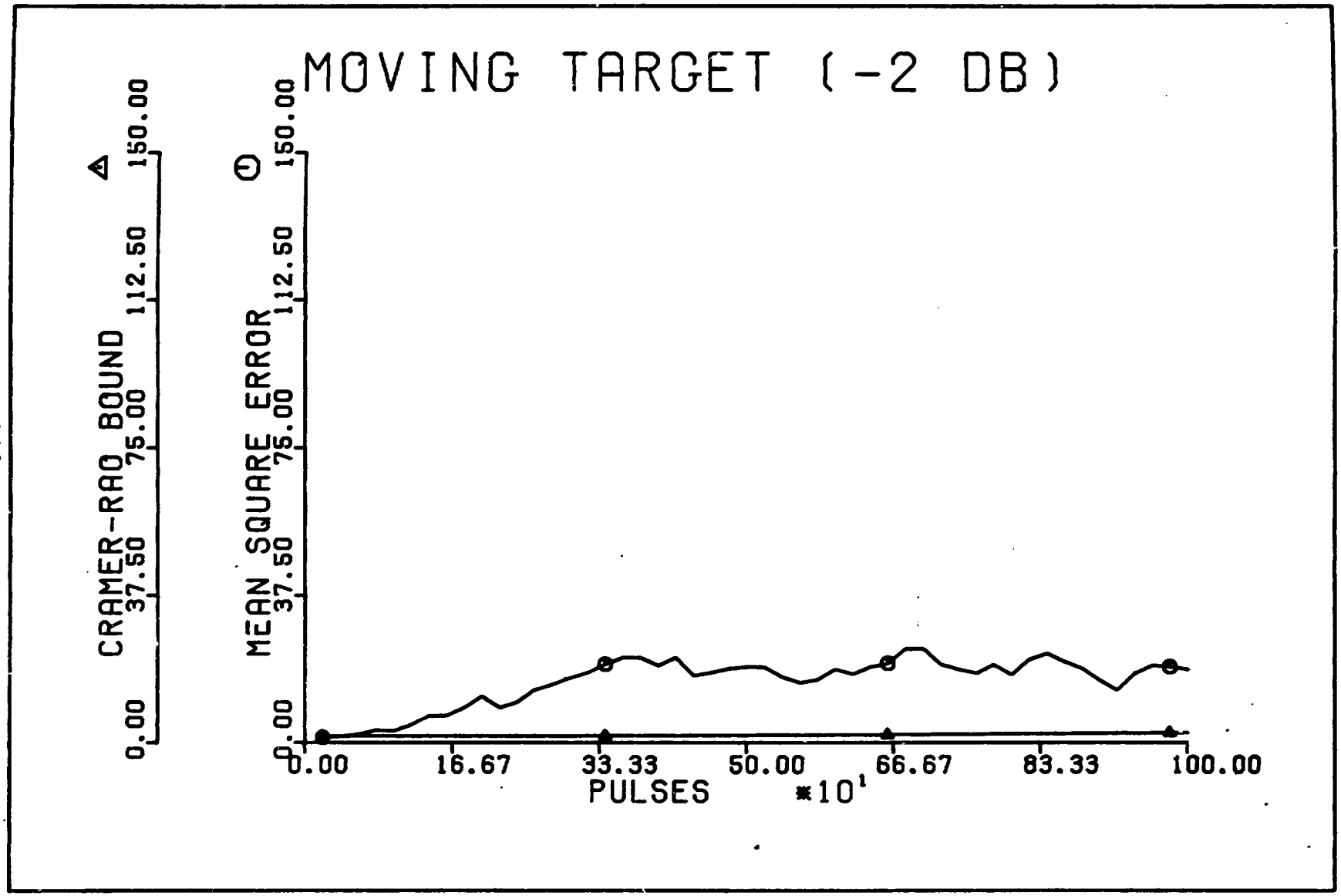
MOVING TARGET (-2 DB)
CRAMER-RAO BOUND
MEAN SQUARE ERROR
0.00
37.50
75.00
112.50
150.00
0.00
16.67
33.33
50.00
66.67
83.33
100.00
PULSES
*10¹

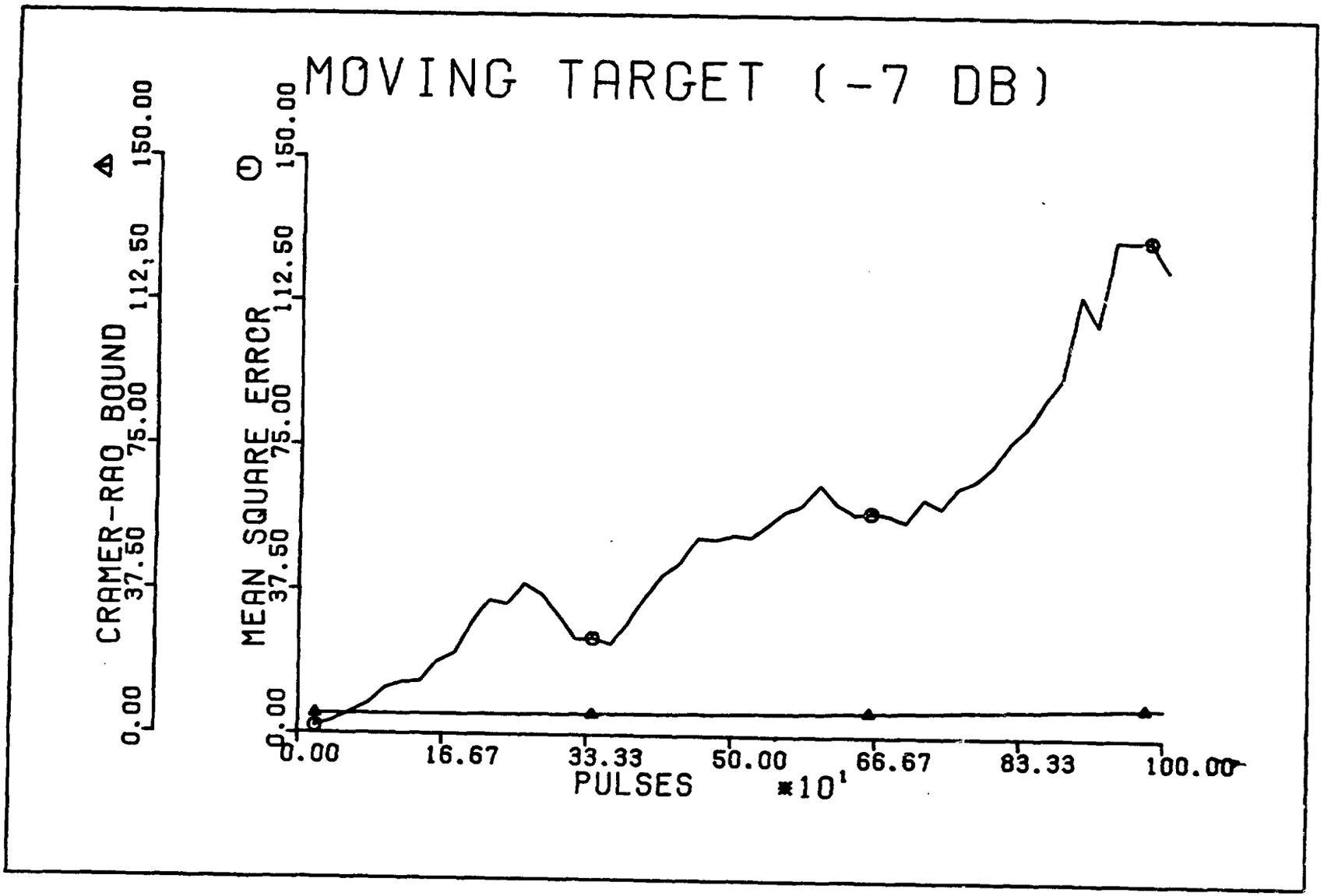
MOVING TARGET (-7 DB)
CRAMER-RAO BOUND
MEAN SQUARE ERROR
0.00
37.50
75.00
112.50
150.00
0.00
16.67
33.33
50.00
66.67
83.33
100.00
PULSES
*10¹

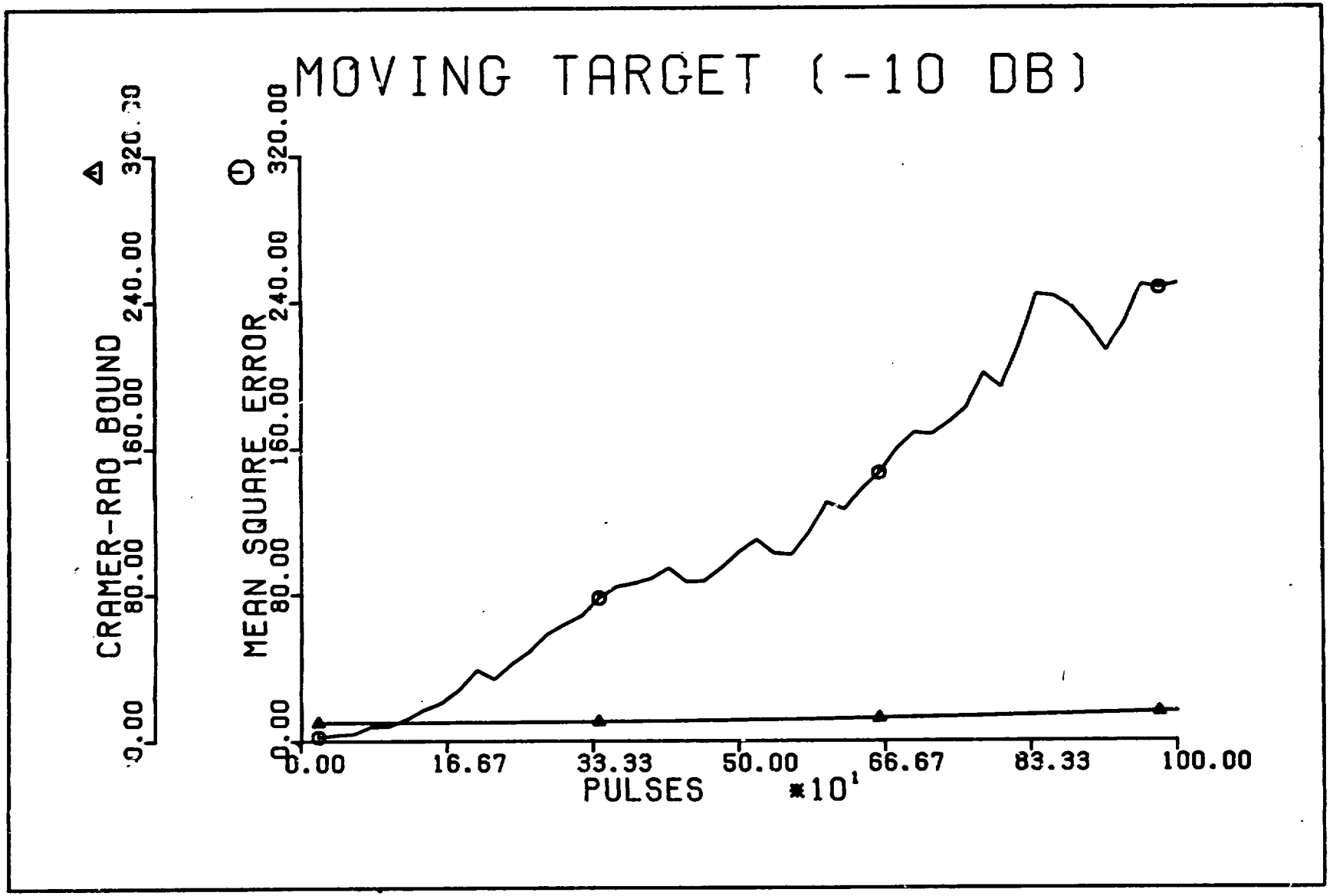
MOVING TARGET (-10 DB)
CRAMER-RAO BOUND
MEAN SQUARE ERROR
0.00
80.00
160.00
240.00
320.00
0.00
16.67
33.33
50.00
66.67
83.33
100.00
PULSES
*10¹

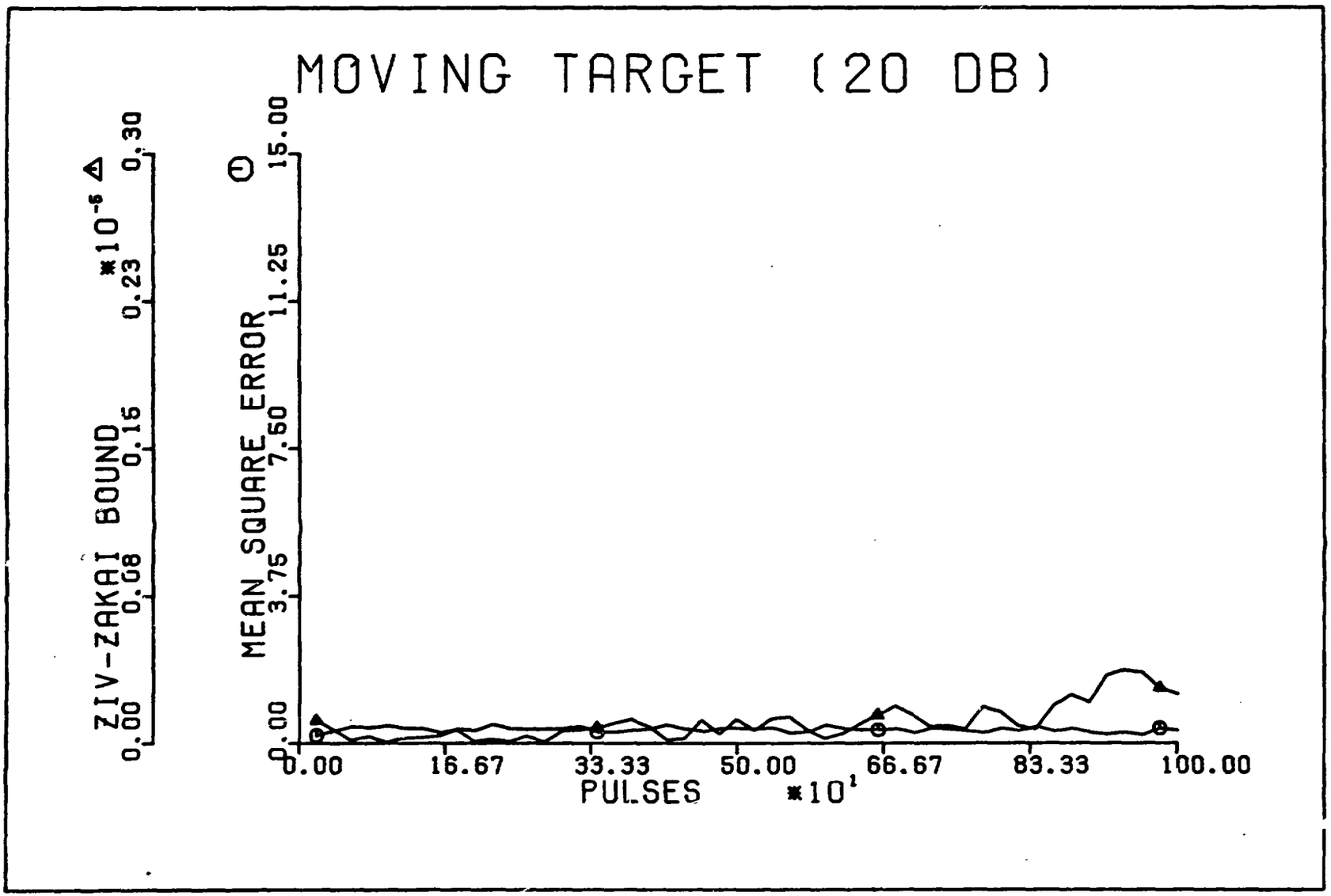
MOVING TARGET (20 DB)
ZIV-ZAKAI BOUND
*10⁻⁵
0.00
0.08
0.15
0.23
0.30
MEAN SQUARE ERROR
0.00
3.75
7.50
11.25
15.00
0.00
16.67
33.33
50.00
66.67
83.33
100.00
PULSES
*10¹

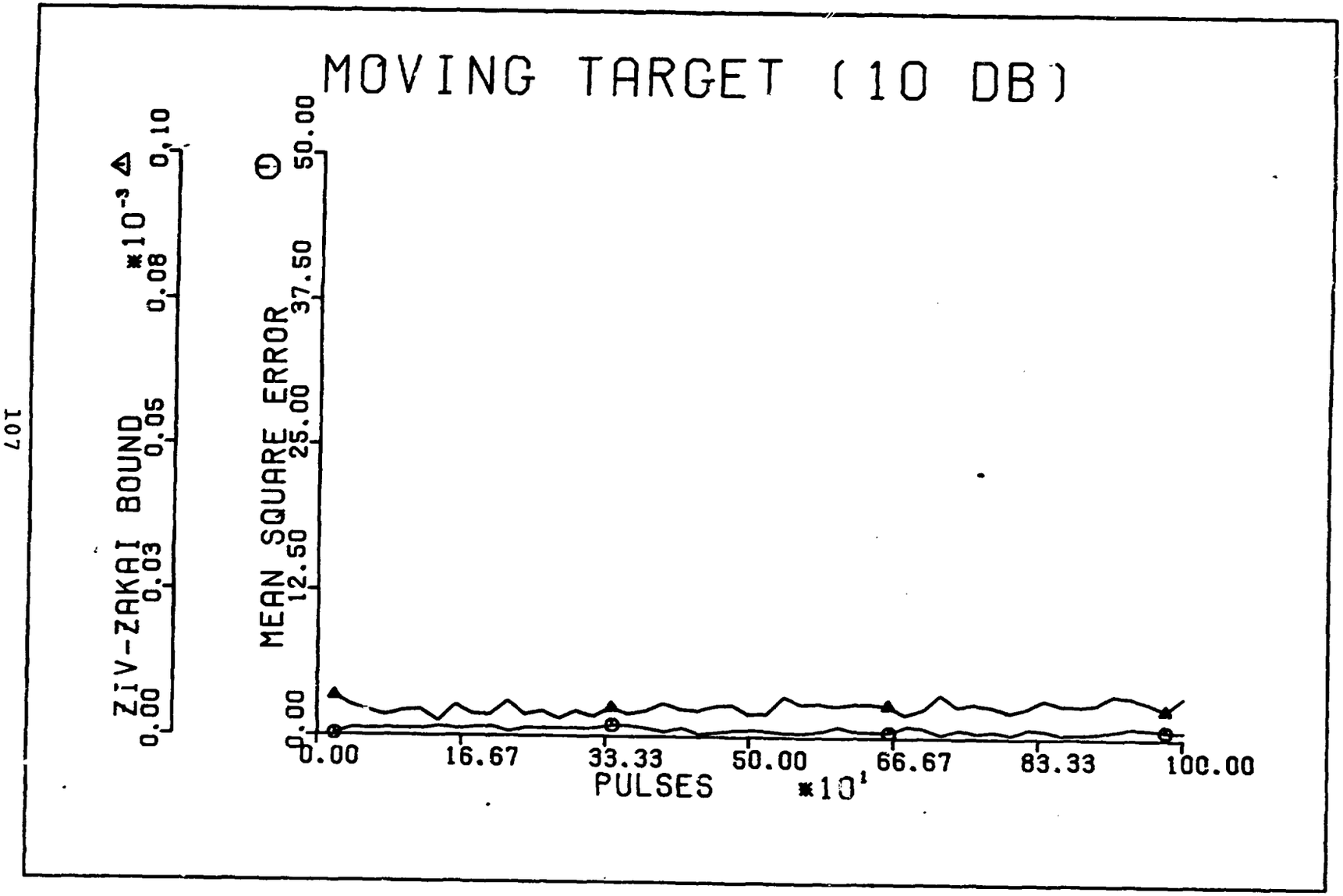
MOVING TARGET (10 DB)
ZIV-ZAKAI BOUND
0.00
0.03
0.05
0.08
0.10
*10⁻³
Δ
MEAN SQUARE ERROR
0.00
12.50
25.00
37.50
50.00
Θ
0.00
16.67
33.33
50.00
66.67
83.33
100.00
PULSES
*10¹

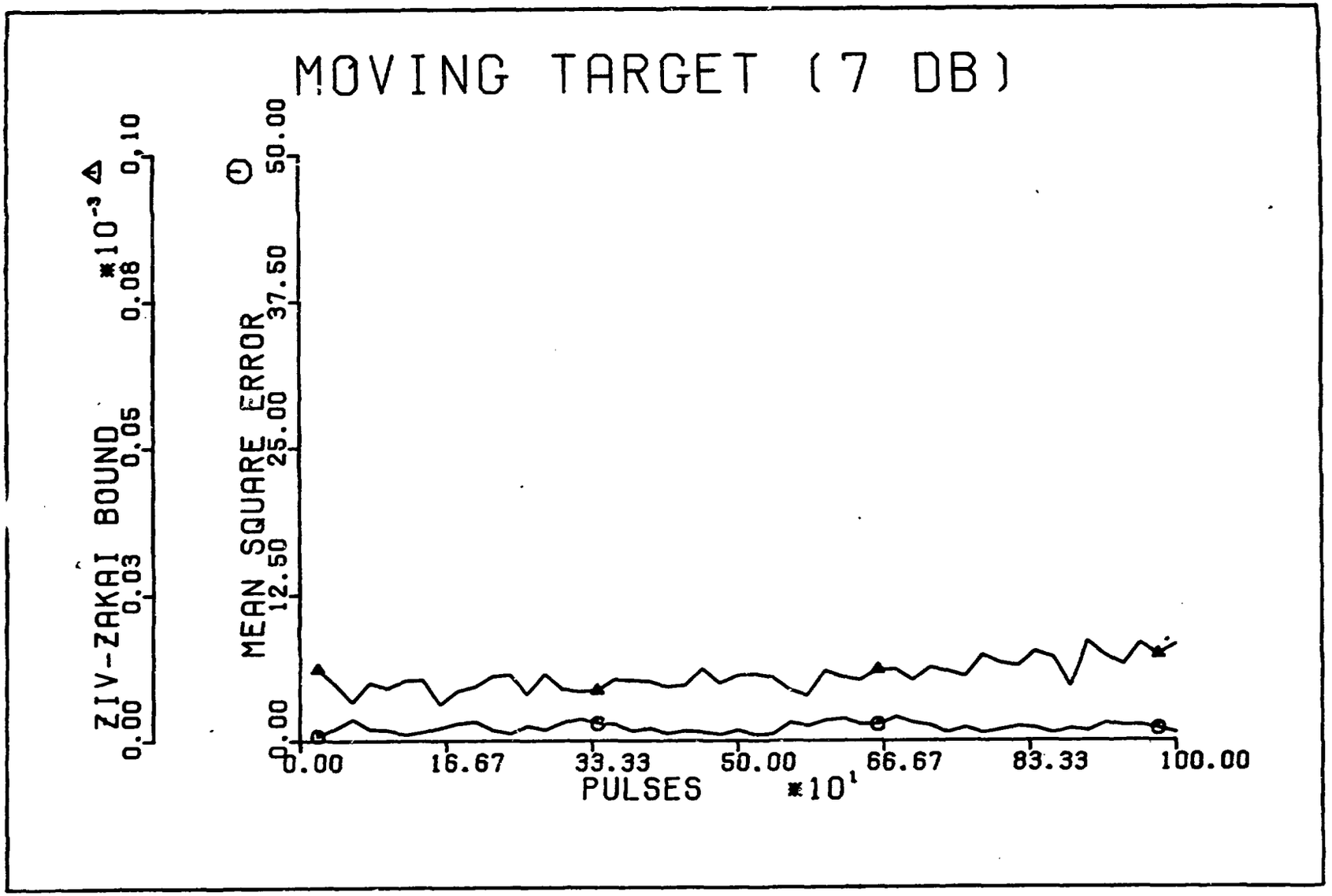
MOVING TARGET (7 DB)
ZIV-ZAKAI BOUND
0.00
0.03
0.05
0.08
0.10
*10^-3
MEAN SQUARE ERROR
0.00
12.50
25.00
37.50
50.00
0.00
16.67
33.33
50.00
66.67
83.33
100.00
PULSES
*10^1

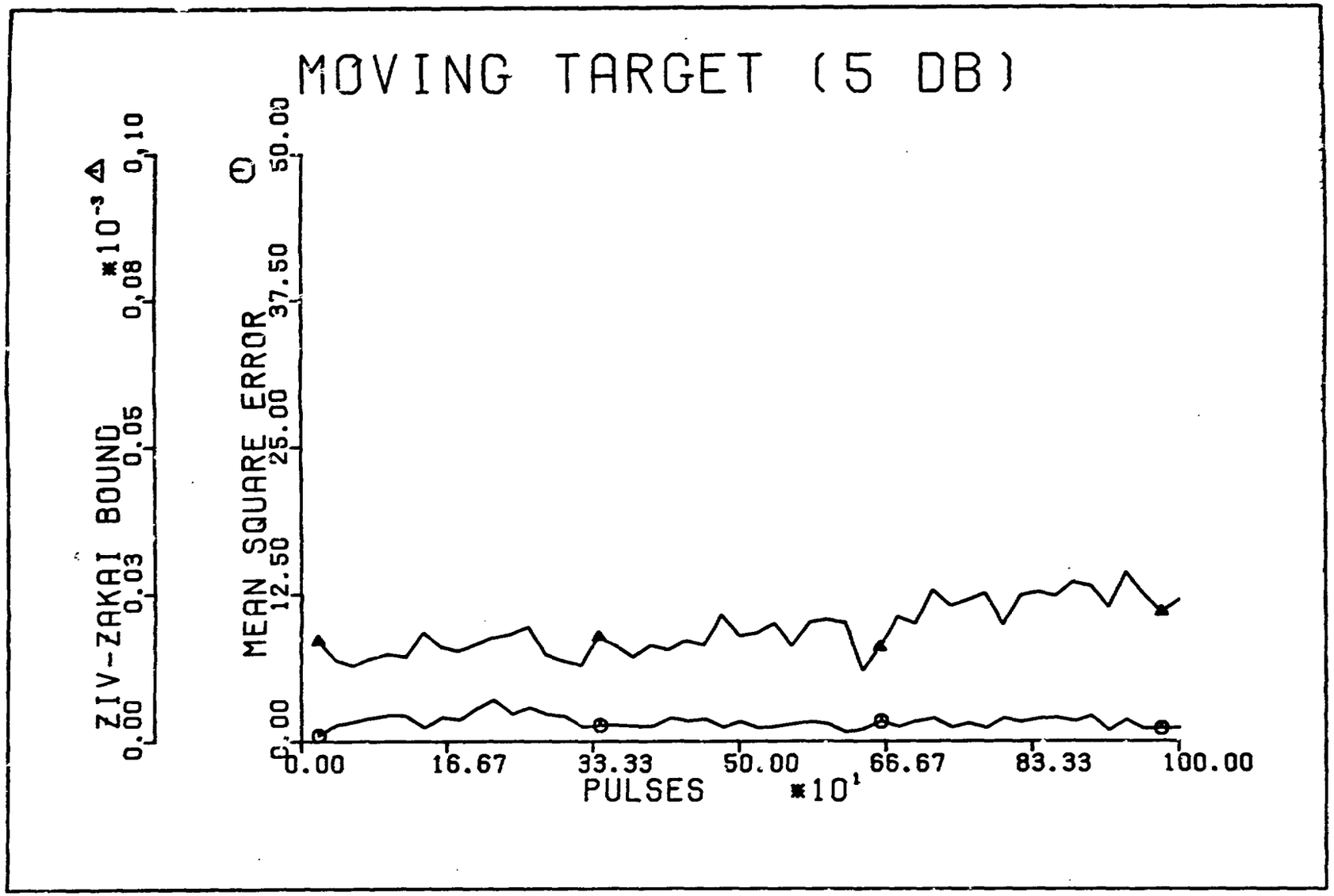
MOVING TARGET (5 DB)
ZIV-ZAKAI BOUND
0.00
0.03
0.05
0.08
0.10
*10⁻³
Δ
MEAN SQUARE ERROR
0.00
12.50
25.00
37.50
50.00
θ
0.00
16.67
33.33
50.00
66.67
83.33
100.00
PULSES
*10¹

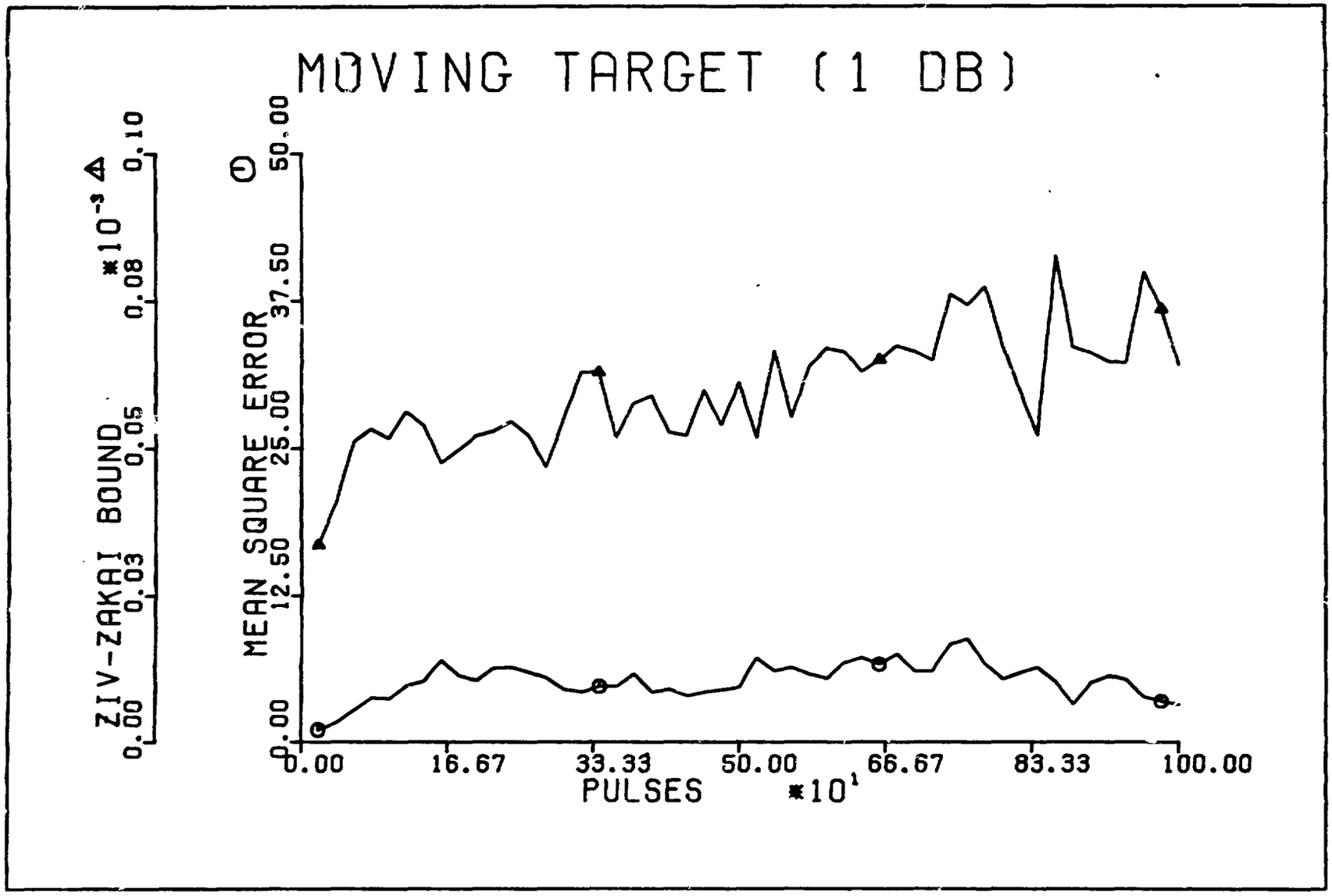
MOVING TARGET (1 DB)
ZIV-ZAKAI BOUND
0.00
0.03
0.05
0.08
0.10
*10^-3
MEAN SQUARE ERROR
0.00
12.50
25.00
37.50
50.00
0.00
16.67
33.33
50.00
66.67
83.33
100.00
PULSES
*10^1

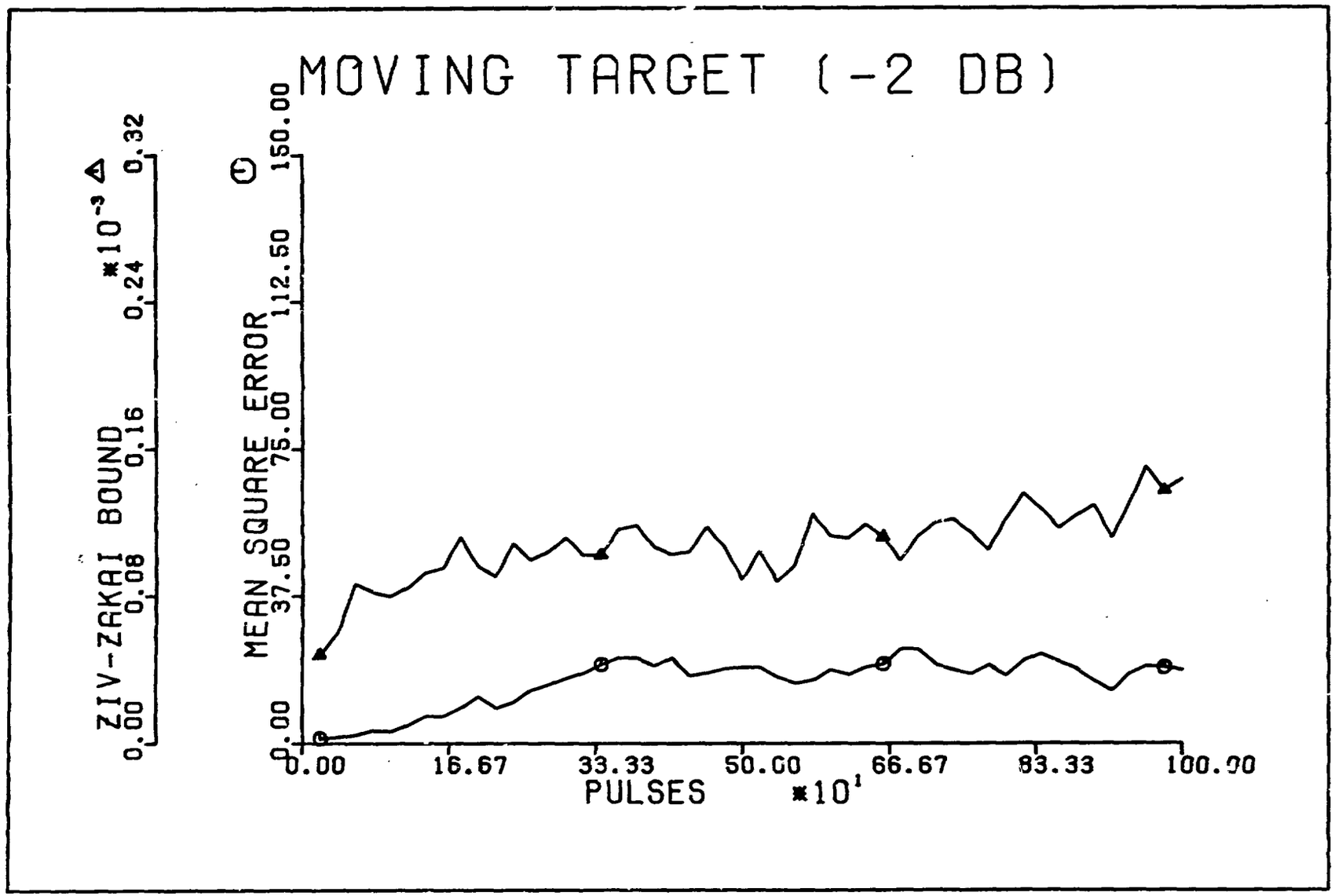
MOVING TARGET (-2 DB)
ZIV-ZAKAI BOUND
0.00
0.08
0.16
0.24
0.32
*10⁻³
Δ
MEAN SQUARE ERROR
0.00
37.50
75.00
112.50
150.00
Θ
0.00
16.67
33.33
50.00
66.67
83.33
100.00
PULSES
*10¹

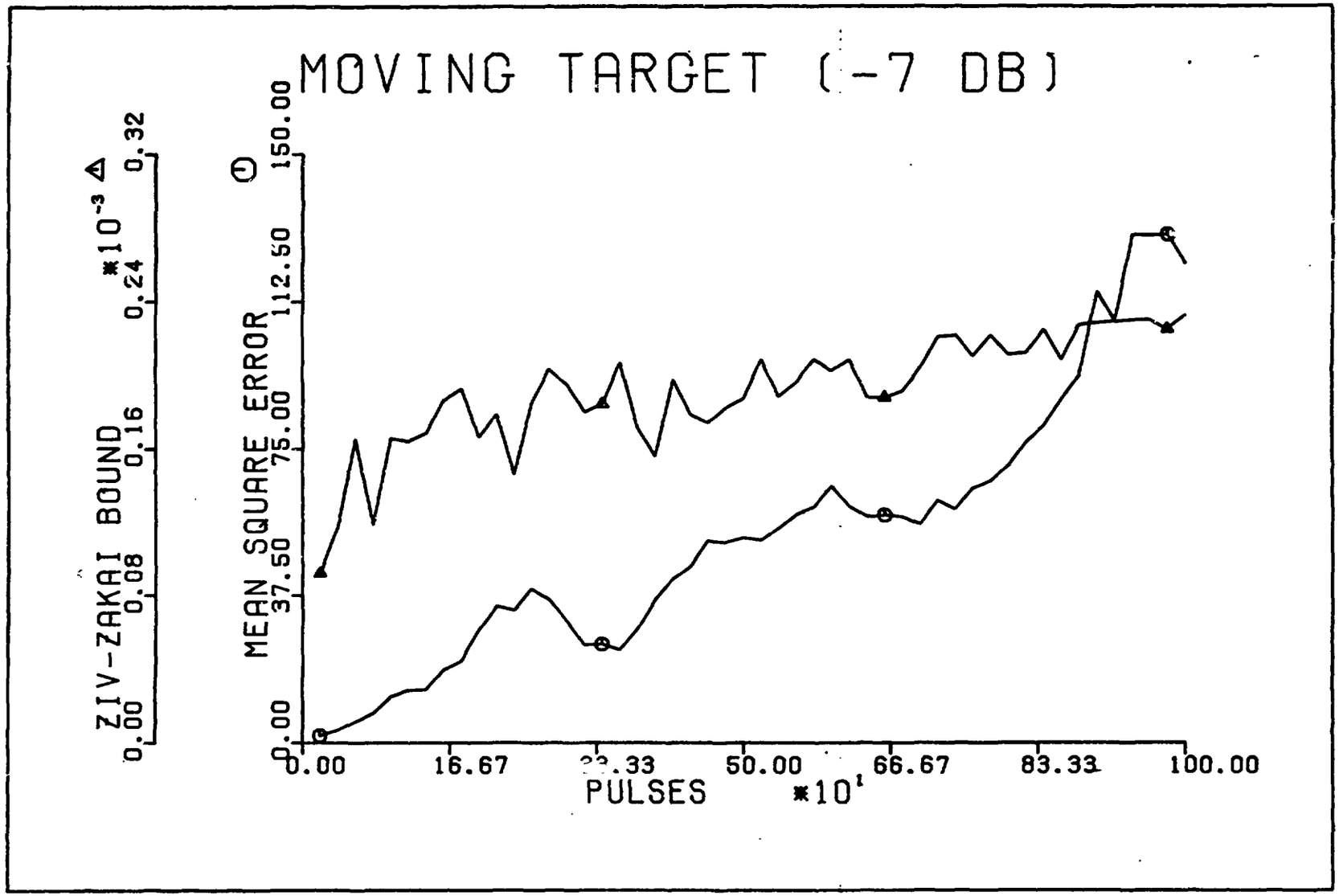
MOVING TARGET (-7 DB)
MEAN SQUARE ERROR
150.00
112.50
75.00
37.50
0.00
ZIV-ZAKAI BOUND
*10⁻³
0.32
0.24
0.16
0.08
0.00
0.00
16.67
33.33
50.00
66.67
83.33
100.00
PULSES
*10¹

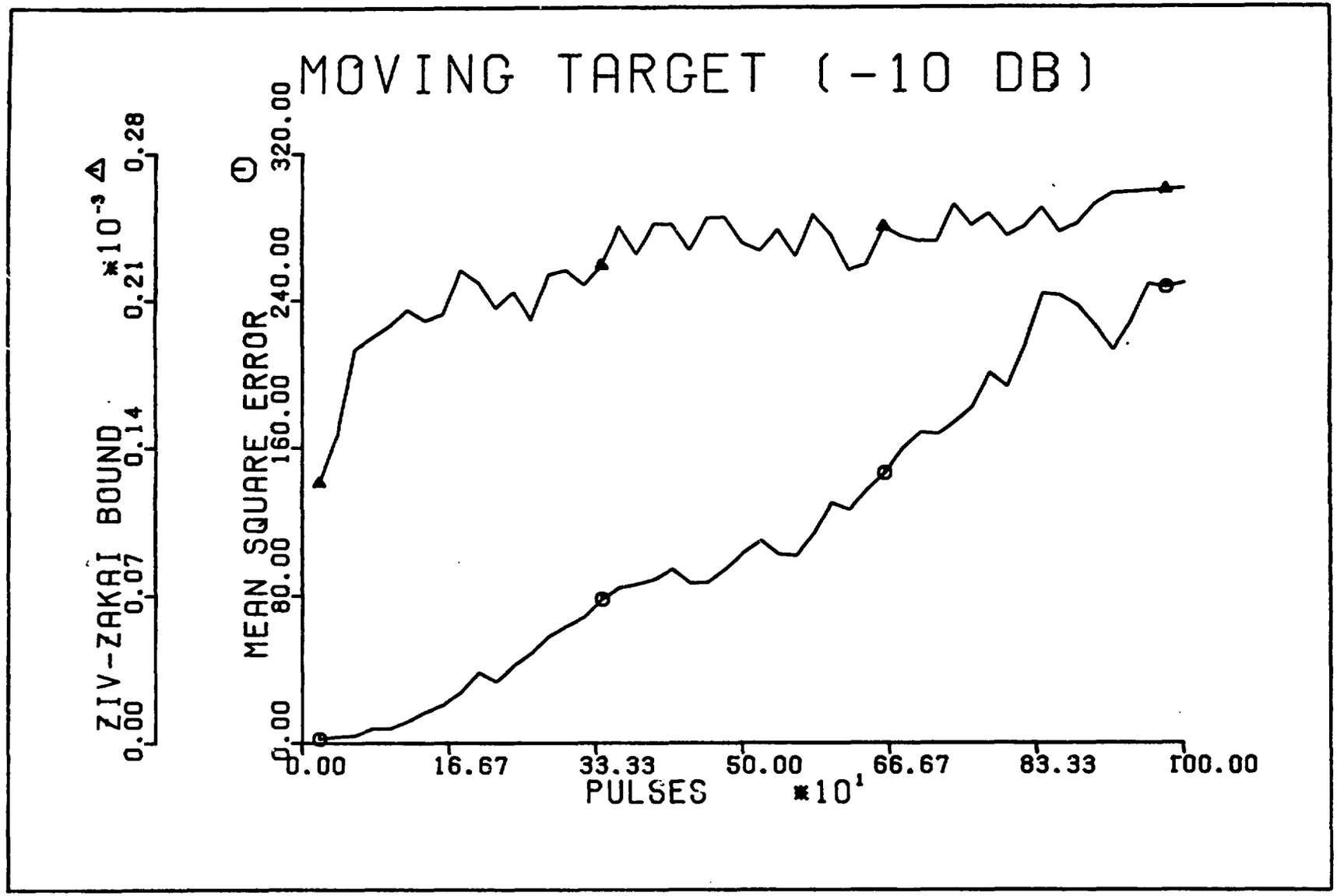
MOVING TARGET (-10 DB)
ZIV-ZAKAI BOUND
0.00
0.07
0.14
0.21
0.28
*10⁻³
Δ
MEAN SQUARE ERROR
0.00
80.00
160.00
240.00
320.00
Θ
0.00
16.67
33.33
50.00
66.67
83.33
100.00
PULSES
*10¹

# Appendix D

## Program Listing

```
      PROGRAM MAIN(INPUT,OUTPUT,LIST,PLOT,TAPE5=INPUT,TAPE6=LIST,
     1 TAPE9=PLOT)
C * THIS PROGRAM SIMULATES A STATIONARY AND MOVING TARGET,
C * BEING TRACKED BY AN AMPLITUDE-COMPARISON MONOPULSE RADAR,
C * CALCULATES THE MEAN-SQUARE ERROR, THE CRAMER-RAO BOUND,
C * THE ZIV-ZAKAI BOUND, AND PLOTS THE RESULTS.
      COMMON/GRAFS/TITLE(3),Y1T(2),Y2T(2),Y3T(2),Y4T(2)
      COMMON/INOU/KIN,KOUT,KP
      DIMENSION TIME(52),TRK(52),TR(52),RMSEA(15,50),RMS(15,50)
      DIMENSION R(100),SNRV(15)
      REAL NPWR,N1,N2
      INTEGER PULSE
      DOUBLE PRECISION DSEED
C * INPUT ALL PARAMETERS
      DATA KIN,KOUT,KP/5,6,9/
      DATA DEPRAD,PI,THETAH/57.3,3.14159,0./
      DATA VT,R0/609.6,6000./
      DATA SNRV/35.,30.,25.,20.,15.,10.,7.,5.,3.,1.,-2.,-5.,-7.,-10.,
     1 -20./
      DATA Y1T/10HMEAN SQUAR,10HE ERROR    /
      DATA Y3T/10HCRAMER-RAO,10H BOUND     /
      DATA Y4T/10HZIV-ZAKAI ,10HBOUND      /
      REWIND 6
      REWIND 9
      CALL PLOTS(0.,0.,9)
 5    CONTINUE
      WRITE*," MOVING OR STATIONARY TARGET(1 OR 2)"
      READ*,IMS
      IF(IMS.LE.0) GO TO 510
      WRITE*,"  C-R OR Z-Z BOUND (1 OR 2)"
      READ*,IB
      WRITE*," ENTER MSE(C-R) AND Z-Z BOUND SCALES"
      READ*,TM,TZ
      WRITE*," ENTER DO LOOP RANGE"
      READ*,I1,I2
      IF(IB.EQ.2) GO TO 20
      Y2T(1)=Y3T(1)
      Y2T(2)=Y3T(2)
      GO TO 25
 20   Y2T(1)=Y4T(1)
      Y2T(2)=Y4T(2)
 25   CONTINUE
      DSEED=2104700000.D0
      WRITE(6,52)
C * TOTAL OBSERVATION INTERVAL
      T=100.E-3
      TX=T/5.E-3
C * SERVO PARAMETERS
      SIG=600./TX
      OM=1483./TX
      NR=100
      TRK(51)=0.
```

```
      TRK(52)=TM/4.
      TR(51)=0.
      IF(IB.EQ.1) TR(52)=TM/4.
      IF(IB.EQ.2) TR(52)=TZ/4.
      TIME(51)=0.
      TIME(52)=50.*TX/6.
      DO 500 IP=I1,I2
      SNR=SNRV(IP)
      SNR0=10.**(SNR/10.)
      SNRR=SNR0
      ROLD=R0
      SPWR=1.E-3
      DO 200 J=1,15
      I=0
      IF(IMS.EQ.2) GO TO 30
      BRSITE=1.5
      TRGT=0.
      GO TO 35
 30   BRSITE=0.
      TRGT=1.
 35   CONTINUE
      THETA=TRGT-BRSITE
C * CALL GGNML AND SET UP THE OBSERVATIONS R1 AND R2
      CALL GGNML(DSEED,NR,R)
      DO 100 PULSE=1,50
      PULSEC=FLOAT(PULSE)
      RNEW=SQRT(R0**2+(VT*PULSEC*T)**2)
      IF(IMS.EQ.1) SNRR=((ROLD/RNEW)**4)*SNR0
      NPWR=SPWR/SNRR
      S=SQRT(NPWR)
      I=I+1
      N1=R(I)*S
      I=I+1
      N2=R(I)*S
      GD=SIN(SIN(THETAH))
      GS=COS(SIN(THETAH))
      THETA=THETA/DEGRAD
      R1=COS(SIN(THETA))+N1
      R2=SIN(SIN(THETA))+N2
C * THE ESTIMATOR AND THE DISCRIMINATOR
      E=R1*GD-R2*GS
      DTHETA=-E*DEGRAD
      IF(DTHETA.GT.1.5) DTHETA=1.5
      IF(DTHETA.LT.-1.5) DTHETA=-1.5
C * THE SERVO
      SERVO=(1.-EXP(-SIG*T)*((SIG/OM)*SIN(OM*T)+COS(OM*T)))
      DTHETP=DTHETA*SERVO
C * MOVE THE ANTENNA
      BRSITE=BRSITE+DTHETP
C * THE EQUATION TO MOVE THE TARGET
```

```
      IF(IMS.EQ.1) TRGT=ATAN((VT*PULSEC*T)/RO)*DEPRAD
C * ADJUST THETA TO REFLECT NEW POSITION OF TARGET WITH RESPECT
C * TO THE BORESITE.
      THETA=TRGT-BRSITE
C * CALCULATE MSE
      TRKER=-THETA
      RMSEA(J,PULSE)=TRKER**2
      IF(THETA.GT.1.5) THETA=1.5
      IF(THETA.LT.-1.5) THETA=-1.5
      THETA=THETA/DEPRAD
      IF(IB.EQ.2) GO TO 40
      SM=1./SNRR/COS(THETA)**2
      GO TO 45
 40   CONTINUE
C * CALCULATE CR AND ZZ BOUNDS.
      UX=SIN(THETA)
      RO=COS(2.*UX)
      AX=SQRT((1.-RO)/NPWR)
      YX=AX
      CALL MONOR(YX,PX)
      PEX=1.-PX
      SM=PEX*UX**2
 45   RMS(J,PULSE)=SM
      TIME(PULSE)=TX*PULSEC
      THETA=THETA*DEPRAD
      SNR=10.*ALOG10(SNRR)
      WRITE(6,50) BRSITE,TRGT,PULSEC,TRKER,RMSEA(J,PULSE)
 100  CONTINUE
 200  CONTINUE
      WRITE(6,53)
      DO 400 K=1,50
      SUM=0.
      SUM1=0.
      DO 300 L=1,15
      SUM=SUM+RMSEA(L,K)
      SUM1=SUM1+RMS(L,K)
 300  CONTINUE
      TRK(K)=SUM/15.
      TR(K)=SUM1/15.
      WRITE(6,54) TRK(K),SNR,RC
 400  CONTINUE
      WRITE*," ENTER TITLE(3A10)",SNRV(IP)
      READ(5,55) TITLE
C * PLOT THE RESULTS
      CALL DRAWCC(TIME,TRK,TR,Y3,Y4,2,0,50,1)
 500  CONTINUE
      GO TO 5
 510  CONTINUE
      WRITE*," * * * ROUTE 'PLOT' TO ON-LINE PLOTTER"
      WRITE*," * * * ROUTE 'LIST' TO PRINTER"
      CALL PLOTE(NDUM)
```

```
      REWIND 6
      REWIND 9
 50   FORMAT(10X,6(3X,E11.5))
 52   FORMAT(15X,"BRSITE",9X,"TRGT",9X,"PULSEC",9X,"TRKER",9X,"MSET")
 53   FORMAT(16X,"MSEE",11X,"SNR",12X,"RO")
 54   FORMAT(10X,3(3X,E11.5))
 55   FORMAT(3A10)
 56   FORMAT(2A10)
      STOP
      END
      SUBROUTINE DRAWCC(X,Y1,Y2,Y3,Y4,NGRAPHS,NSCALE,NPOINTS,JOIN)
      COMMON/GRAFS/TITLE(3),Y1TITLE(2),Y2TITLE(2),Y3TITLE(2),Y4TITLE(2)
      COMMON/INCU/KIN,KOUT,KPUNCH
      DIMENSION X(1),Y1(1),Y2(1),Y3(1),Y4(1),BIG(4),SMALL(4),XTITLE(4)
C
C     ----CHECK CALL PARAMETERS FOR ERRORS
      IBOOBOO=0
      IF(NGRAPHS.LE.4)GO TO 7
      WRITE(KOUT,10)
      IBOOBOO=1
   7  IF(NSCALE.LE.NGRAPHS)GO TO 9
      WRITE(KOUT,11)
      IBOOBOO=1
   9  IF(JOIN .GE. -1 .AND. JOIN .LE. 1)GO TO 14
      WRITE(KOUT,13)
      IBOOBOO=1
C
C     ----ERROR MESSAGES FOR CALL PARAMETERS
  10  FORMAT(1H-,10X,*????? TOO MANY ORDINATES FOR DRAWCC [[[[[*)
  11  FORMAT(1H-,10X,*????? 'NSCALE' LARGER THAN NGRAPHS [[[[[*)
  13  FORMAT(1H-,10X,*????? 'JOIN' IS OUTSIDE ALLOWABLE RANGE     [[[[*)
C
C
C
  14  CONTINUE
C     ----AUTOMATIC SPECIFICATIONS
      ORD=4. $ ABSC=6.  $ SIZE=.25 $ LETTERS=30
      NX=8$XTITLE(1)=6HPULSEC
      NY1=NY2=NY3=NY4=20
C
  30  IF(IBOOBOO .NE. 1)GO TO 33
      WRITE(KOUT,27)
 27   FORMAT(1H-,5X,*ERROR IN CALL TO DRAWCC - - NO PLOTS*//)
      RETURN
C
C     ----CENTER THE Y-AXES
 33   BOTTOM=(11.-ORD-SIZE)/2.
C     ----FIX ORIGIN FOR Y1
      GRAPHS=NGRAPHS-1
      CALL PLOT(GRAPHS,BOTTOM,-3)
C
```

```
      IF(NSCALE .EQ. 0)GO TO 34
C     ----CALCULATE SCALE FACTORS FOR EACH ARRAY
      CALL SCALE(X,ABSC,NPOINTS,1)
      IF(NSCALE .NE. 1)GO TO 80
      CALL SCALE(Y1,ORD,NPOINTS,1)
      IF(NGRAPHS.EQ.1) GO TO 34
      CALL SCALE(Y2,ORD,NPOINTS,1)
      IF(NGRAPHS.EQ.2) GO TO 34
   31 CALL SCALE(Y3,ORD,NPOINTS,1)
      IF(NGRAPHS.EQ.3) GO TO 34
   32 CALL SCALE(Y4,ORD,NPOINTS,1)
      GO TO 34
C
C     ----THIS SECTION ACCOMPLISHES IDENTICAL SCALING
C
C     ----SEARCH Y1( ) AND Y2( ) FOR MAX AND MIN VALUES
   80 BIG(1)=SMALL(1)=Y1(1)
      BIG(2)=SMALL(2)=Y2(1)
      DO 85 I=2,NPOINTS
      IF(Y1(I) .GT. BIG(1) ) BIG(1)=Y1(I)
      IF(Y2(I) .GT. BIG(2) ) BIG(2)=Y2(I)
      IF(Y1(I) .LT. SMALL(1) ) SMALL(1)=Y1(I)
      IF(Y2(I) .LT. SMALL(2) ) SMALL(2)=Y2(I)
   85 CONTINUE
      XMAX=AMAX1( BIG(1),BIG(2) )
      XMIN=AMIN1(SMALL(1),SMALL(2) )
      IF(NSCALE .LT. 3)GO TO 100
C
C     ----SEARCH Y3( ) FOR ITS MAX AND MIN VALUES
      BIG(3)=SMALL(3)=Y3(1)
      DO 90 I=2,NPOINTS
      IF(Y3(I) .GT. BIG(3) ) BIG(3)=Y3(I)
      IF(Y3(I) .LT. SMALL(3) ) SMALL(3)=Y3(I)
   90 CONTINUE
      IF(XMAX .LT. BIG(3) )XMAX=BIG(3)
      IF(XMIN .GT. SMALL(3) )XMIN=SMALL(3)
      IF(NSCALE .LT. 4)GO TO 100
C
C     ----SEARCH Y4( ) FOR ITS MAX AND MIN VALUES
      BIG(4)=SMALL(4)=Y4(1)
      DO 95 I=2,NPOINTS
      IF(Y4(I) .GT. BIG(4) ) BIG(4)=Y4(I)
      IF(Y4(I) .LT. SMALL(4) ) SMALL(4)=Y4(I)
   95 CONTINUE
      IF(XMAX .LT. BIG(4) )XMAX=BIG(4)
      IF(XMAX .LT. BIG(4) )XMAX=BIG(4)
      IF(XMIN .GT. SMALL(4) )XMIN=SMALL(4)
C
C     ----FIND THE ADJUSTED MIN AND INCREMENT PER INCH
  100 BIG(1)=XMIN
      BIG(2)=XMAX
```

```
      CALL SCALE(BIG,ORD,2,1)
      XMIN=BIG(3)
      DELTA=BIG(4)
C
C     ----PUT THE SCALING INFORMATION INTO THE ARRAYS
      GO TO (34,115,110,105),NSCALE
C
  105 Y4(NPOINTS+1)=XMIN
      Y4(NPOINTS+2)=DELTA
  110 Y3(NPOINTS+1)=XMIN
      Y3(NPOINTS+2)=DELTA
  115 Y2(NPOINTS+1)=XMIN
      Y2(NPOINTS+2)=DELTA
      Y1(NPOINTS+1)=XMIN
      Y1(NPOINTS+2)=DELTA
C
C     ----IS ANY INDEPENDENT SCALING NEEDED?
      IF(NSCALE .EQ. 2  .AND.  NGRAPHS .GT. 2)GO TO 31
      IF(NSCALE .EQ. 3  .AND.  NGRAPHS .EQ. 4)GO TO 32
C
   34 A=ORD-.1
C
C     ----DRAW AN AXIS AND A SYMBOL FOR THAT AXIS
      CALL AXIS(0.,0.,Y1TITLE,NY1,ORD,90.,Y1(NPOINTS+1),Y1(NPOINTS+2))
      IF(JOIN.EQ.0)GO TO 35
      CALL SYMBOL(-.4,A,.15,1,90.,-1)
   35 IF(NGRAPHS.EQ.1) GO TO 51
      CALL AXIS(-1.,0.,Y2TITLE,NY2,ORD,90.,Y2(NPOINTS+1),Y2(NPOINTS+2))
      IF(JOIN.EQ.0)GO TO 36
      CALL SYMBOL(-1.4,A,.15,2,90.,-1)
   36 IF(NGRAPHS.EQ.2) GO TO 51
      CALL AXIS(-2.,0.,Y3TITLE,NY3,ORD,90.,Y3(NPOINTS+1),Y3(NPOINTS+2))
      IF(JOIN.EQ.0)GO TO 37
      CALL SYMBOL(-2.4,A,.15,5,90.,-1)
   37 IF(NGRAPHS.EQ.3) GO TO 51
      CALL AXIS(-3.,0.,Y4TITLE,NY4,ORD,90.,Y4(NPOINTS+1),Y4(NPOINTS+2))
      IF(JOIN.EQ.0)GO TO 51
      CALL SYMBOL(-3.4,A,.15,4,90.,-1)
C
   51 CALL AXIS(0.,0.,XTITLE,-NX,ABSC,0.,X(NPOINTS+1),X(NPOINTS+2))
C
C     ----DECIDE HOW MANY POINTS SHOULD BE MARKED WITH A SYMBOL
      IF(JOIN .NE. 0)GO TO 72
      J=0
      GO TO 53
   72 IF(JOIN .EQ. 1)GO TO 68
      J=-1
      WRITE(KOUT,71)
   71 FORMAT(1H-,5X,*EVERY POINT IS MARKED WITH A SYMBOL*)
      GO TO 53
```

```
   68 NUM=ABSC*.25 + 1.
      IF(NUM .LT. 3)NUM=3
      J=NPOINTS/NUM
      IF(J .LT. 1)J=1
   69 JJ=IABS(J)
      WRITE(KOUT,70) JJ
   70 FORMAT(1H-,5X,*EVERY*,I4,* TH  POINT IS MARKED WITH A SYMBOL*)
C
C     ----PLOT X VS Y1
   53 CALL LINE(X,Y1,NPOINTS,1,J,1)
      IF(NGRAPHS .EQ. 1)GO TO 60
C     ----PLOT X VS Y2
   56 CALL LINE(X,Y2,NPOINTS,1,J,2)
      IF(NGRAPHS .EQ. 2)GO TO 60
C     ----PLOT X VS Y3
   57 CALL LINE(X,Y3,NPOINTS,1,J,5)
      IF(NGRAPHS .EQ. 3)GO TO 60
C     ----PLOT X VS Y4
   58 CALL LINE(X,Y4,NPOINTS,1,J,4)
C
C     ----SEE IF A TITLE IS DESIRED
   60 IF(LETTERS.EQ.0)GO TO 61
C     ----CENTER TITLE OVER GRAPH
      XX=0.
      CALL SYMBOL(XX,ORD+.425,SIZE,TITLE,0.,LETTERS)
C     ----DRAW BOX AROUND PLOT
      RLM=-(GRAPHS+1.)
      RRM=ABSC+1.
      RBM=-1.
      RTM=ORD+1.
      CALL PLOT(RLM,RBM,3)
      CALL PLOT(RRM,RBM,2)
      CALL PLOT(RRM,RTM,2)
      CALL PLOT(RLM,RTM,2)
      CALL PLOT(RLM,RBM,2)
C     ----POSITION PEN FOR THE NEXT CALL DRAWCC
   61 CALL PLOT(ABSC+5.,-BOTTOM,-3)
      RETURN
      END
```

## Vita

William P. Tross was born on 28 April 1951 in Holyoke, Massachusetts. He graduated from high school in Orange, Virginia in 1969. He joined the Air Force in February 1973 as an Electronic Warfare Systems Specialist. In 1977, he was accepted into the Airmans Education and Commissioning Program, and then attended Brigham Young University from which he received the degree of Bachelor of Science in Electrical Engineering in April 1979. Upon graduation he received a commission in the U.S. Air Force through OTS. His first assignment was at the Warner Robins Air Logistics Center in the Systems Management Division of the Directorate of Material Management at Robins AFB, Georgia. He later transferred to the Electronic Warfare Management Division at Robins AFB, where he developed software for the APR-38 Advanced Wild Weasel until entering the School of Engineering, Air Force Institute of Technology, in June 1981.

Permanent Address: Box 634
Gordonsville, Virginia 22942

UNCLASSIFIED

SECURITY CLASSIFICATION OF THIS PAGE (When Data Entered)

## REPORT DOCUMENTATION PAGE

READ INSTRUCTIONS BEFORE COMPLETING FORM

| | |
|---|---|
| 1. REPORT NUMBER: AFIT/GE/EE/82D-66 | 2. GOVT ACCESSION NO.: AD-A135806 |
| 3. RECIPIENT'S CATALOG NUMBER: | |
| 4. TITLE (and Subtitle): Lower Bounds Applied to the Mean-Square Tracking Error of an Amplitude-Comparison Monopulse Radar | 5. TYPE OF REPORT & PERIOD COVERED: Ms Thesis |
| | 6. PERFORMING ORG. REPORT NUMBER: |
| 7. AUTHOR(s): William P. Tross, BSEE<br>1Lt, USAF | 8. CONTRACT OR GRANT NUMBER(s): |
| 9. PERFORMING ORGANIZATION NAME AND ADDRESS: Air Force Institute of Technology (AFIT-EN)<br>Wright-Patterson AFB OH 45433 | 10. PROGRAM ELEMENT, PROJECT, TASK AREA & WORK UNIT NUMBERS: |
| 11. CONTROLLING OFFICE NAME AND ADDRESS: | 12. REPORT DATE: December 1981 |
| | 13. NUMBER OF PAGES: 124 |
| 14. MONITORING AGENCY NAME & ADDRESS (if different from Controlling Office): | 15. SECURITY CLASS. (of this report): UNCLASSIFIED |
| | 15a. DECLASSIFICATION/DOWNGRADING SCHEDULE: |

16. DISTRIBUTION STATEMENT (of this Report)

Approved for public release; distribution unlimited

17. DISTRIBUTION STATEMENT (of the abstract entered in Block 20, if different from Report)

18. SUPPLEMENTARY NOTES

Approved for public release; IAW AFR 190-17

9 SEP 1983

Approved for public release: IAW AFR 190-17.

LYNN E. WOLAVER
Dean for Research and Professional Development
Air Force Institute of Technology (ATC)
Wright-Patterson AFB OH 45433

19. KEY WORDS (Continue on reverse side if necessary and identify by block number)

Lower Bounds
Ziv-Zakai Bound
Mean-Square Error
Parameter Estimation
Bearing Estimation
Threshold Effect

20. ABSTRACT (Continue on reverse side if necessary and identify by block number)

This thesis addresses the problem of estimating the target angle with respect to the boresight of an Amplitude-Comparison Monopulse Radar. The maximum likelihood estimate is used to track the target which produces a mean-square error. This error is approximated from a computer simulated tracking loop and then compared to the Cramer-Rao and Ziv-Zakai bounds.

At high signal-to-noise ratios (SNR), the Cramer-Rao bound is useful to lower bounding the mean-square error. At low SNR levels a phenomena known as the threshold effect occurs and the Cramer-Rao bound becomes unreliable as a

DD FORM 1 JAN 73 1473 EDITION OF 1 NOV 65 IS OBSOLETE

UNCLASSIFIED

SECURITY CLASSIFICATION OF THIS PAGE (When Data Entered)

lower bound. The Ziv-Zakai bound is a tighter bound and can be used to lower bound the mean-square error at very low SNR levels. It also proves useful in determining the SNR level at which the threshold effect occurs.